Master's degree programme in
Territorial, Urban, Environmental and Landscape Planning
Planning for the Global Urban Agenda

MASTER THESIS

URBAN HEAT ISLAND IMPACT IN TURIN
- the role of urban pavements -

Supervisors: Candidate:

Prof. Mutani Guglielmina   Zampese Althea

Prof. Bassani Marco

Prof. Tefa Luca

Master's degree programme in
Territorial, Urban, Environmental and Landscape Planning
Planning for the Global Urban Agenda
Academic Year 2023/2024

MASTER THESIS

URBAN HEAT ISLAND IMPACT IN TURIN
- the role of urban pavements -

Supervisors: Candidate:

Prof. Mutani Guglielmina   Zampese Althea

Prof. Bassani Marco

Prof. Tefa Luca

a Mario

TABLE OF CONTENTS

ABSTRACT

The urban heat island (UHI) effect has been the subject of extensive research over the years. This phenomenon refers to the localized increase in air temperatures in urban areas compared to surrounding rural or less developed regions. The UHI effect is associated with a range of environmental and public health risks, which are well-documented and significant.

Albedo is a key factor in determining the intensity of the Urban Heat Island (UHI) effect. It refers to how much sunlight is reflected by a surface. Materials like asphalt, which have a low albedo, absorb more heat, making them common in road surfaces. This contributes to higher temperatures in urban areas. This thesis aims to explore the UHI effect and investigate how different types of urban pavements contribute to it. Specifically, it examines how materials used in the construction of urban infrastructure affect temperature, with the application of "cool" materials serving as a potential strategy to reduce surface heat.

This study, which utilizes weather station data and Landsat 8 satellite imagery, takes an appropriate approach for measuring and quantifying the UHI effect. The temporal data taken from one or more of these data sources are considered as reasonable indicatives of a typical time frame for the effects of one another. An array of urban indices based on satellite imagery, such as the Normalized Difference Vegetation Index (NDVI) and Land Surface Temperature (LST), will prove useful in framing the phenomenon as well as providing directions in developing suitable strategies for reducing such effects.

The present thesis aims to focus on taking albedo measurements of various road pavements in the city of Turin. These pavements provided a great variation in the application of the albedo measurement with regard to the warming up of urban environments and how they influence UHI. Measurements thus undertaken are the first of their kind in Turin and are included in an area where such studies are few.

1 LITERATURE REVIEW

The heat island effect is a phenomenon characterized by significantly warmer temperatures in urban areas compared to the surrounding rural regions.
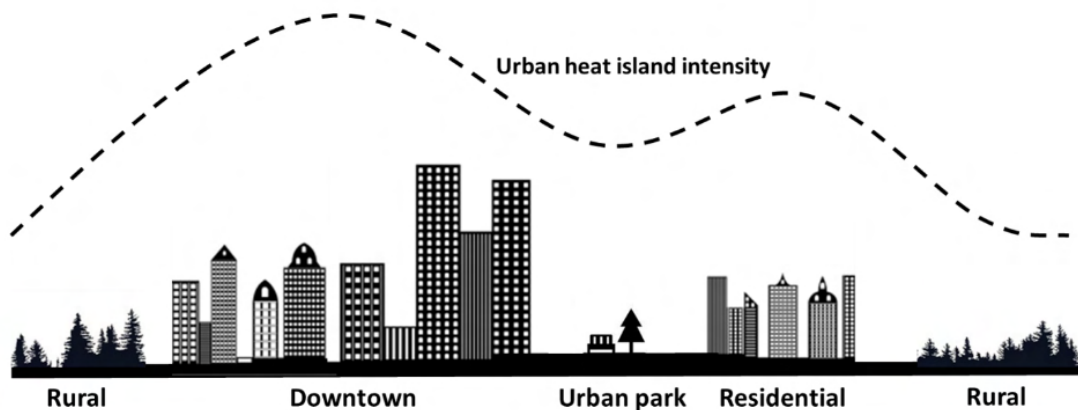

Figure 1 - Urban Heat Island intensity diagram

The concept of the Urban Heat Island (UHI) effect was first proposed by Luke Howard [31] in the early 19th century. By analyzing the city of London and its surrounding areas, he examined the impact of urbanization and the factors contributing to the phenomenon. As a result, in 1833, Howard identified four causes, which can be summarized as follows:

• The geometry of the urban area can trap solar radiation;

• Human activities contribute to rising temperatures due to winter heating;

• Humidity resulting from evaporation;

• The irregular surfaces of the city can alter the direction and speed of the wind.

In 1982, Oke [34] asserted that the topography of the environment is relatively insignificant, emphasizing the boundaries between rural and urban areas: the city center exhibits higher temperatures compared to the surrounding regions. Furthermore, within urban areas, it is also possible to find hotter and cooler zones corresponding to areas of varying building density. In the case of parks and lakes, temperatures will therefore be lower than in industrial, commercial, or urban center areas.

The vertical aspect of the Urban Heat Island (UHI) effect can be understood by looking at three key layers of a city: the Urban Canopy, the Urban Canyon, and the Urban Boundary. These components help explain how heat is trapped and distributed in urban areas. This framework was developed by Oke in 1976 [32].

The Urban Canopy refers to the space between the average height of buildings and the ground level. The Urban Canyon describes the enclosed areas within a city, created by buildings and other structures that block airflow and natural light. The Urban Boundary is the layer of the atmosphere that is directly affected by the features and activities of urban areas.

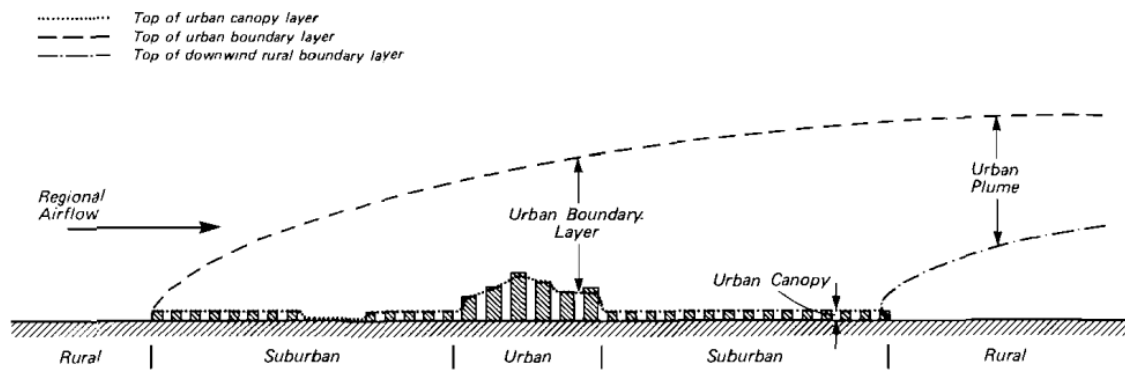Below is the model proposed by Oke in 1976:

Figure 2 - Two-layer classification of thermal modification of urban atmosphere (Oke, 1976)

In conclusion, the primary causes of the Urban Heat Island (UHI) effect are:

• Anthropogenic activities: anthropogenic activities contribute to the expansion of the phenomenon. Industrial facilities, heating systems, and CO2 emissions from traffic and pollution exacerbate the greenhouse effect;

• Urban geometry: the construction of infrastructure and buildings reduces the ground's capacity to absorb water. Additionally, buildings obstruct wind circulation. The denser the city, the greater the discomfort and perceived temperature increase;

• Sparse vegetation: urban areas tend to have fewer trees and green spaces compared to surrounding regions. Central areas are characterized by denser development and high population density. Trees and green spaces provide permeable soils that contribute to a greater level of comfort in cities, as they offer shade and, notably, possess the capacity for evapotranspiration. This process facilitates the absorption of air heat, thereby lowering temperatures.

• Surface materials: Dark surfaces, like asphalt, absorb more heat than natural materials like soil covered with vegetation. Common urban materials such as asphalt, concrete, and mortar have a high ability to absorb and hold onto heat. Albedo is the term used to describe how much sunlight a material reflects.

The Protocollo ITACA a Scala Urbana SINTETICO [24] identify and list the factors for quantifying and assessing the Urban Heat Island (UHI) effect according to the guidelines of the protocol itself.

Solar Reflectance Index (SRI): is a measure that combines how much sunlight a surface reflects (solar reflectance) and how much heat it releases (thermal emittance). It's given on a scale from 0 to 100, lower values indicate lower heat dissipation ability.

Sky View Factor (SVF): it defines and measures the visible portion of the sky from a given observation point. Expressed on a scale from 0 to 1, the maximum value indicates that the sky is completely visible from every angle of the observation point. This factor is particularly important in urban environments, as building density can restrict sky visibility and consequently limit heat exchange.

H/D ratio: it is defined by the ratio of building height (H) to the width of the open space (D). Open spaces allow for greater radiation and convection, facilitating heat

exchange with the atmosphere. Buildings act as "barriers" between the Earth's surface and the atmosphere.

Soil permeability: the ability of the ground to absorb or let fluids pass through it. Soils with low permeability tend to hold onto water, while those with higher permeability allow water to drain more easily. In the context of the urban heat island effect, permeable soils are preferred.

Urban anthropogenic activities: transportation, air conditioning, and industrial facilities generate heat that contributes to the formation of the Urban Heat Island (UHI) effect.

Green roof and vegetation: Urban greenery plays a key role in cooling the air by releasing moisture through evapotranspiration, providing shade, and improving air quality. Plants and trees help lower surrounding temperatures, making cities more comfortable and healthier to live in.

Presence of water: fountains, ponds, and puddles help to reduce air temperatures through the process of evapotranspiration.

Materials: in urban areas, the materials used are fundamental. For instance, it is well known that asphalt on roads tends to retain heat. For this reason, it is preferable to use reflective materials (also known as cool materials).

[31] Howard, L. (1833), The Climate of London. London, UK: Harvey and Darton.

[34] Oke, T. R. (1982), The energetic basis of the urban heat island.

[32] Oke T.R. (1976), The distinction between canopy and boundary-layer urban heat islands, Atmosphere.

[24] (2020), Istituto per l'innovazione e trasparenza degli appalti e la compatibilità ambientale Itaca, Protocollo ITACA a scala urbana Sintetico, Metodologia e strumento di verifica.

Effects of UHI on environment and human health

Urban heat islands, if no interventions are made, are destined to worsen in terms of temperatures and pollutant gases within cities. The direct consequence of the urban heat island effect is the increase in temperatures, which leads to reduced comfort, higher consumption of water and electricity, and difficulties in mobility.

The urban microclimate modifies and influences the quality of life. Elevated temperatures have multiple consequences, such as increased air pollutants, heightened thermal stress, deteriorating water quality, and a general degradation of the environment.

The effects of Urban Heat Island (UHI) on human health are manifold and are primarily caused by prolonged exposure to elevated temperatures above the average. The human body requires significant amounts of energy to rebalance and adapt to temperature variations. The health consequences can be outlined as follows:

- Heat Stroke: occurs after prolonged exposure to high temperatures, high humidity, and lack of ventilation.
- Dehydration: arises when the amount of fluids consumed is less than those expelled through sweating.
- Edema: localized swelling due to the dilation of blood vessels as a result of circulatory dysfunction.
- Fainting: happens when there is a sudden drop in blood pressure, which can cause a person to faint or lose consciousness quickly.
- Blood Pressure Variations: heat acts as a vasodilator, lowering blood pressure and causing the heart to beat more rapidly. Abrupt drops can result in general malaise and fainting.
- Worsening of Pre-existing Conditions: the ongoing increase in temperatures can make health conditions worse for people who already have underlying health issues. Those with heart or blood vessel problems, lung diseases, metabolic disorders, and neurological conditions are especially vulnerable to the effects of extreme heat.

Figure 3 - Sustaibable Development Goals

Italy has adhered to the 2030 Agenda for Sustainable Development [41]. Sustainable Development Goal 11 aims to make cities safe, resilient, inclusive, and sustainable, thereby addressing climate change with a focus on microclimates. Specifically, Target 11.7 emphasizes the importance of reducing Urban Heat Islands (UHI).

Target 11.7 highlights that air pollution is no longer limited to just urban areas. It stresses the need to ensure everyone has access to safe, inclusive, and accessible public spaces, especially in cities. These spaces are crucial not only for helping to fight climate change, like reducing the urban heat island effect, but also for improving air quality and overall well-being. SDG 11 is closely connected to the concept of the microclimate. Achieving its goals - such as creating sustainable and resilient cities, improving urban infrastructure, and promoting green spaces - can positively influence the microclimate of urban areas. By considering microclimatic factors in urban planning and design, cities can enhance human comfort, reduce the urban heat island effect, mitigate climate change impacts, and foster sustainable development.

SDG 13 aims to take actions to combat climate change and its impacts: specifically, Target 13.2 aims to "integrate climate change measures into national policies, strategies and planning".

SDG 7 promote the access to affordable, reliable, sustainable and modern energy. Target 7.1 and 7.2 are the most coherent with the scope of this work, as they want to ensure affordable, reliable and modern energy services, and increase share of renewable energy in the global energy mix.

The following indicators can be used to quantify the issue and assess whether improvements have been made after implementation:

- 11.6.2: Annual average levels of fine particulate matter (PM2.5, PM10) in cities, weighted by population.
- 11.7.1: Average proportion of urban built-up areas that is designated as open space for public use, broken down by sex, age, and persons with disabilities.
- 11.a.1: Number of countries with national urban policies or regional development plans that address population dynamics, ensure balanced territorial development, and expand local fiscal capacity.
- 11.b.2: Proportion of local governments that adopt and implement disaster risk reduction strategies at the local level, in alignment with national disaster risk reduction frameworks.
- 13.1.3: Proportion of local governments that adopt and implement local disaster risk reduction strategies in line with national disaster risk reduction strategies.
- 13.b-1: Number of least developed countries and small island developing States with nationally determined contributions, long-term strategies, national adaptation plans and adaptation communications.

2 MATERIALS & METHODS

The Role Of Urban Pavement

Recent studies focus on the role of pavement surfaces in the Urban Heat Island effect. Asphalt is the most commonly used material for roads because it's practical, easy to maintain, quick to apply, and provides a smooth, comfortable surface for vehicles. However, it's also very sensitive to temperature changes. Asphalt absorbs a lot of heat from the sun, which can cause it to expand and contract, leading to cracks and damage over time.This occurs because asphalt accumulates thermal radiation from solar energy, leading to cracks and fractures in the pavement. The asphalt mixtures are affected by the viscoelastic behavior of the binder, which is sensitive to changes in temperature.
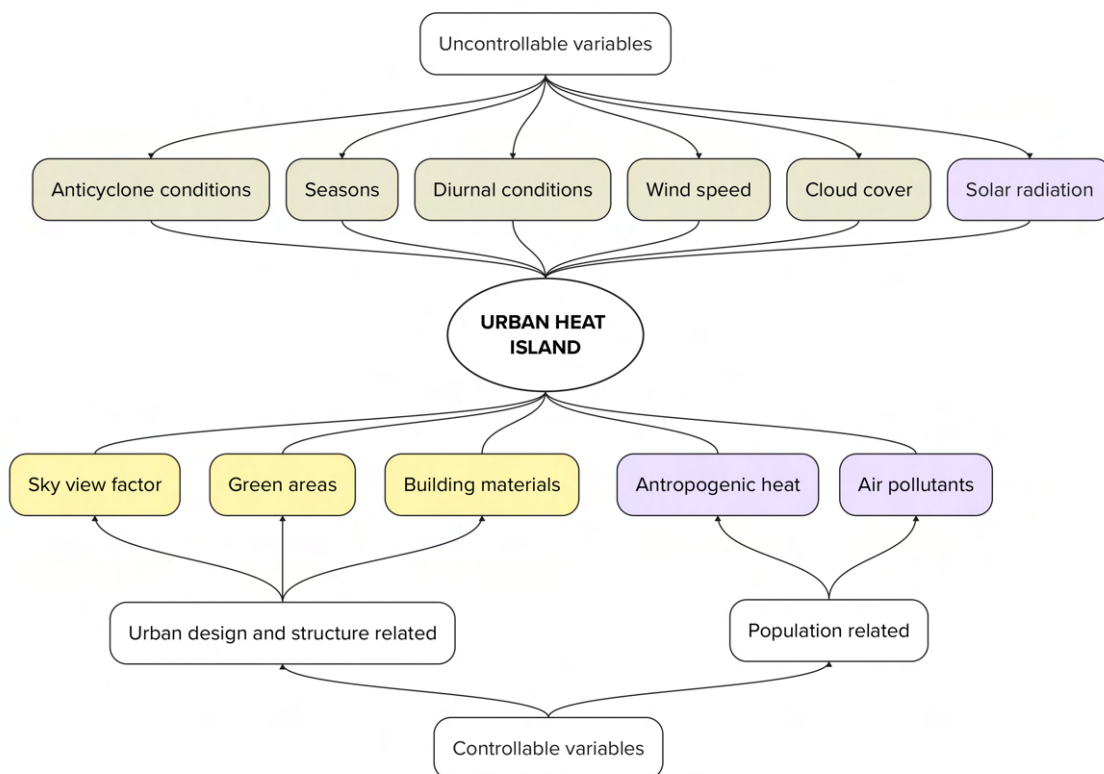
Figure 4 - Urban Heat Island's causes

As mentioned in Section 1, the causes of the Urban Heat Island (UHI) effect are numerous [37]. Figure 4 illustrates the connections between controllable and uncontrollable variables: the permanent effect variables are highlighted in yellow, the temporary effect variables in gray, and the cyclic effect variables in yellow.

It can be stated that modifications and increases in urban density are closely associated with changes in surface cover, as the expansion of urbanization necessitates an increase in built-up areas at the expense of green spaces. Surface temperatures, hydraulic, and thermal properties are strongly dependent on the type of cover: studies [1] indicate that vegetated surfaces with moist soil can reach 18°C under direct sunlight, while dark and impervious surfaces can reach temperatures as high as 88°C.

The heat exchange in asphalt pavements is significantly high, considering their thermal susceptibility; thus, the surrounding environment is consequently influenced by these pavements. For this reason, it can be asserted that a large portion of the Urban Heat Island effect is attributable to asphalt pavements.

• Heat exchange occurs through radiation, convection, and conduction in asphalt pavement [13]:

• Radiation: heat transfer occurs via electromagnetic waves;

• Convection: heat transfer due to fluid movement (observed between air and the asphalt pavement surface);

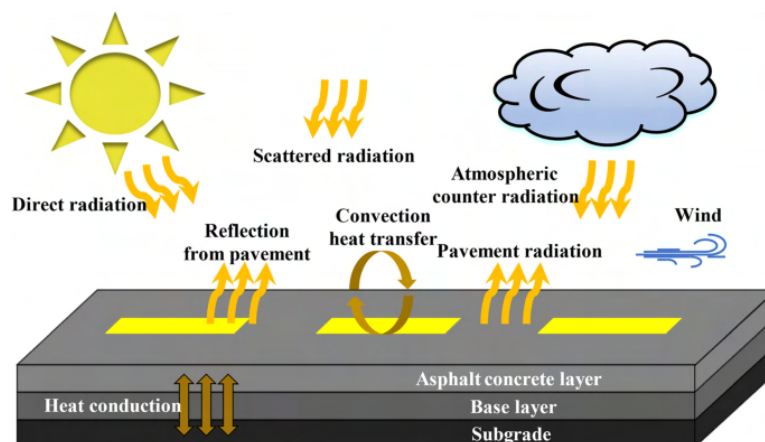• Conduction: heat transfer occurs between objects through direct contact.

Figure 5 - Heat transfer scheme in asphalt pavements

It should be emphasized that other parameters must also be considered: heat transfer in asphalt pavements is related to factors such as color, material conductivity, and surface texture. In conclusion, the physical properties of the material play an essential role in heat transfer.

Given the characteristics and effects of asphalt, studies and research have been conducted on pavements that could minimize the urban heat island effect: to date, studies suggest using construction materials that absorb less heat (such as reflective pavements) and that are characterized by high albedo. On average, roads cover 30% of urban areas [1], considering roads, parking lots, streets, and cycle paths.

"Cool pavements" are characterized by materials and methodologies that help keep the surfaces cooler. As a result, the use of these technologies can significantly reduce daily temperatures. There are various types of cool pavements, which can be divided into three main categories [27]:
• Porous/permeable (a): Their internal structure allows water to infiltrate through interconnected pores, reaching the lower layers;
• Interlocking (b): These can be permeable or non-permeable, created from precast blocks placed a few centimeters apart to allow water to pass through the gaps and infiltrate the natural soil;
• Concrete/plastic grid (c): Also known as "honeycomb," aggregates or natural soil are placed within the grid to permit water passage through the voids.
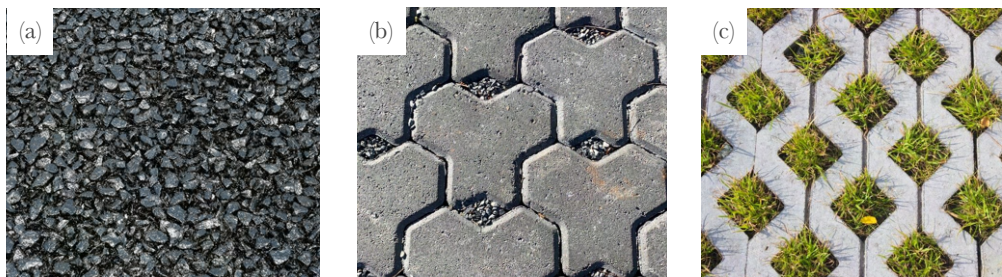

Figure 6 - (a) porous, (b) interlocking, (c) grid

These pavements offer various advantages, including the reduction of flooding risk (by decreasing surface runoff) and the mitigation of the Urban Heat Island (UHI) effect through evaporation.

To help lower surface temperatures, it's important to reduce the amount of heat absorbed by the ground. This can be done by increasing the albedo (the reflectivity of surfaces), improving how well pavements conduct heat, and encouraging evaporation, which helps cool the area.Albedo can be increased by applying layers of light-colored paint with high albedo on conventional pavements. Evaporation can be enhanced by increasing porosity and permeability, making the pavements more suitable for retaining water.

"Cool pavements" can also be further divided into three categories: reflective, evaporative, and thermally modified pavements [8].

Reflective Pavements

Reflective pavements are made by covering asphalt with a thin layer of light-colored material. These lighter materials help improve the surface's albedo, meaning they reflect more sunlight and absorb less heat. However, they're not always the most practical solution because producing these materials requires adjusting the mixture formulas, which can drive up construction costs. The use of light colors for painting and micro-coating can enhance reflection. However, this type may cause glare issues; to address this, non-white pigments with infrared reflectivity (rather than visible light reflectivity) are employed.

Surface roughness affects the reflectivity of pavements, but if surfaces are too smooth (and thus more reflective), they can negatively impact the skid resistance of asphalt pavements. Despite the significant benefits of this type of pavement, it is important to note that they are very costly and increase production expenses. Additionally, maintenance costs are also relatively high.

Evaporative pavements

Evaporative Pavements (also defined as "cool pavements with water existance") can retain water within their structure to reduce temperature. These pavements are utilized because they are permeable, porous, and directly evaporative. Pavements in this category can therefore retain water internally and consequently lower surface temperatures through the evaporation effect. However, it is important to consider that this type of pavement should be used where water runoff is available; otherwise, the result may have the opposite effect—warming the environment as it could have a higher surface temperature compared to conventional pavements.

The study by Higashiyama et al. (2016) looked at how different types of pavements affect the temperature of the surrounding environment. The findings showed that traditional asphalt pavements can reach temperatures over 60°C, while water-retaining pavements were about 10°C cooler. These water-retaining pavements not only help reduce heat but also help manage stormwater, making them a good solution for mitigating urban flooding.

Permeable pavements are characterized by a surface layer that allows water to flow through. In contrast, pervious pavements are not suitable for road construction, as water passes to the base course. Porous pavements are characterized by voids filled with grass or gravel, but they have a relatively negligible cooling effect.

Thermally modified pavements

The last type of pavement, thermally modified pavements, allows for the alteration of the thermal conductivity of asphalt pavements: in this case, the materials in the asphalt mixture are fundamental for thermal performance. Aggregates, binders, additives, and fillers are added to the mixture to modify the thermal properties of the asphalt. This is because conventional pavements attract and absorb more solar radiation during the summer and release more heat during the winter.

The thermal behavior of materials depends on the thermal properties associated with radiation, conduction, and convection, as well as properties related to thermodynamic equilibrium [40].

Material	Density [kg/m³]	Specific heat [J/gK]	Heat capacity [J/gK]	Thermal conductivity [W/mK]	Thermal diffusivity [m² s⁻¹]	Thermal admittance [W/m²K]
Asphalt	2.11	0.92	1.94	0.75	0.38	1205
Concrete	0.32	0.88	0.28	0.08	0.29	150
Stone	2.68	0.84	2.25	2.19	4.93	2220
Brick	1.83	0.75	1.37	0.83	0.61	1.65
Clay tiles	1.92	0.92	1.77	0.84	0.47	1220

Table 1 - materials and related features

The thermal balance is related to the amount of solar radiation absorbed and stored, the heat transferred to the air by convection, the heat conducted to the ground, and the heat stored within the material.

Thermal inertia refers to a material's ability to resist changes in temperature. It's the time it takes for a material to heat up or cool down after being exposed to a temperature change. In other words, materials with high thermal inertia take longer to reach a new temperature balance. Generally, construction materials, like concrete and asphalt, have a higher heat capacity than natural materials like trees and soil, meaning they can store more heat for longer periods.

[37] Busato F. et al (2014), Three years of study of the Urban Heat Island in Padua: Experimental results.

[13] Gartland L. (2008), Heat Islands: Understanding and Mitigating Heat in Urban Areas.

[1] Shamsaei M. et al (2022), A review on the heat transfer in asphalt pavements and urban heat island mitigation methods.

[27] Wardeh Y. et al (2022), Review of the optimization techniques for cool pavements solutions to mitigate Urban Heat Island.

[8] Kousis i. et al (2023), Evaluating the performance of cool pavements for urban heat island mitigation under realistic conditions: A systematic review and meta-analysis.

[40] Vujovic S. et al (2021), Urban Heat Island: Causes, Consequences, and Mitigation Measures with Emphasis on Reflective and Permeable Pavements

The role of albedo

Albedo is defined as the ratio of incident solar radiation to reflected radiation from a surface. Albedo is a non-dimensional quantity with values ranging from 0 to 1—where "0" corresponds to surfaces that fully absorb radiation, and "1" corresponds to surfaces that fully reflect radiation. In conclusion, a surface with low albedo will reflect less than a surface with high albedo.As previously summarized, cities are composed of combinations of these types of surfaces, with asphalt being the predominant material used for roads. Materials with low albedo tend to absorb a greater amount of radiation, resulting in higher land surface temperatures. By increasing the albedo of surfaces, it is possible to decrease surface temperatures and consequently reduce the Urban Heat Island effect, thereby improving thermal comfort and mitigating impacts on the environment and human health.

Regarding pavements, the transport of energy is related to albedo and emissivity. Albedo changes over time due to weather conditions, dirt accumulation, and material aging. A portion of energy is constantly retained and dissipated from the pavements to the atmosphere; this is referred to as emissive power [22].

Soil	Albedo	Emissivity	Soil	Albedo	Emissivity
Asphalt (old)	0,125	0,85	Roof	0,27	0,9
Asphalt (new)	0,05	0,95	Tile	0,225	0,9
Concrete	0,205	0,93	Tar roof	0,13	0,92
Brick	0.03	0,91	Forest	0,15	0,97
Stone	0,15	0,9	Water	0,5	0,97

Table 2 - albedo and emissivity for materials

Albedo and emissivity both play an important role in regulating surface temperatures. Pervious concrete pavements have lower reflectivity, thermal conductivity, and heat storage capacity, which means they absorb more heat compared to other materials. This can lead to higher temperatures on surfaces made from pervious concrete.
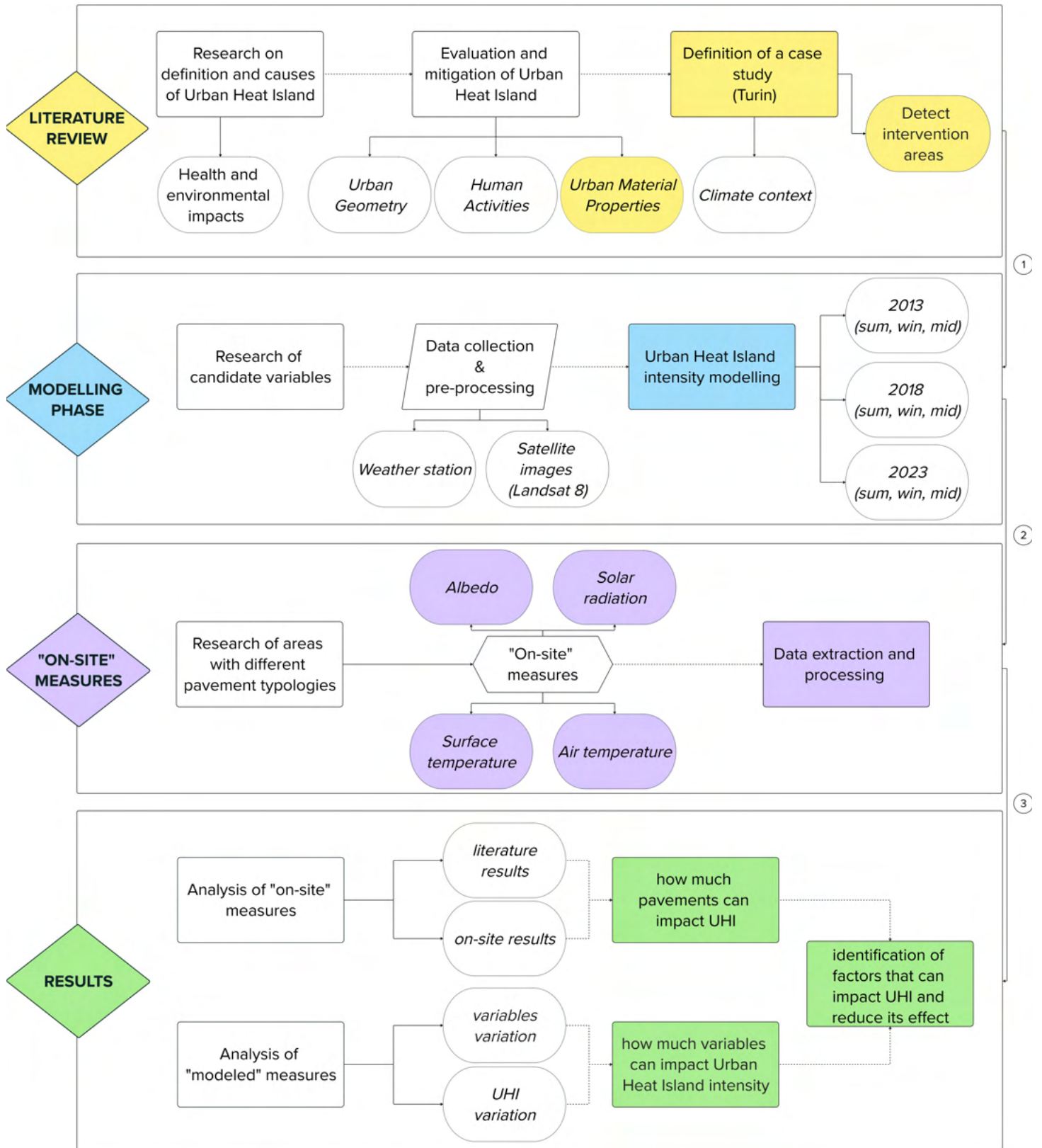
UHI analysis in Turin

As mentioned in the previous sections, the Urban Heat Island (UHI) effect primarily characterizes urban areas. This thesis will explore and define the UHI effect in the city of Turin, focusing on how pavements influence it.

In recent years, the city of Turin has undergone numerous changes, making it interesting to analyze the developments in how and to what extent the UHI phenomenon has evolved over time. The analysis will be structured along two main threads:

- Definition of the "status quo": the characteristics of Turin and its transformations will be examined. Starting with an analysis of the city's climate using data from weather stations, a picture of the historical and contemporary situation in Turin will be established. Candidate variables that define the city's characteristics, such as road coverage or the percentage of built-up areas, will then be identified. This step will help understand how and to what extent urban regeneration has impacted the UHI effect, as well as which regeneration efforts have been most effective in mitigating it;

- Research on mitigation strategies: based on the analyses conducted with the identified variables, it will be possible to establish and propose mitigation strategies to reduce the UHI effect. Solutions will be suggested both in light of the analytical results and in accordance with previously proposed solutions by the city.

The research aims to bring together data and analysis to address urban redevelopment challenges, with the goal of creating urban spaces that are resilient, comfortable, and sustainable.

Flowchart overview

3 PERFORM UHI ANALYSIS

Turin - understand climate context

A useful starting point for understanding climatic dynamics is the analysis of data from weather stations. This allows for the identification of factors such as seasonal variations, average temperatures, and climate patterns.

The first factor to be analyzed is temperature, focusing on the annual averages to understand seasonal climate variations between 2013 and 2023. The second factor is precipitation, looking at the average yearly rainfall and its distribution throughout the seasons. This helps identify the wettest and driest periods.

Understanding the climatic context is a necessary and fundamental step in defining the UHI effect and its impact on climate change in the area. This step also serves to identify seasonal variations and climate-related challenges.

The selected weather station for meteorological data is located at Via della Consolata 10, Turin. The reason for this selection is that it is situated in the city center, within a relatively dense urban context with a low percentage of green areas. Below is the location of the weather station and its details:
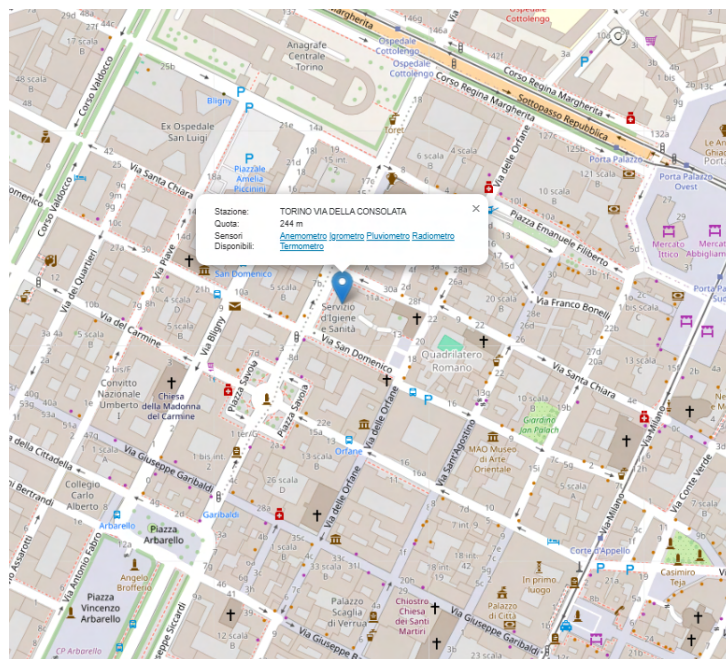
Figure 7 - Weather station localization: Via della Consolata - Torino

YEAR	J	F	M	A	M	J	J	A	S	O	N	D
2013	4,6	3,9	7,9	13,6	16,0	22,4	25,9	24,6	20,5	14,6	9,2	5,5
2014	5,7	7,1	12,0	15,6	17,9	22,7	22,6	22,2	20,1	16,2	10,6	6,3
2015	5,6	5,4	10,8	15,1	19,2	23,4	28,3	24,4	18,9	13,6	9,8	6,4
2016	5,1	7,2	10,0	14,9	17,1	22,0	25,5	24,7	22,0	13,5	9,6	5,5
2017	2,9	6,9	12,9	15,1	19,4	24,9	25,6	25,7	19,0	15,8	8,7	3,1
2018	6,5	4,0	7,9	16,2	18,5	23,7	26,0	25,9	21,7	15,7	9,7	4,9
2019	4,0	7,6	12,1	13,5	15,9	24,4	26,0	24,8	20,3	15,7	8,8	6,7
2020	4,3	9,4	9,8	15,0	19,0	21,0	24,9	25,0	20,8	13,3	9,9	5,1
2021	3,9	8,0	10,9	12,6	16,9	23,7	24,3	24,3	21,5	14,2	8,8	4,8
2022	4,8	8,2	9,6	14,1	20,5	25,4	28,0	25,9	20,4	17,8	10,1	4,6
2023	5,7	7,6	12,1	14,4	17,5	23,1	26,0	25,7	21,8	17,5	9,3	7,0
Mean	4,8	6,8	10,5	14,6	18,0	23,3	25,7	24,8	20,6	15,3	9,5	5,4
Std	1,0	1,7	1,7	1,0	1,5	1,3	1,6	1,1	1,1	1,6	0,6	1,1
Std +	5,9	8,6	12,2	15,6	19,5	24,6	27,3	25,9	21,7	16,8	10,1	6,6
Std -	3,8	5,1	8,9	13,5	16,5	22,0	24,2	23,8	19,6	13,7	8,9	4,3

Table 3 - Mean monthly temperature 2013 - 2023 [°C]

YEAR	J	F	M	A	M	J	J	A	S	O	N	D
2013	J	F	M	A	M	J	J	A	S	O	N	D
2014	5,2	7,3	9,7	11,9	17,6	20,3	20,4	19,2	13,6	6,2	5,6	5,4
2015	4,5	6,5	12,8	14,9	18,2	19,0	17,4	15,7	12,7	7,8	4,6	3,8
2016	5,5	7,3	11,4	16,9	17,4	19,4	20,6	16,9	13,3	8,0	6,8	4,6
2017	5,6	6,4	12,6	15,8	17,2	19,0	20,6	19,6	14,3	8,2	5,1	5,1
2018	5,7	6,4	12,1	17,0	19,3	21,3	21,5	18,7	14,1	9,7	5,9	5,3
2019	5,3	6,3	9,5	14,8	15,1	20,7	20,8	17,9	15,1	9,3	3,7	5,2
2020	6,7	10,5	16,9	16,2	19,4	23,4	22,8	17,9	14,7	8,4	4,5	4,9
2021	6,6	10,3	11,6	18,9	21,0	21,2	22,6	20,0	15,2	8,6	6,0	3,8
2022	6,2	8,4	15,1	17,0	21,4	22,7	20,9	20,7	14,9	10,1	5,3	5,5
2023	7,0	10,4	13,1	18,5	19,7	23,0	25,3	21,1	15,6	9,4	6,5	4,6
Mean	5,8	8,1	12,7	16,5	18,5	21,0	21,4	19,0	14,4	8,7	5,6	4,8
Std	0,8	1,7	2,3	2,1	1,9	1,6	2,0	1,8	0,9	1,1	1,0	0,6
Std +	6,6	9,8	14,9	18,6	20,4	22,5	23,3	20,7	15,3	9,8	6,6	5,4
Std -	5,0	6,4	10,4	14,3	16,6	19,4	19,4	17,2	13,5	7,5	4,5	4,2

Table 4 - Mean monthly solar irradiance 2013 - 2023 [W/m²]

The tables present the average temperatures and solar irradiance, expressed respectively in degrees Celsius and W/m2. The statistical values have been utilized to create the climograph. The following graph - a climograph - combines the precipitation and temperature data into a single visualization. The selected data spans from 2013 to 2023:
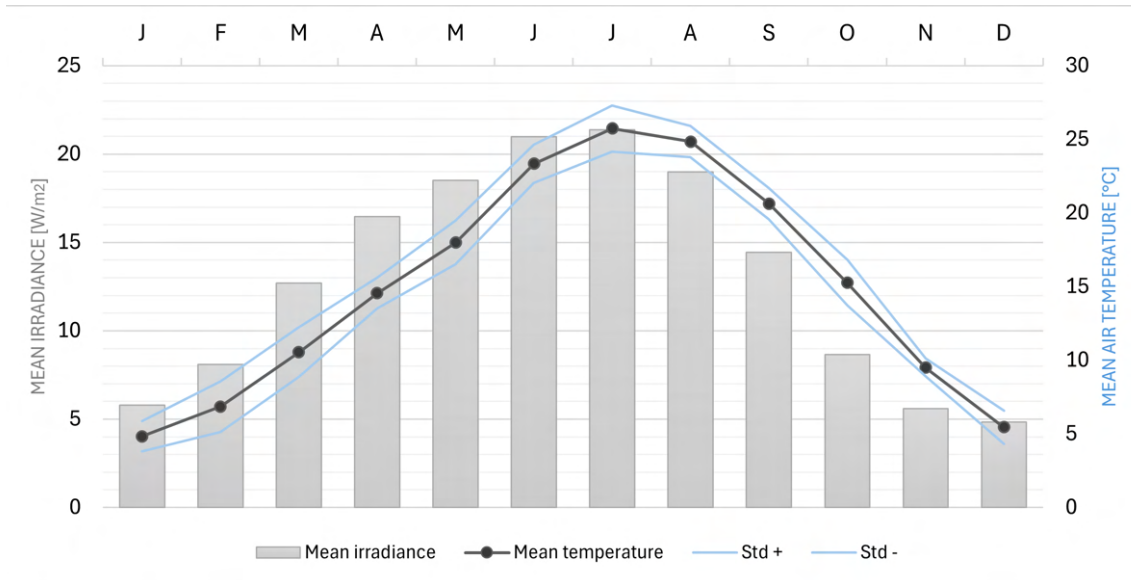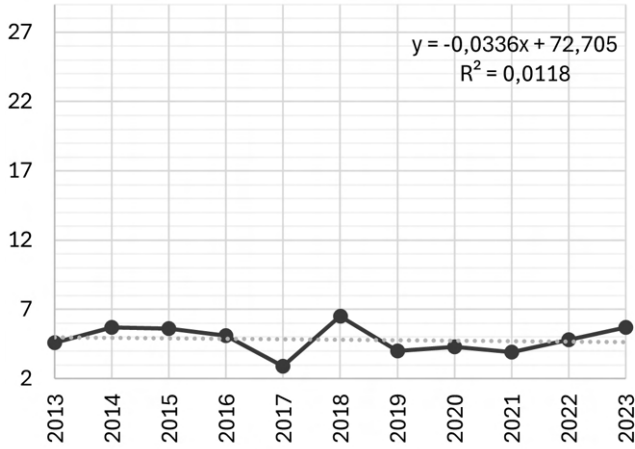

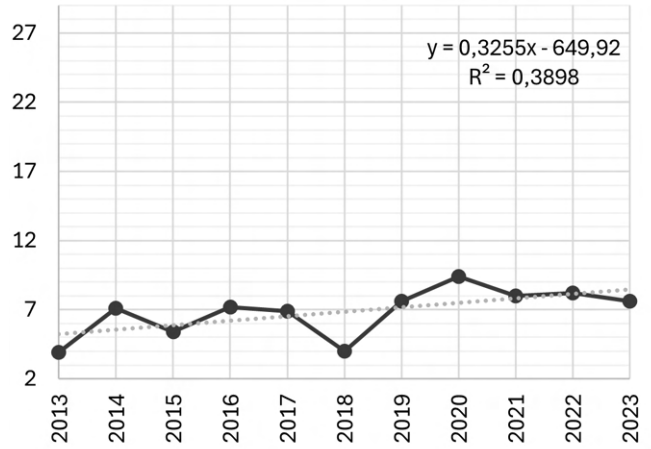Graph 1 - Climograph (temperature and precipitation)

The graph clearly illustrates the patterns of temperature and solar irradiance during the selected period, serving as a useful starting point for subsequent analyses by calculating trends over the study years.

Given that this thesis focuses on the influence of pavements, trends in temperature and global radiation will be analyzed. To calculate these trends, a monthly graph was created with average temperature/irradiance data along with a trend line. The trend was calculated by considering the monthly averages for each year multiplied by the angular coefficient of the corresponding graph equation.

January
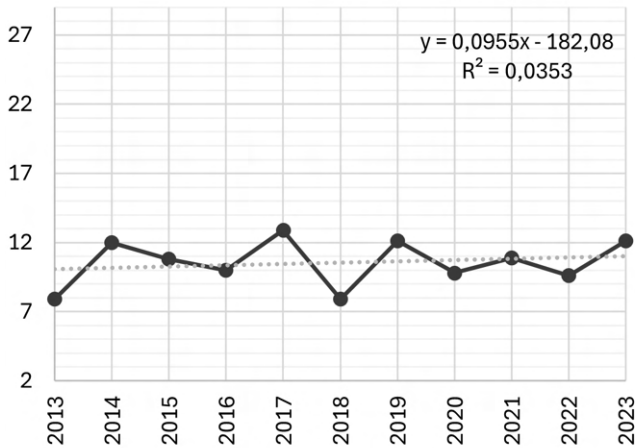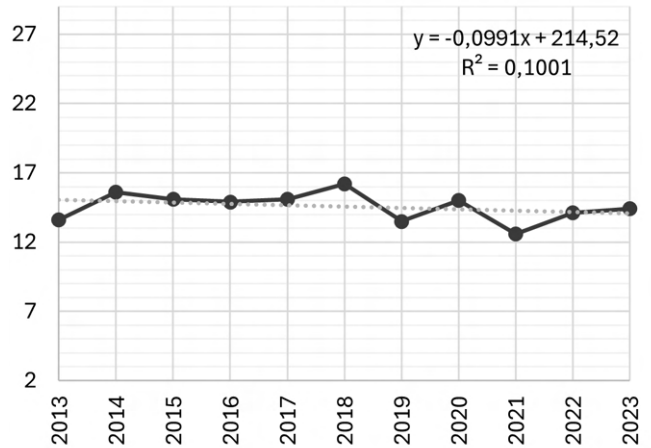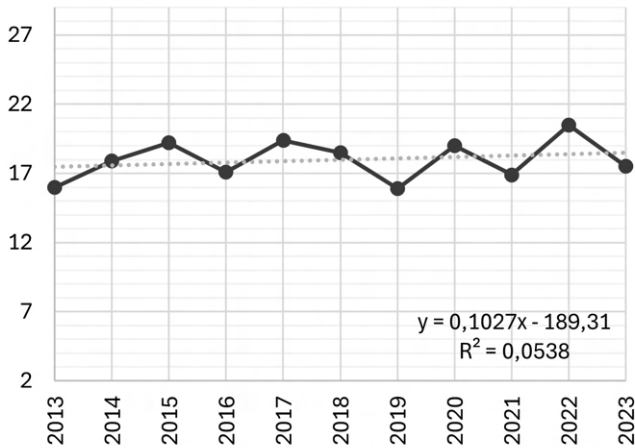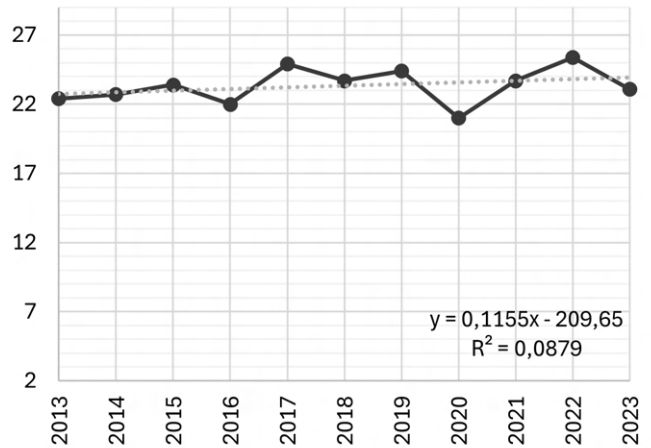
y = -0,0336x + 72,705
R² = 0,0118

February

y = 0,3255x - 649,92
R² = 0,3898

March

y = 0,0955x - 182,08
R² = 0,0353

April

y = -0,0991x + 214,52
R² = 0,1001

May

y = 0,1027x - 189,31
R² = 0,0538

June

y = 0,1155x - 209,65
R² = 0,0879

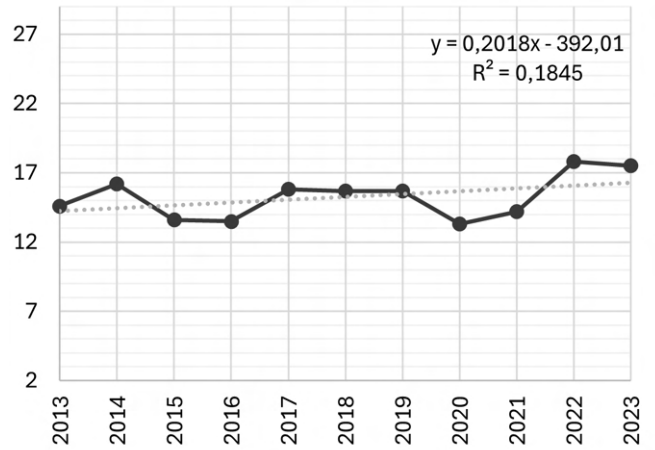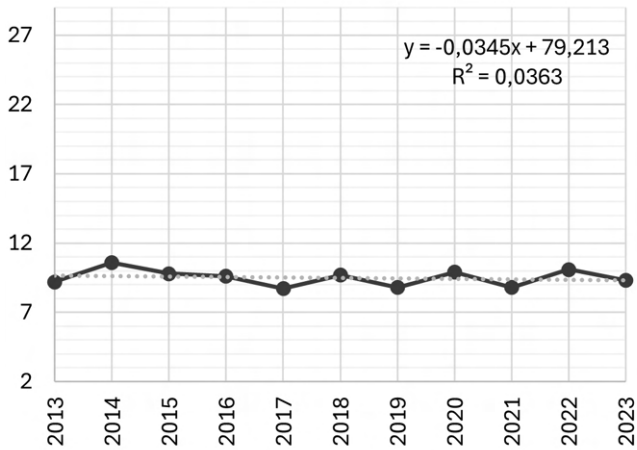Graph 2 - Temperature trends 2013 - 2023 (from January to June)

July

y = 0,0845x - 144,88
R^2 = 0,032

August

y = 0,1791x - 336,57
R^2 = 0,3126

September

y = 0,1309x - 243,54
R^2 = 0,167

October

y = 0,2018x - 392,01
R^2 = 0,1845

November

y = -0,0345x + 79,213
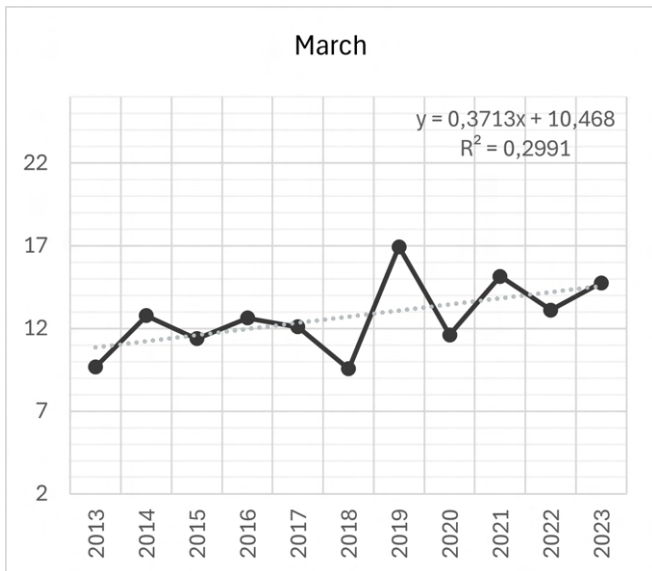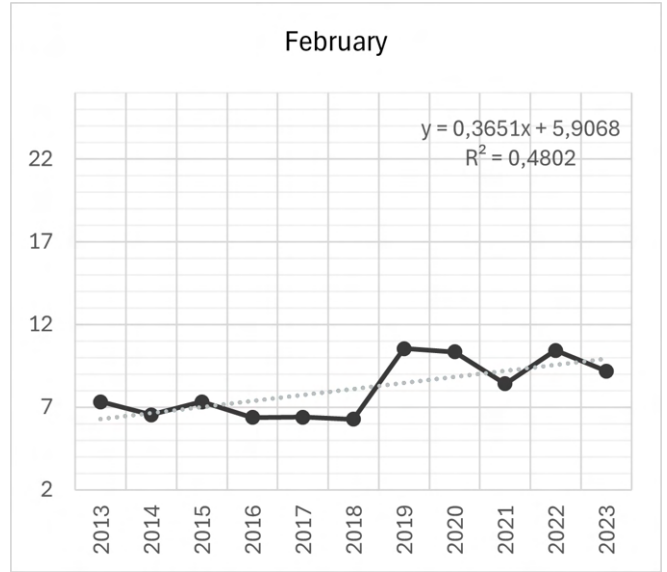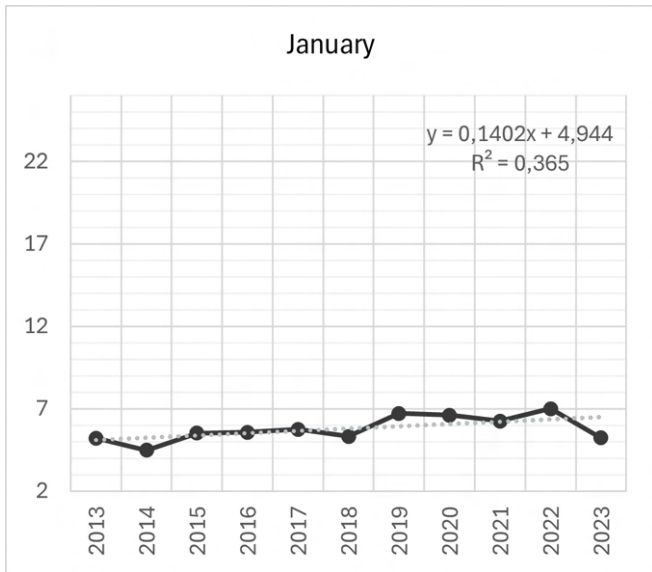R^2 = 0,0363

December

y = -0,0118x + 29,295
R^2 = 0,0012
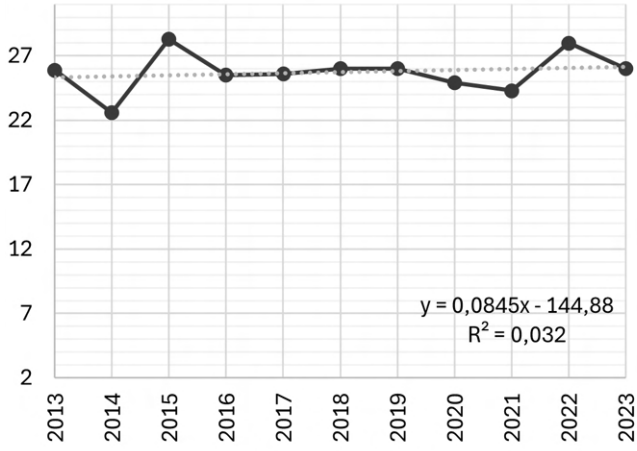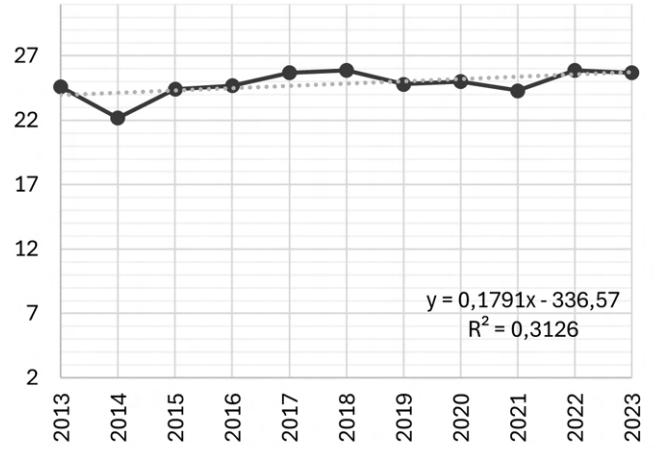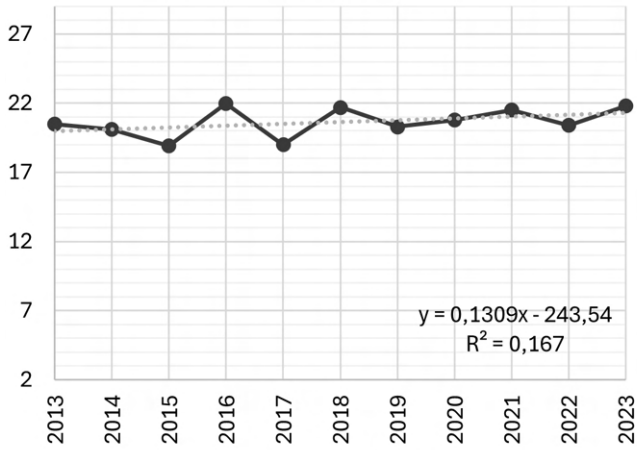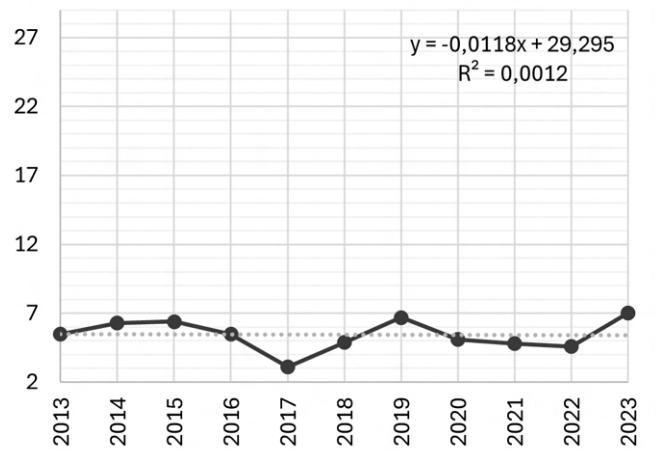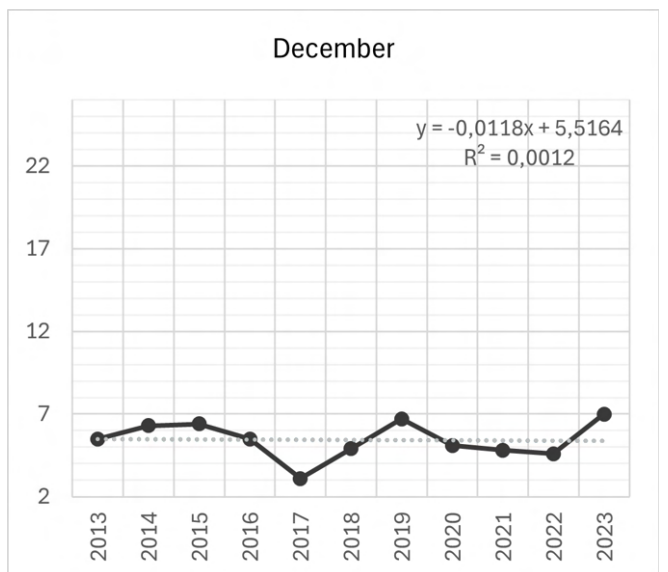
Graph 3 - Temperature trends 2013 - 2023 (from July to December)
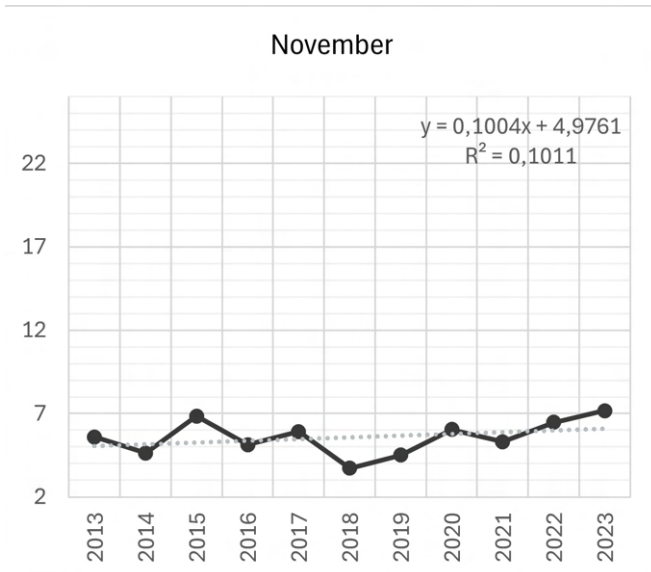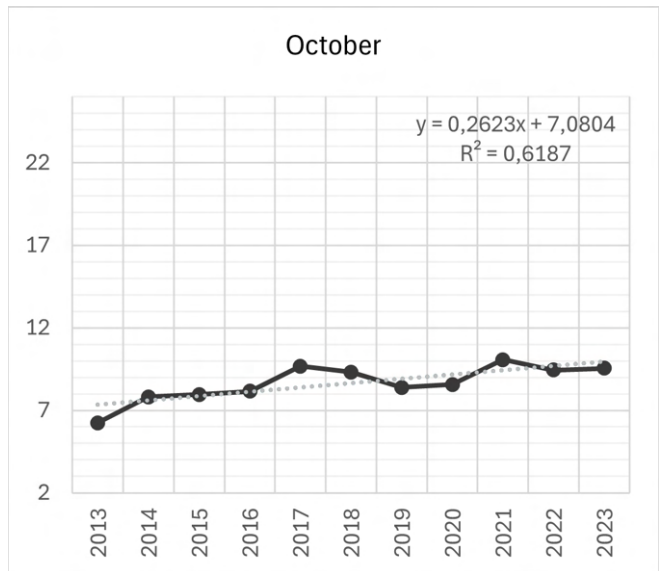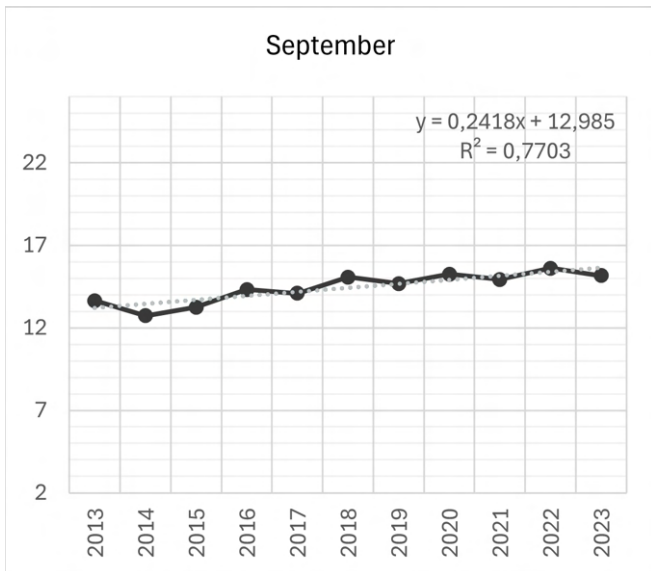
	J	F	M	A	M	J	J	A	S	O	N	D
Mean temperature 2013-2023 [°C]	4,8	6,8	10,5	14,6	18,0	23,3	25,7	24,8	20,6	15,3	9,5	5,4
Trend (from graphs)	0,1518	0,439	0,0143	0,0609	0,0008	0,1564	0,0538	0,1174	0,0715	0,2607	0,0089	0,0854
Calculated trend	0,733	3,005	0,151	0,886	0,014	3,650	1,385	2,916	1,476	3,979	0,085	0,465
Average trend 2013-2023	1,562											

Table 5 - Temperature trends

The temperature data from 2013 to 2023 provide insights into the climatic dynamics of the city. The calculated trend, equal to 1.562, indicates a gradual increase in average temperatures. This leads to a warming trend: Turin has experienced a rise in average temperatures over the selected decade, reinforcing the theme of climate change. This effect has a significant impact on the ecosystem, making it essential to consider these results in order to propose adaptation solutions and develop resilient strategies.
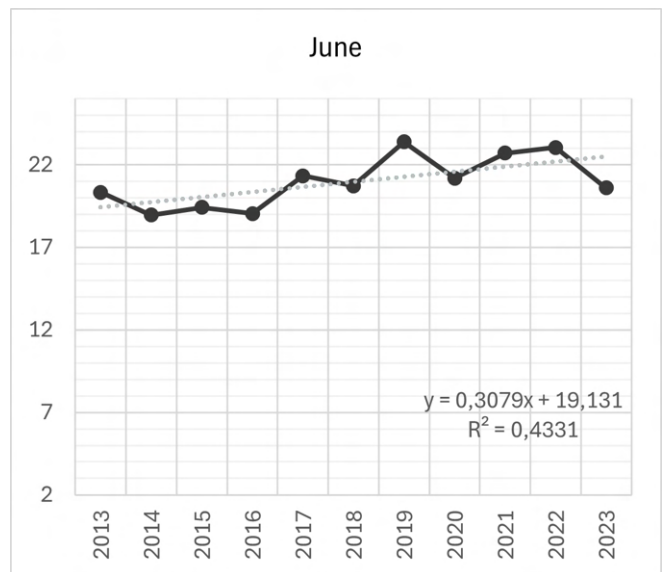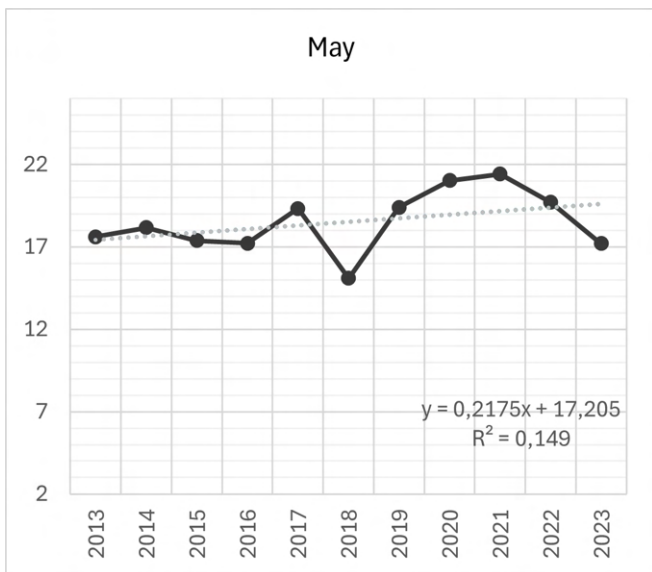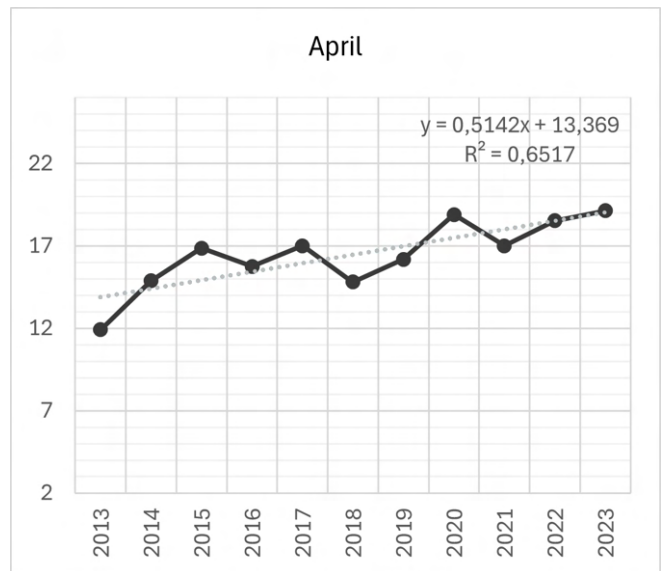
January

y = 0,1402x + 4,944
R² = 0,365

February

y = 0,3651x + 5,9068
R² = 0,4802

March

y = 0,3713x + 10,468
R² = 0,2991

April

y = 0,5142x + 13,369
R² = 0,6517

May

y = 0,2175x + 17,205
R² = 0,149

June

y = 0,3079x + 19,131
R² = 0,4331

Graph 4 - Irradiance trends 2013 - 2023 (from January to June)

July

$$y = 0{,}4312x + 18{,}788$$
$$R^2 = 0{,}5298$$

August

$$y = 0{,}3886x + 16{,}64$$
$$R^2 = 0{,}541$$

September

$$y = 0{,}2418x + 12{,}985$$
$$R^2 = 0{,}7703$$

October

$$y = 0{,}2623x + 7{,}0804$$
$$R^2 = 0{,}6187$$

November

$$y = 0{,}1004x + 4{,}9761$$
$$R^2 = 0{,}1011$$

December

$$y = -0{,}0118x + 5{,}5164$$
$$R^2 = 0{,}0012$$
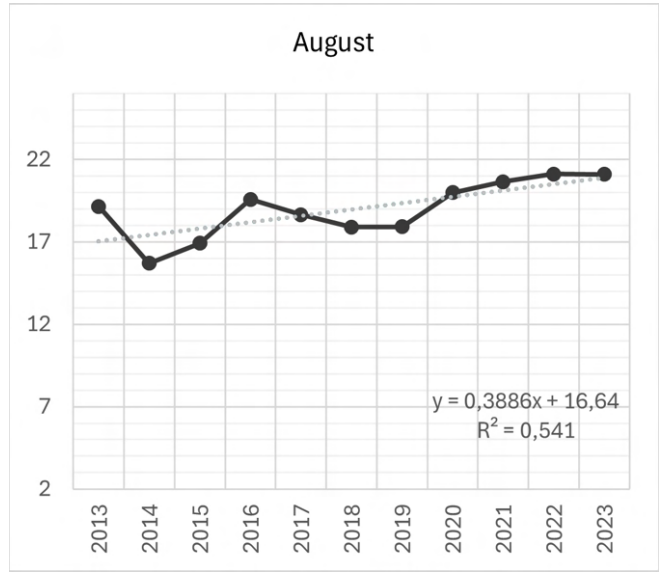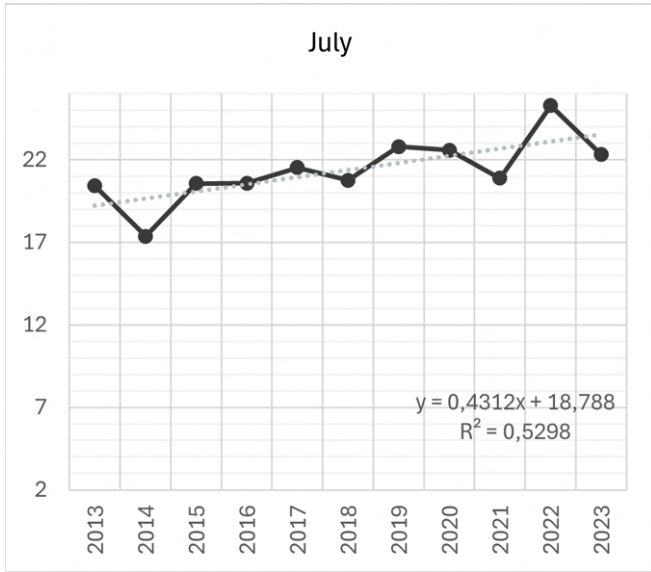
Graph 5 - Irrandiace trends 2013 - 2023 (from July to December)

|	J	F	M	A	M	J	J	A	S	O	N	D
Mean solar radiation 2013-2023 [°C]	5,8	8,1	12,7	16,5	18,5	21,0	21,4	19,0	14,4	8,7	5,6	4,8
Trend (from graphs)	0,3344	0,1819	0,1895	0,2088	0,0013	0,4464	0,1798	0,1315	0,2298	0,0951	0,0363	0,0854
Calculated trend	1,935	1,473	2,406	3,436	0,024	9,365	3,843	2,495	3,317	0,823	0,203	0,412
Average trend 2013-2023	2,478											

Table 6 - Irradiance trends [MJ/m²]

Analyzing the monthly trend of global irradiance, it is evident that this trend is also on the rise, with a value of 2,478. This outcome may be attributed to a more permeable atmosphere, allowing greater radiation to reach the Earth's surface. Certainly, regulations regarding anthropogenic emissions have played a role, but another possible factor could be the reduction in cloud cover. The impact of atmospheric conditions and the decrease in pollution is thus significant.

However, it is important to highlight that this also has negative implications, as atmospheric transparency can accelerate climate warming.

Turin - interventions in urban context

The city of Turin is currently experiencing and has undergone numerous changes and modifications to its pavements as a result of the Piano Nazionale di Ripresa e Resilienza, along with funding from national and European Union sources [b].

<u>Soil maintenance and pedestrian access at Borgo Dora</u> *(in progress)*
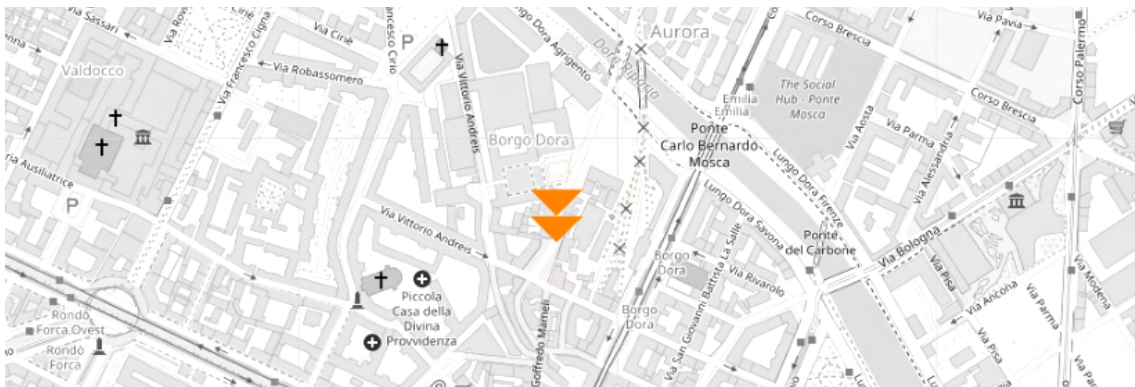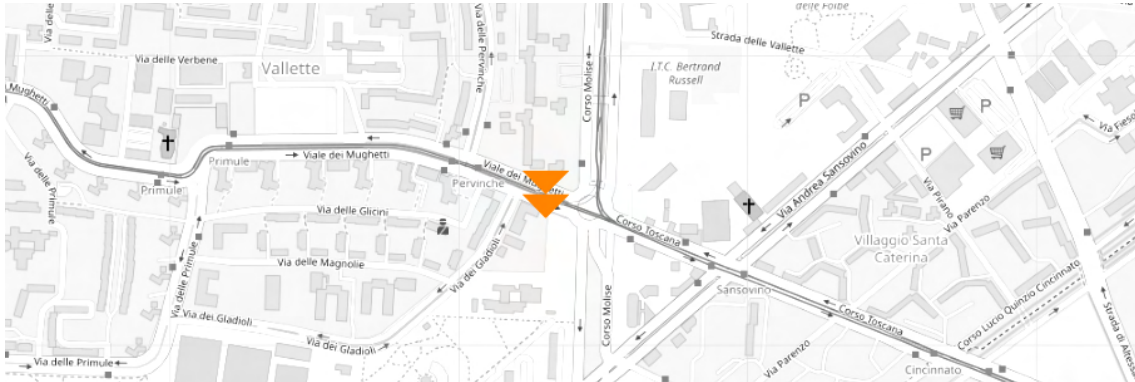

The aim of the initiative is to standardize the improvement of conditions between Piazza della Repubblica, Via Cigna, the Dora Riparia, and Corso XI Febbraio. Solutions that promote greater soil permeability will be adopted, including the use of traditional stone materials.

<u>Don Gnocchi garden</u> (*concluded*)
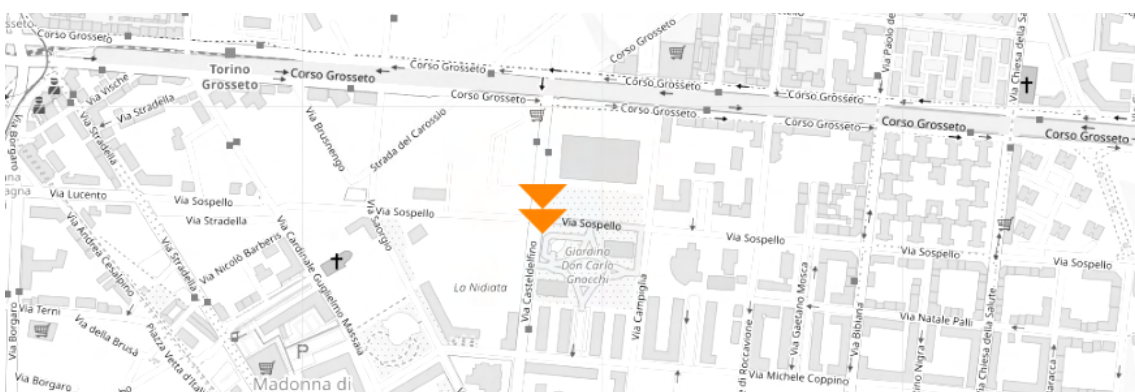
Among all the planned interventions in the Don Gnocchi Garden, measures aimed at increasing soil permeability and the planting of new trees are included.

<u>Corso Marconi</u> (*concluded*)

New pavements have been installed in the boulevard between Via Madama Cristina and Corso Massimo D'Azeglio, along with the addition of two tree-lined sidewalks. The degraded roadway surface has been replaced with permeable pavements.

<u>Livable Valdocco</u> (*concluded*)

The project includes the refurbishment of intersections and parking areas, incorporating green spaces where possible to capture rainwater and mitigate runoff during intense precipitation events.

Soil in Vallette (*in progress*)

The interventions include the installation of sound-absorbing mats on Viale dei Mughetti, modifications to parking areas through the removal of asphalt and the installation of permeable interlocking pavers (aimed at increasing permeability and reducing heat release), as well as the reconstruction of sidewalks using permeable materials with high albedo.

Livable Via Stradella (*concluded*)
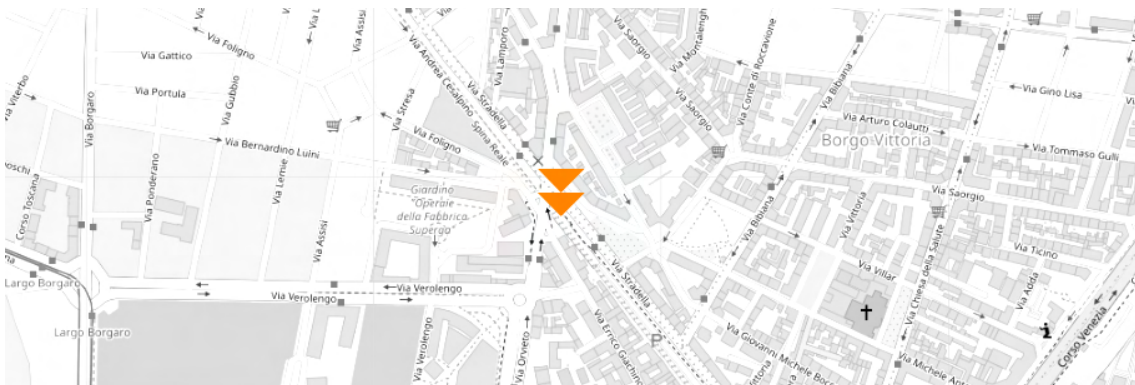
Improvement of the former Turin-Ceres railway, the intervention involves the redevelopment of the parking surface with the planting of trees (ensuring shading) and the replacement of asphalt with cool materials. The new drainage system is designed to prevent flooding during intense precipitation events.

<u>Permeable surfaces on the northern tramway line 4</u> (*concluded*)
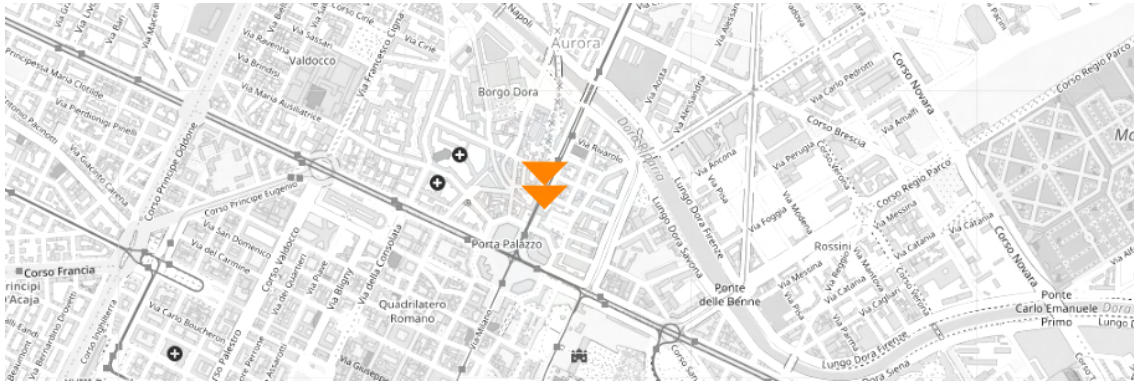
In a 500-meter section of line 4 (north), the asphalt has been removed and a drainage system has been installed for water management, along with a green surface. The result is a replacement of the impermeable and warm surface, facilitating a reduction in the heat island effect, increased permeability, and lower maintenance costs.

<u>Redevelopment Corso Belgio</u> (*in progress*)
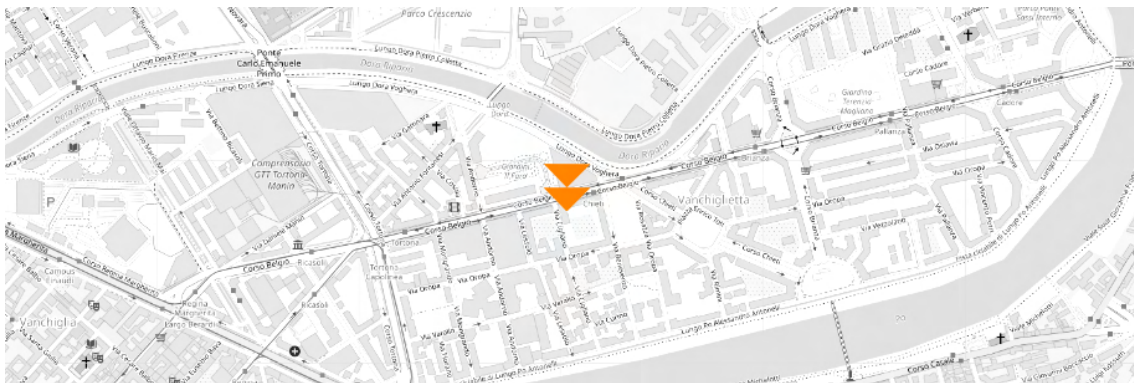
The project involves replacing the existing trees with new ones to ensure proper canopy development. The new row of trees will be aligned at the center of the sidewalk to avoid interference with the tram line. The sidewalks will feature drainage planters and the restoration of the parking surface.

Madre Teresa di Calcutta Garden (*concluded*)

The garden will be expanded, and new structures will be installed. Additionally, there will be planting of trees and the installation of new permeable pavements.

Valentino Park (*in progress*)

Various interventions are planned throughout the park. These include the restoration of park components, the planting of tree-lined areas, the rehabilitation of the banks, the resizing of certain pathways to increase green spaces, and the replacement of asphalt with permeable pavements.

The municipality has also planned to renovate public transportation shelters, including replacing the asphalt paving with more permeable materials to help reduce surface heat and improve water drainage.

Additionally, the planting of trees is proposed for re-naturalization, aimed at increasing CO_2 capture and providing shade.

Finally, the redevelopment of play areas has been proposed to mitigate climate vulnerability through planting and the renovation of permeable pavements to enhance the soil's absorptive capacity.

Intervention	Investment	Requalified Soil [m²]	CO₂ Saved [t/year]	PM10 Not Emitted [kg/year]	Expected Completion Date
Soil Maintenance Borgo Dora	€2.4 million	65,750			2025
Don Gnocchi Garden	€6.5 million	23,660	10.03	25	Completed
Corso Marconi	€1.2 million		23.36	4.06	Completed
Livable Valdocco	€3.5 million				Completed
Soil at Vallette	€2 million	119,000			2025
More Livable Via Stradella	€1 million	6,000	7.08	23	Completed
Tram Network North Line 4	€1 million	300	7.08	23	Completed
Redevelopment of Corso Belgio		15,000			2024
Mother Teresa of Calcutta Garden	€6.5 million	7,500	10.03	25	Completed
Valentino Park	€13 million	300,000	139.16	305	2025
Public Transport Stops	€1 million		7.08	23	Completed
Tree and Shrub Planting	€1 million				2027
Climate-Proof Play Areas	€1.5 million				2027

Table 7 - Summary interventions, "*Torino Cambia*"

4 ENVIRONMENTAL VARIABLES

Data collection and processing

Landsat-8, launched in February 2013, is equipped with two onboard sensors: the Operational Land Imager (OLI), which measures in the visible, near-infrared, and shortwave infrared spectra, and the Thermal Infrared Sensor (TIRS), which measures land surface temperature in thermal bands.

Band	Wavelenght [μm]	Resolution [m]
Coastal Aerosol (1)	0,43 - 0,45	30
Blue (2)	0,45 - 0,51	30
Green (3)	0,53 - 0,59	30
Red (4)	0,64 - 0,67	30
NIR (5)	0,85 - 0,88	30
SWIR 1 (6)	1,57 - 1,65	30
SWIR 2 (7)	2,11 - 2,29	30
PAN (8)	0,50 - 0,68	15
Cirrus (9)	1,36 - 1,38	30
TIRS 1 (10)	10,6 - 11,19	100
TIRS 2 (11)	11,5 - 12,51	100

Table 8 - Landsat8 OLI and TIRS

Multispectral satellite images of the city of Turin were obtained through the EarthExplorer geoplatform service of the United States Geological Survey (USGS).

For the preprocessing of the Landsat images, has been used the "Semi-Automatic Classification Plugin (SCP)" in QGIS. This tool helps with radiometric calibration, geometric correction, and atmospheric correction to ensure the images are accurate and ready for analysis.

Satellite images were selected using a methodology related to the previous climatic analyses. "Typical days" were identified within the patterns of seasonal temperatures. Below are the climatic data for the selected days:

Seasonality	2013		2018		2023	
	Day	Air temperature [°C]	Day	Air temperature [°C]	Day	Air temperature [°C]
Winter	28/11	-0,8	11/2	1,6	10/2	-1,9
Mid – season	18/4	21,3	25/4	21,7	24/5	19,7
Summer	1/8	32,3	6/8	34,9	21/8	35,9

Table 9 - Landsat8 image selection

Specifically, the details for each selected image are provided below. The years under analysis are 2013, 2018, and 2023.

Landsat product ID	LC08_L1TP_195029_20131128_20200912_02_T1
Date acquired	2013/11/28
Scene time (start/stop)	10:18:39 / 10:19:11
Cloud cover	5.20
Grid Cell Size Reflective/Thermal	30

Landsat product ID	LC08_L1TP_195029_20130418_20200912_02_T1
Date acquired	2013/04/18
Scene time (start/stop)	10:18:51 / 10:19:21
Cloud cover	4,32
Grid Cell Size Reflective/Thermal	30

Landsat product ID	LC08_L1TP_194029_20130801_20200912_02_T1
Date acquired	2013/08/01
Scene time (start/stop)	10:12:51 / 10:13:23
Cloud cover	1.78
Grid Cell Size Reflective/Thermal	30

Landsat product ID	LC08_L1TP_195029_20180211_20200902_02_T1
Date acquired	2018/02/11
Scene time (start/stop)	10:16:52 / 10:17:23
Cloud cover	22.91
Grid Cell Size Reflective/Thermal	30

Landsat product ID	LC08_L1TP_194029_20180425_20200901_02_T1
Date acquired	2018/04/25
Scene time (start/stop)	10:10:04 / 10:10:36
Cloud cover	14.09
Grid Cell Size Reflective/Thermal	30

Landsat product ID	LC08_L1TP_195029_20180806_20200831_02_T1
Date acquired	2018/08/06
Scene time (start/stop)	10:16:23 / 10:16:55
Cloud cover	24.32
Grid Cell Size Reflective/Thermal	30

Landsat product ID	LC09_L1TP_194029_20230210_20230310_02_T1
Date acquired	2023/02/10
Scene time (start/stop)	10:11:22 / 10:11:53
Cloud cover	1.84
Grid Cell Size Reflective/Thermal	30

Landsat product ID	LC09_L1TP_195029_20230524_20230601_02_T1
Date acquired	2023/05/24
Scene time (start/stop)	10:16:30 / 10:17:02
Cloud cover	39.05
Grid Cell Size Reflective/Thermal	30

Landsat product ID	LC09_L1TP_194029_20230821_20230823_02_T1
Date acquired	2023/08/21
Scene time (start/stop)	10:10:41 / 10:11:12
Cloud cover	1.49
Grid Cell Size Reflective/Thermal	30

Land cover variables

The study and analysis of land cover allows for the identification and differentiation of various types. As previously mentioned, types of land cover concrete, vegetation, open spaces, and asphalt play a significant role in the urban heat island effect. Thus, evaluating land uses facilitates the assessment of how different areas contribute to heat generation and absorption.

The fractional roof cover enables the examination of the relationship between "paved" roof areas and the overall area of the city:

Asphalt area (m²)	Metropolitan area (m²)	Fractional roof cover (%)
26422378,63	130378112,5	20,3%

Table 10 - Fractional Roof Cover

The data used for the analyses were downloaded from the Copernicus Land Monitoring Service, the European model proposed by EAGLE. The land cover Piemonte model was enhanced with information from the regional Piedmont database (BDTRE 2023), satellite images, and cadastral maps.

The categories, defined based on the BDTRE, are quantified below in relation to the total area of the city:

Category	Total area [m²]	Fractional soil cover [%]
Residential	11990869,86	9,2%
Industrial	6521742,16	5%
Commercial and services	7909766,61	6,1%
Paved roads and related areas	45214814,54	34,7%
Resource extraction and waste disposal	1043801,79	0,8%
Urban green	27600517,92	21,2%
Agricultural	7841587,43	6%
Forest	15828942,76	12,1%
Grazing	2738534,77	2,1%
Water	3687534,65	2,8%
TOTAL [m²]	130378112,5	

Table 11 - Fractional Soil Cover

For a more immediate visualization, a chart has been created to display the percentage of each category with respect to the total metropolitan area:
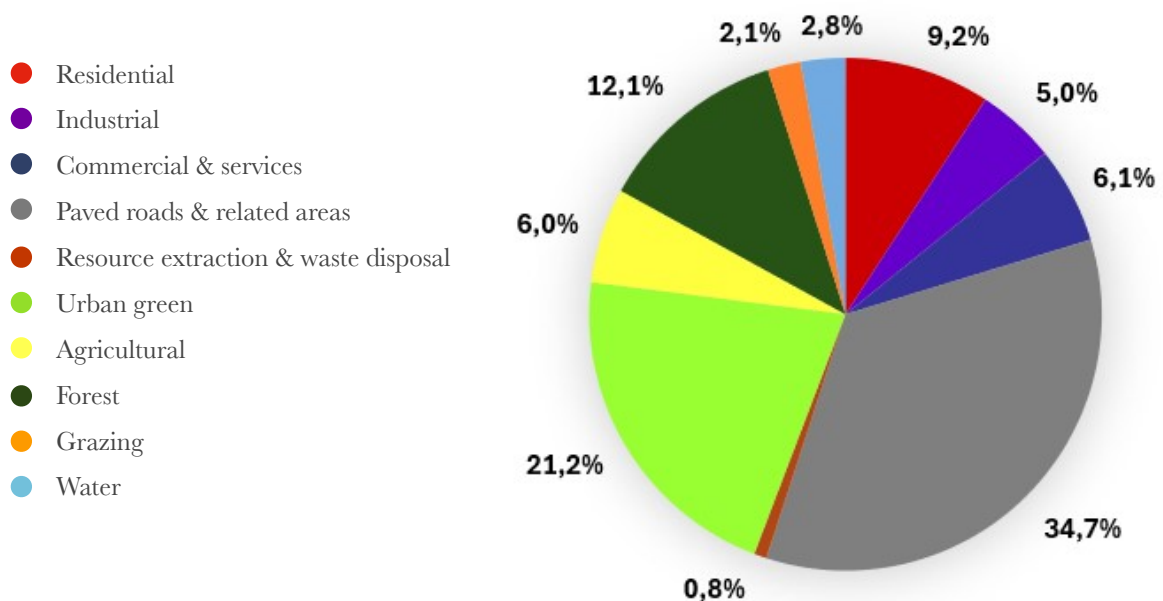
Graph 6 - Percentage of use of soil in Turin
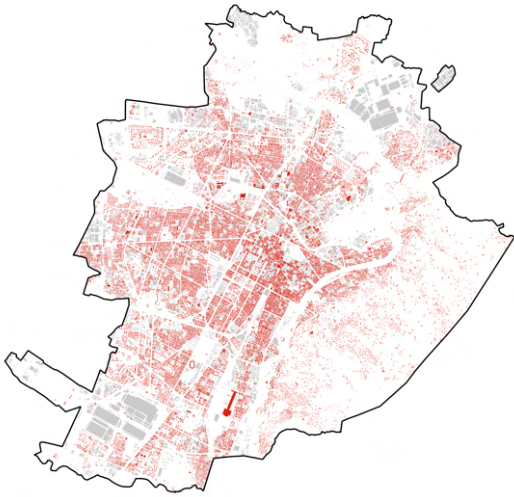
Figure 8 - Residential
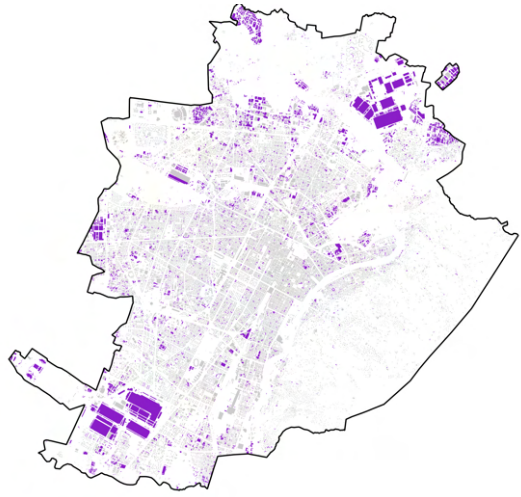
Figure 9 - Industrial
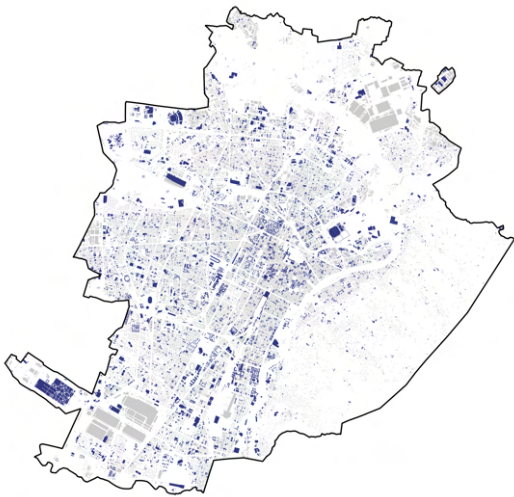
Figure 10 - Commercial and services

Figure 11 - Paved roads and related areas
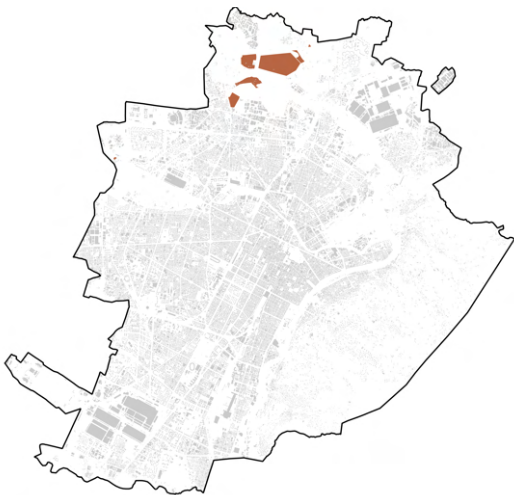
Figure 12 - Resource extraction and waste disposal
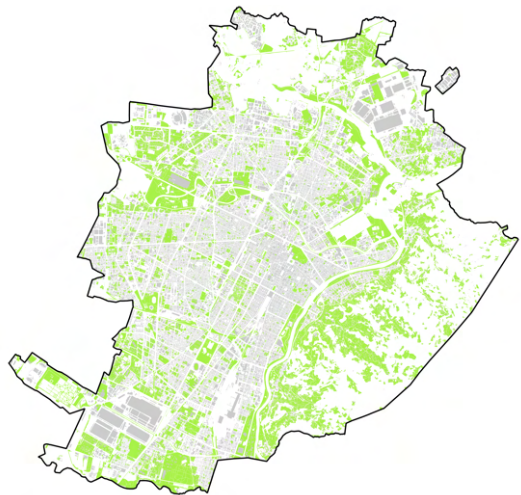
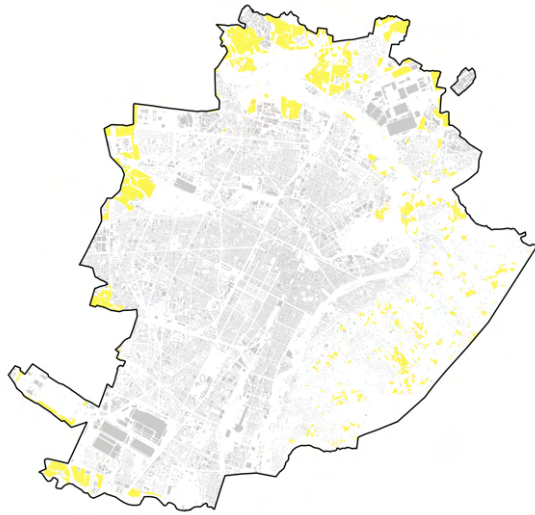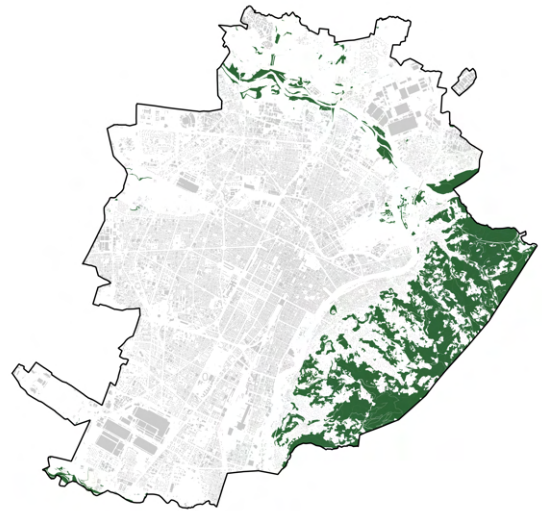Figure 13 - Urban green

44

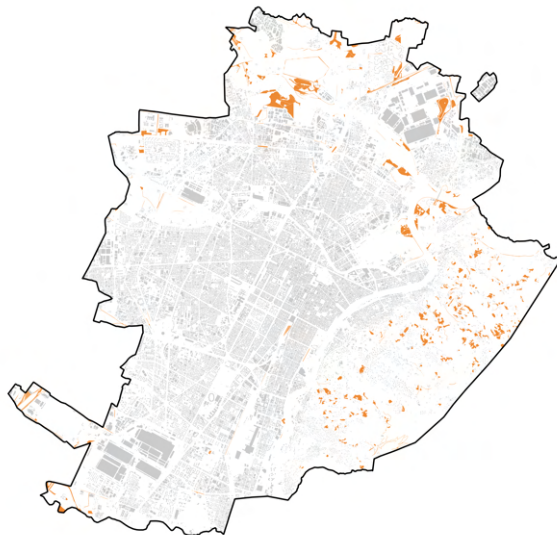Figure 14 - Agricultural

Figure 15 - Forest

Figure 16 - Grazing

Figure 17 - Water

From the images and the chart, it is evident that the most prevalent category in the city of Turin is logistical, that comprehends roads and related areas (34,7%). Residential areas are primarily located in the central part of the municipality, while the hilly zone is characterized by a predominance of forested areas (as shown in Figure 15). This characteristic will need to be considered when interpreting the results of the heat island analysis. Below is the land cover map that integrates the previous categories into a single visualization (Figure 18).
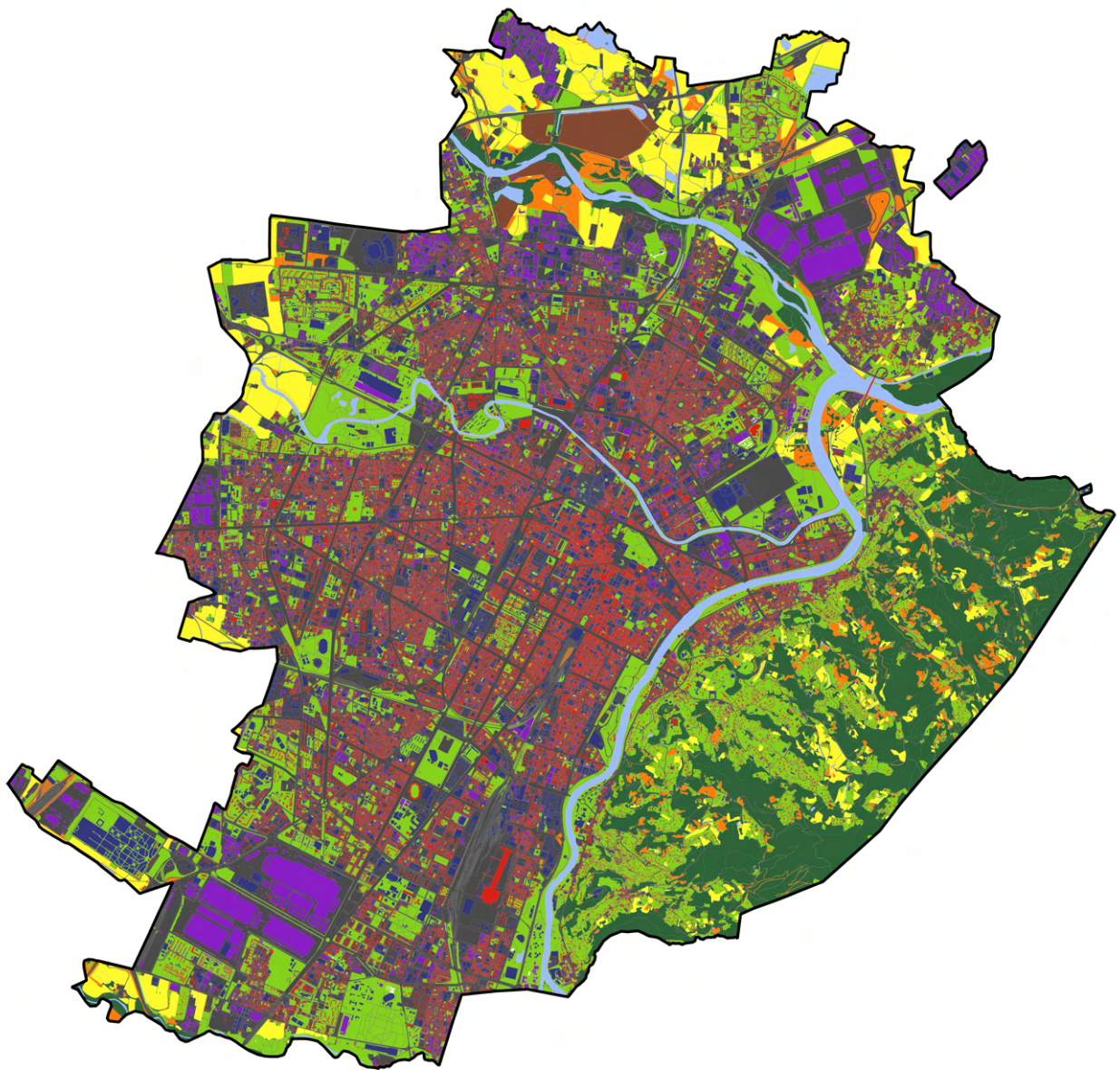
Figure 18 - Use of soil

- ● Residential
- ● Industrial
- ● Commercial & services
- ● Logistical
- ● Resource extraction & waste disposal

- ● Urban green
- ● Agricultural
- ● Forest
- ● Grazing
- ● Water

Radiometric indices are the quantitative features of targets obtained by combining several spectral bands.

Name	Purpose	Type
NDVI	Normalized Difference Vegetation Index	Vegetation Index
NDWI	Normalized Difference Water Index	Water Index
NDMI	Normalized Difference Moisture Index	Vegetation Index
Albedo	Albedo	Soil Index
PVI	Proportion Vegetation Index	Soil Index
Emissivity	Emissivity	Soil Index

Table 12 - Indeces

NDVI - Normalized Difference Vegetation Index:

This index describes the level of vigor vegetation and is calculated as:

$$\frac{(NIR - Red)}{(NIR + Red)}$$

The interpretation of the NDVI absolute value is highly informative, since it allows for an immediate identification of areas that have more or less vegetation. The NDVI is a simple index to interpret since its values range between -1 and 1, each one representing a different situation.

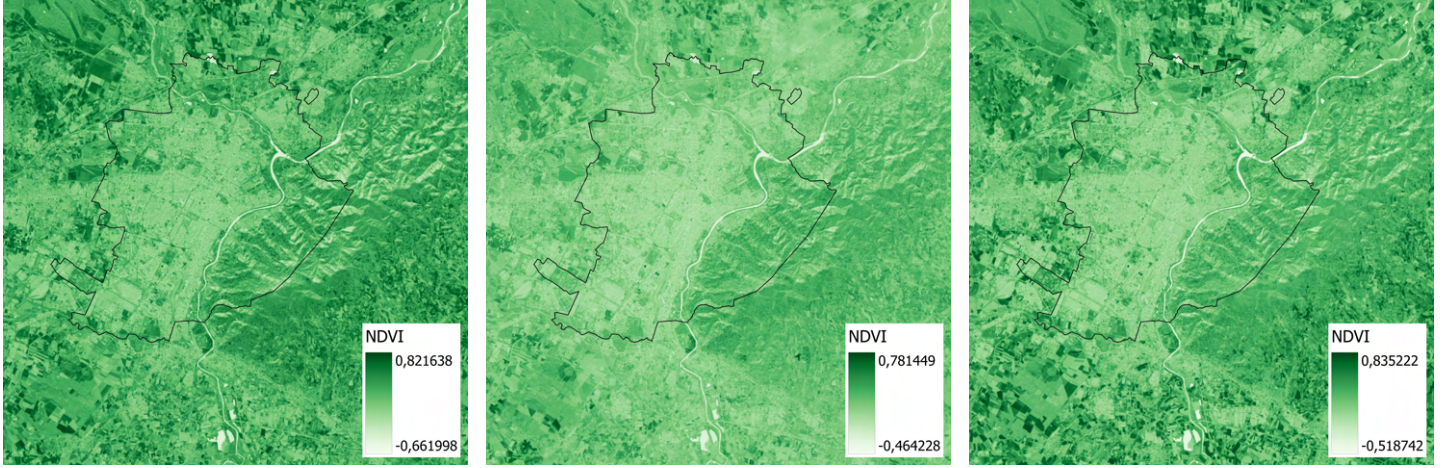| NDVI value	Interpretation	NDVI value	Interpretation
<0,1	Bare soil	0,5 - 0,6	Average canopy cover
0,1 - 0,2	Almost absent canopy	0,6 - 0,7	Mid-hig canopy cover
0,2 - 0,3	Very low canopy	0,7 - 0,8	High canopy cover
0,3 - 0,4	Low canopy cover	0,8 - 0,9	Very high canopy cover
0,4 - 0,5	Mid-low canopy cover	0,9 - 1	Total canopy cover

Table 13 - NDVI values

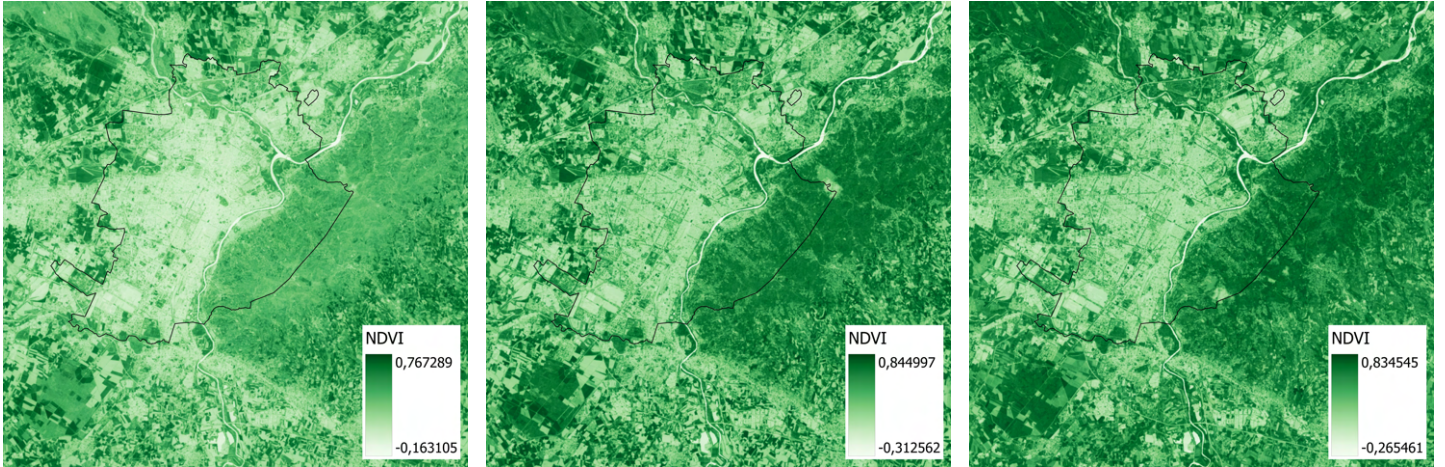Figure 19 - NDVI winter 2013, 2018, 2023
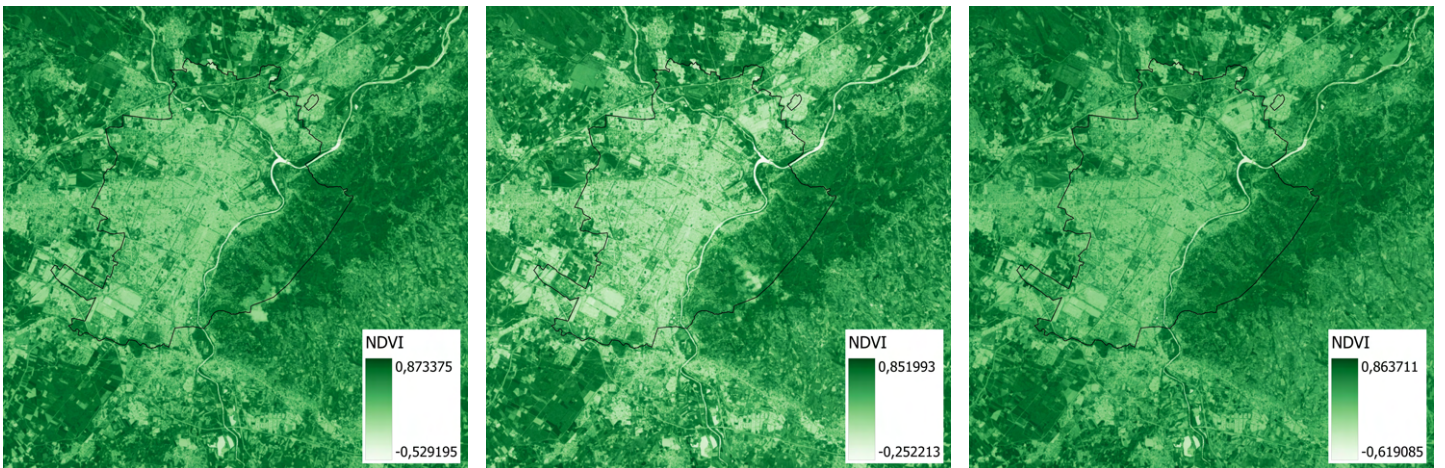

Figure 20 - NDVI mid-season 2013, 2018, 2023

Figure 21 - NDVI summer 2013, 2018, 2023

From the images, it is evident that vegetation undergoes significant changes throughout the seasons. The winter images appear more "flat" in color compared to the others, highlighting a clear seasonal trend. Taking 2023 as an example, below are the summary histograms for each class (in order: winter, mid-season, summer):
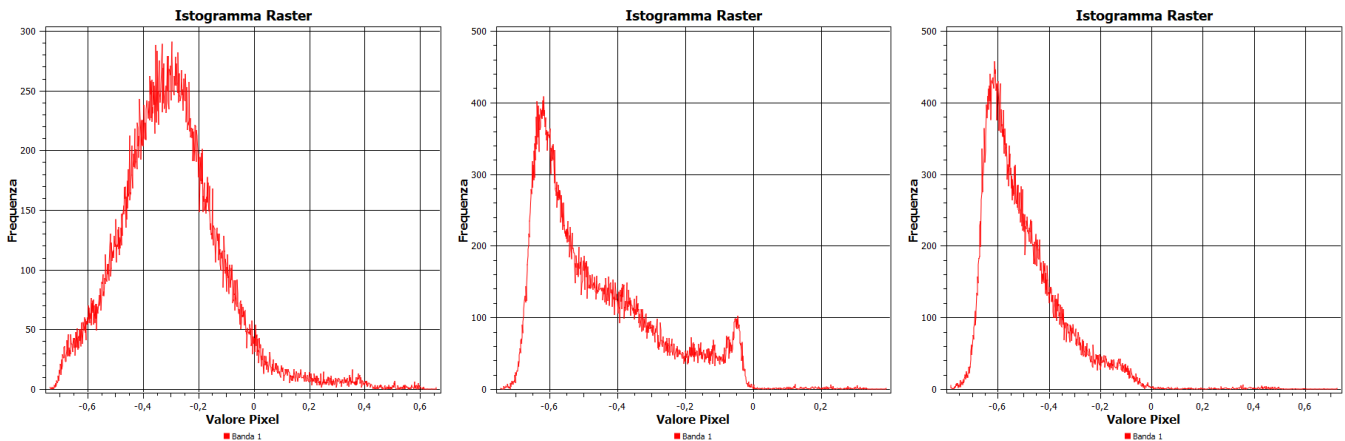
Graph 7 - Histograms winter, mid-season. summer 2023, NDVI

The peaks in value during winter are around 0.3 (very low/low canopy cover), while for the mid-season and summer, the peak is approximately 0.7 (mid-high/high canopy cover).

NDWI - Normalized Difference Water Index

The NDWI is commonly used to observe variations of water content in water bodies. When detecting water bodies, the principle of NDWI is based on visible light to infrared electromagnetic spectrum where water bodies absorb a lot of light and it uses green and near infra-red bands. This index is calculated as:

$$\frac{(\text{Green - NIR})}{(\text{Green + NIR})}$$

The NDWI values correspond to ranges:

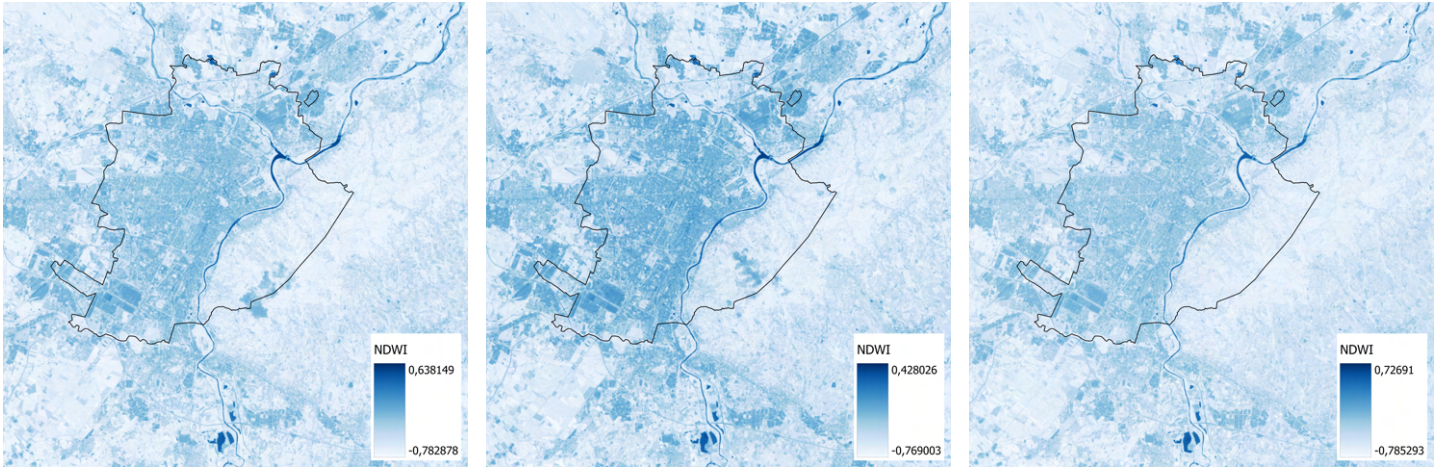| NDWI value	Interpretation
-1 - -0,3	Non-acqueous surfaces
-0,3 - 0	Moderate drought
0 - 0,2	Flooding humidity
0,2 - 1	Water surfaces

Table 14 - NDWI values

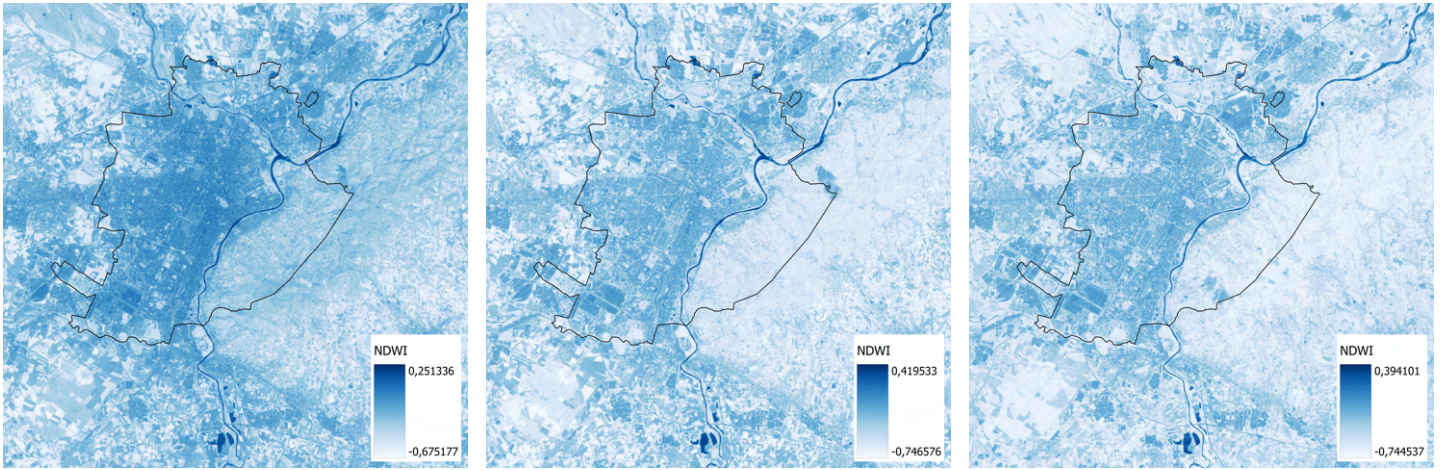Figure 22 - NDWI summer 2013, 2018, 2023
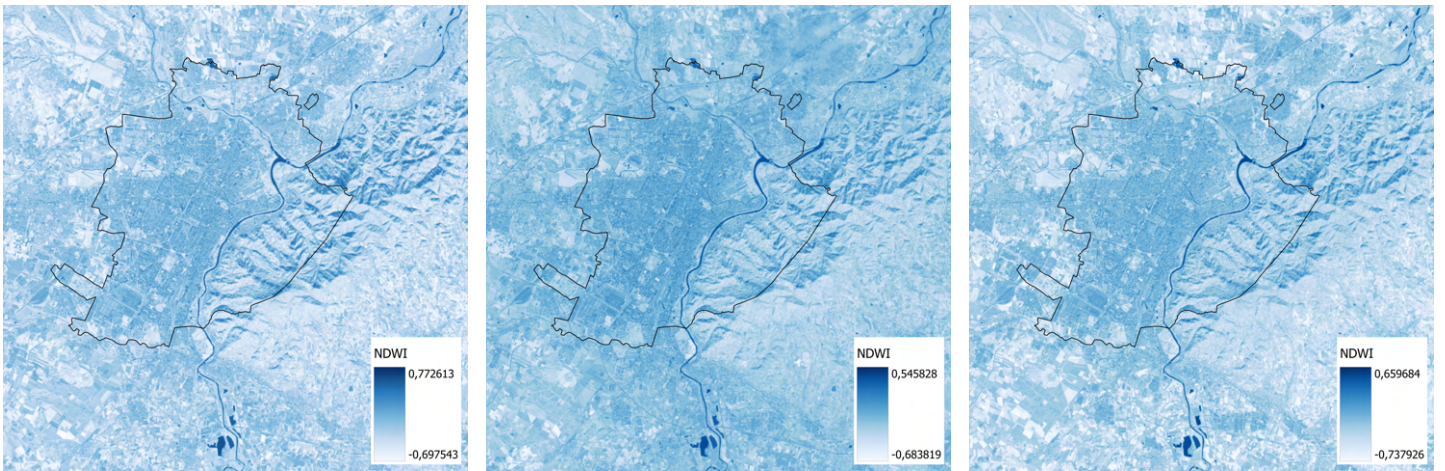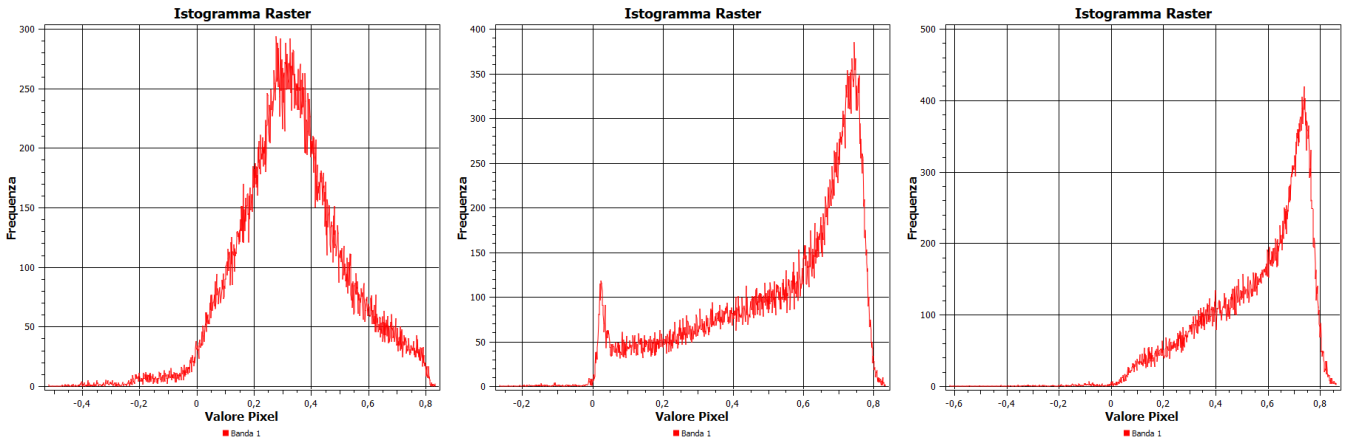

Figure 23 - NDWI mid-season 2013, 2018, 2023

Figure 24 - NDWI winter 2013, 2018, 2023

In contrast to NDVI, NDWI exhibits higher values in winter than in summer. This occurs because, in winter, rainwater is retained in the soil and evaporates at a lower rate. Considering the year 2023, the following are the summary histograms for each class (in order: winter, mid-season, summer):

Graph 8 - Histograms winter, mid-season. summer 2023, NDVWI

NDMI - Normalized Difference Moisture Index

This index indicates the amount of moisture in vegetation with near-infrared and short-wave infrared spectral bands. NDMI is calculated as:

$$\frac{(\text{NIR - SWIR})}{(\text{NIR + SWIR})}$$

NDMI is bounded between -1 and 1.

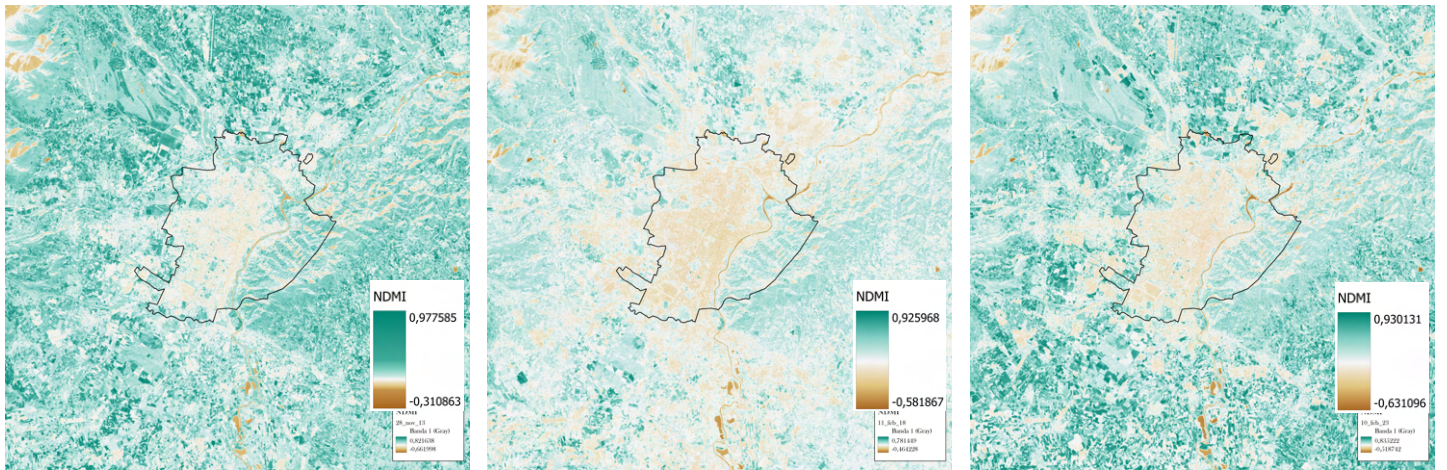| NDMI value	Interpretation	NDMI value	Interpretation
-1; -0,8	Bare soil	0; 0,2	Average canopy cover
-0,8; -0,6	Almost absent canopy	0,2; 0,4	Mid-hig canopy cover
-0,6; -0,4	Very low canopy	0,4; 0,6	High canopy cover
-0,4; -0,2	Low canopy cover	0,6 - 0,8	Very high canopy cover
-0,2; 0	Mid-low canopy cover	0,8 - 1	Total canopy cover

Table 15 - NDMI values

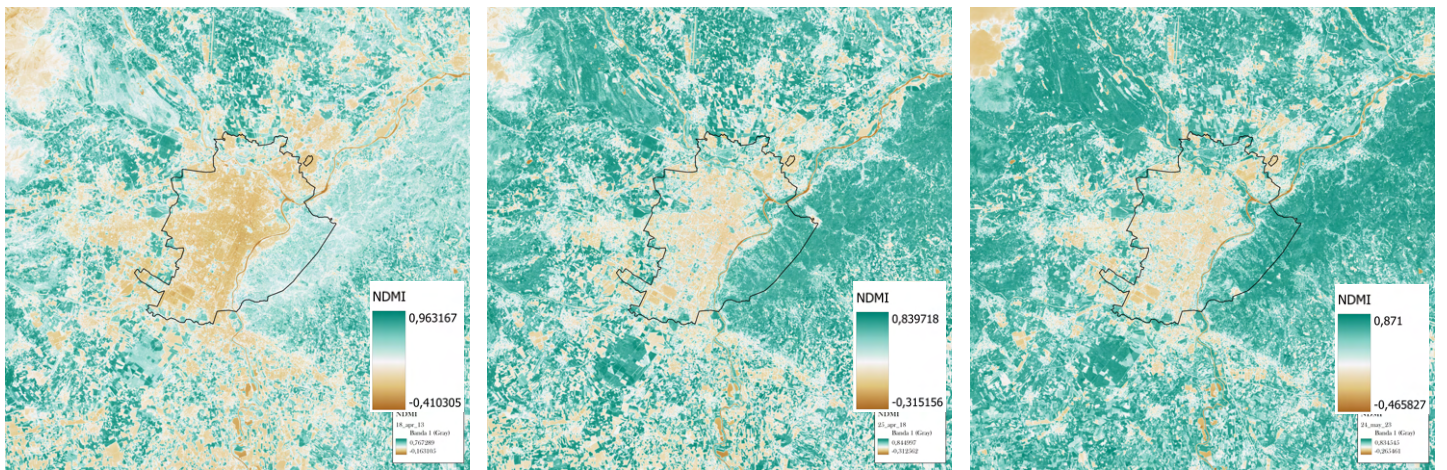Figure 25 - NDMI winter 2013, 2018, 2023
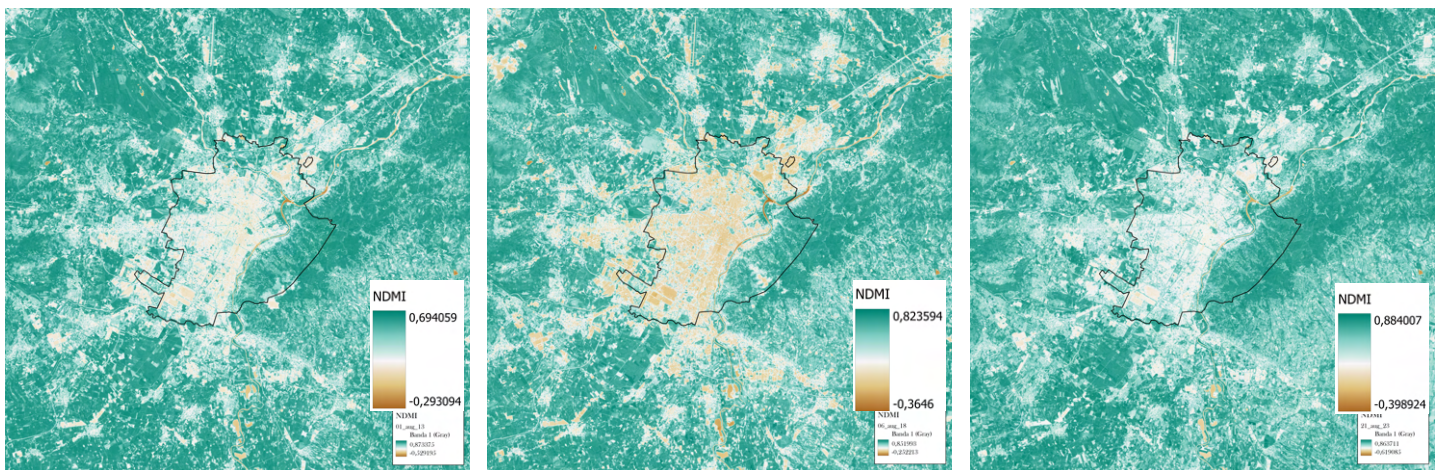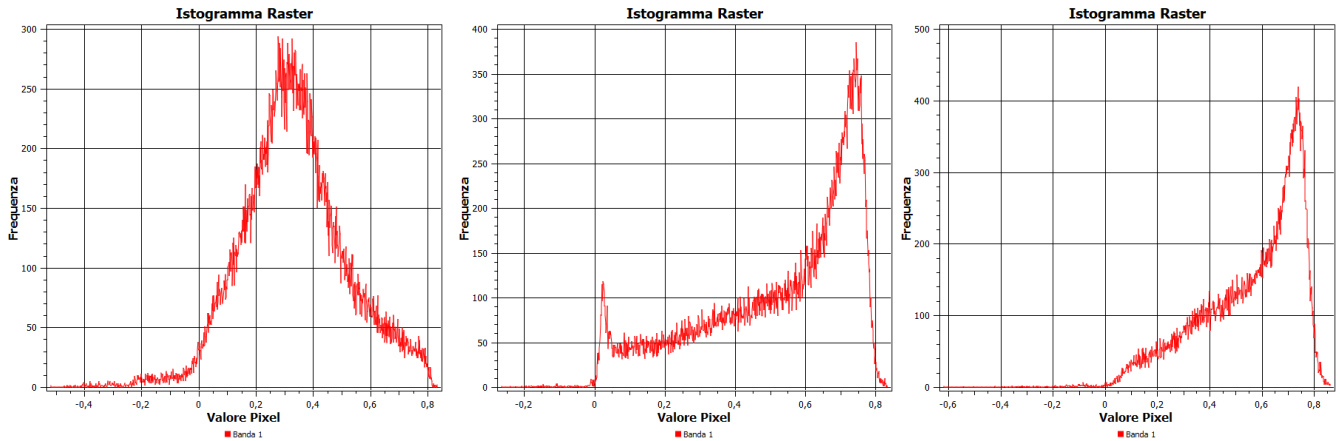

Figure 26 - NDMI mid-season 2013, 2018, 2023

Figure 27 - NDMI summer 2013, 2018, 2023

This index is closely related to NDVI, but it is designed to detect moisture content in plants. Considering the year 2023, the following are the summary histograms for each class (in order: winter, mid-season, summer):

Graph 9 - Histograms winter, mid-season. summer 2023, NDMI

The value peaks in winter are around 0.3 (mid-high canopy cover), whereas for mid-season and summer, the peak reaches approximately 0.7 (very high canopy cover).

Albedo

The surface albedo was estimated using the equation [29]:

$$b_{BLUE} * \rho_{BLUE} + b_{GREEN} * \rho_{GREEN} + b_{RED} * \rho_{RED} + b_{NIR} * \rho_{NIR} + b_{SWIR1} * \rho_{SWIR1} +$$
$$b_{SWIR2} * \rho_{SWIR2} + b_0$$

Below are the values of the band conversion coefficients (Landsat 8):

b_{BLUE}	b_{GREEN}	b_{RED}	b_{NIR}	b_{SWIR1}	b_{SWIR2}	b_0
0,2453	0,0508	0,1804	0,3081	0,1332	0,0521	0,0011

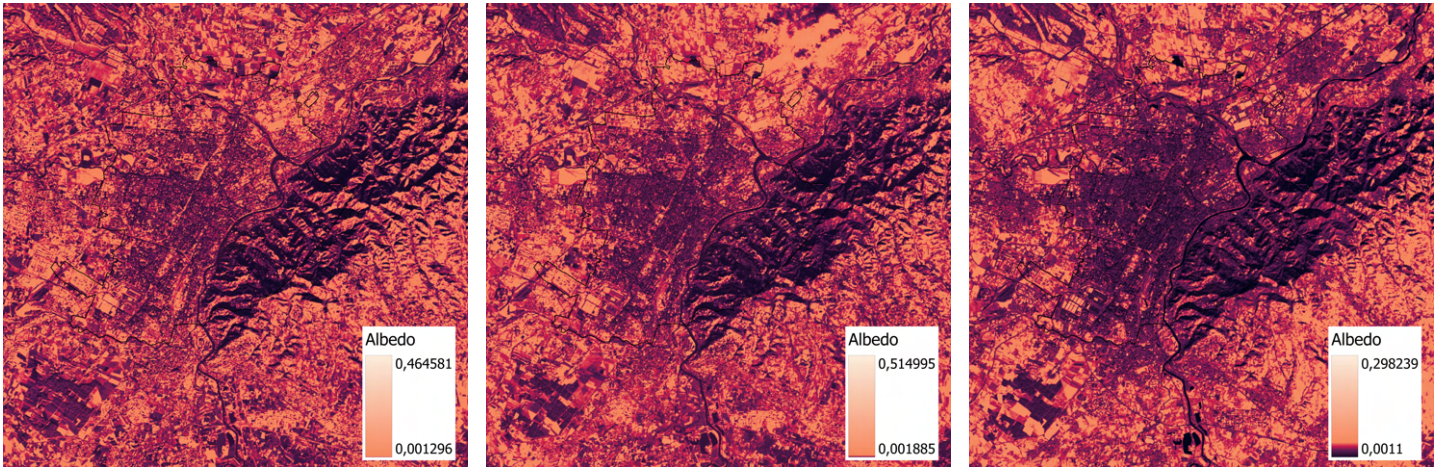The values of albedo, as previously mentioned in earlier chapters, range from 0 to 1.

Figure 28 - Albedo winter 2013, 2018, 2023
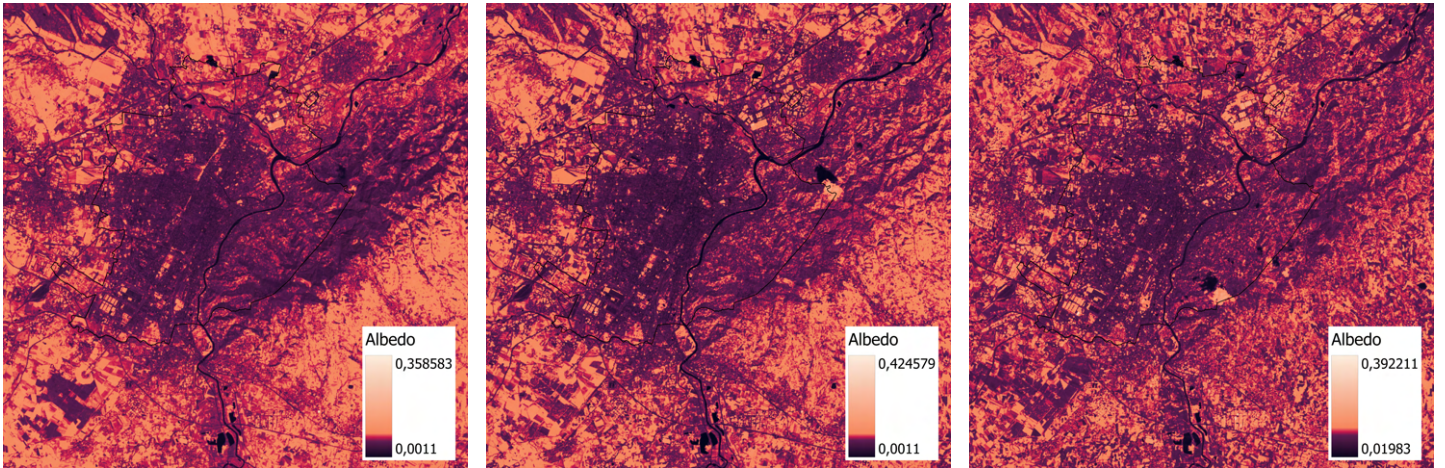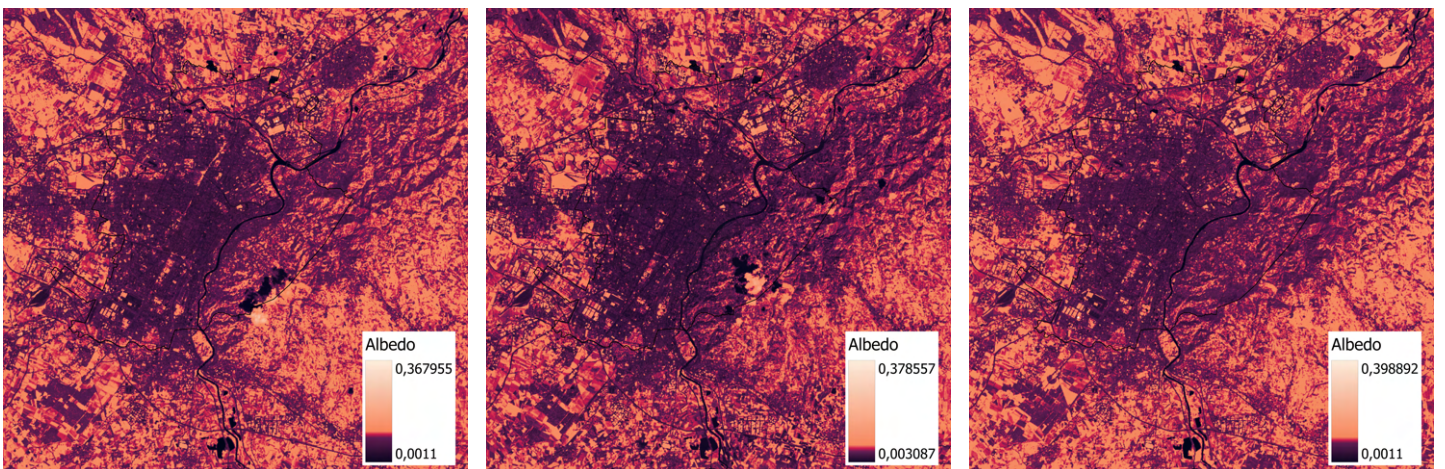

Figure 29 - Albedo mid-season 2013, 2018, 2023

Figure 30 - Albedo summer 2013, 2018, 2023

[29] Cunha J. et al (2020),Surface albedo as a proxy for land-cover clearing in seasonally dry forests: Evidence from the Brazilian Caatinga.

Even in the case of albedo, significant seasonality is observed, likely due to the surfaces being less distinct compared to other months. It should be noted that the analyses were conducted using Landsat 8 bands with a resolution of 100 meters resampled to 30 meters; this may affect the results of the analyses. Therefore, the images should be considered as relatively representative.
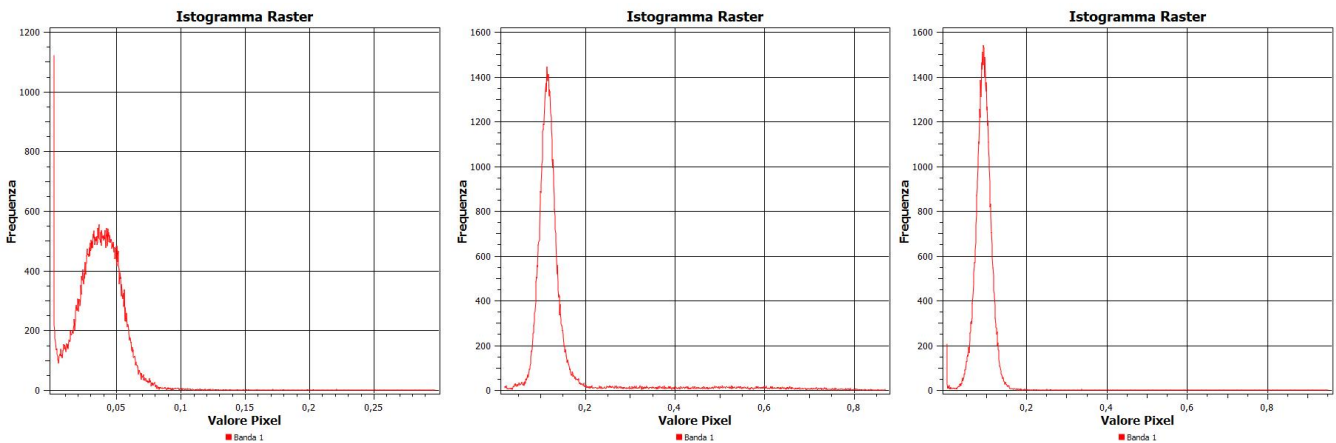
Graph 10 - Histograms winter, mid-season. summer 2023, Albedo

Nonetheless, the results of the albedo analyses yield clear findings: over the years, albedo indicates that the urban area has experienced a decline in the index, suggesting that less reflective surfaces have increased at the expense of reflective surfaces (this is particularly evident between 2013 and 2018). This effect is especially noticeable in the images related to the winter analyses.

PVI - Proportion Vegetation Index

This index is closely linked to the NDVI and shows the amount of vegetation in a given area. The index value ranges from 0 to 1, with higher values indicating more vegetation.

PVI is calculated as:

$$\left(\frac{(\mathrm{NDVI} - \mathrm{NDVI_{min}})}{(\mathrm{NDVI_{max}} + \mathrm{NDVI_{min}})} \right)^2$$

It is calculated by considering the reflectance of non-vegetation and vegetation elements. Values close to 0 correspond to non-vegetated areas, while values close to 1 correspond to vegetated areas.
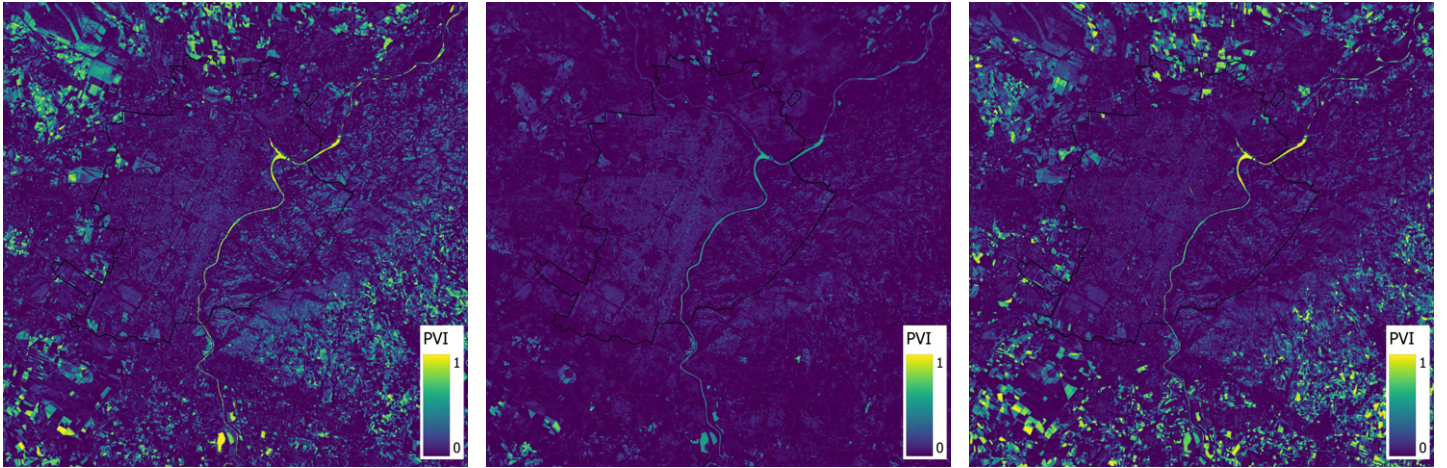
Figure 31 - PVI winter 2013, 2018, 2023
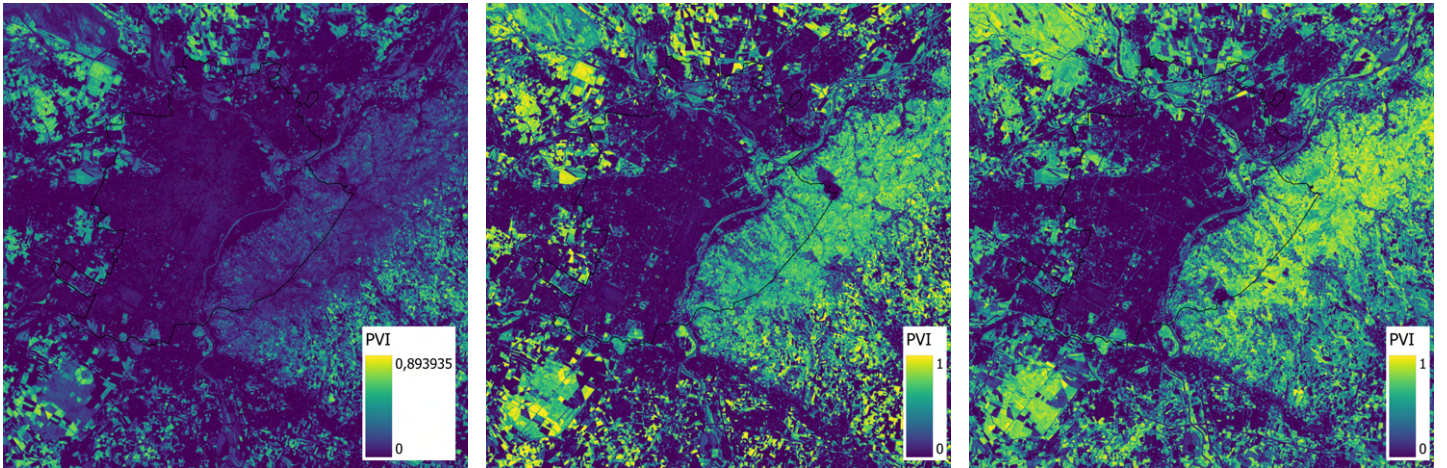
Figure 32 - PVI mid-season 2013, 2018, 2023
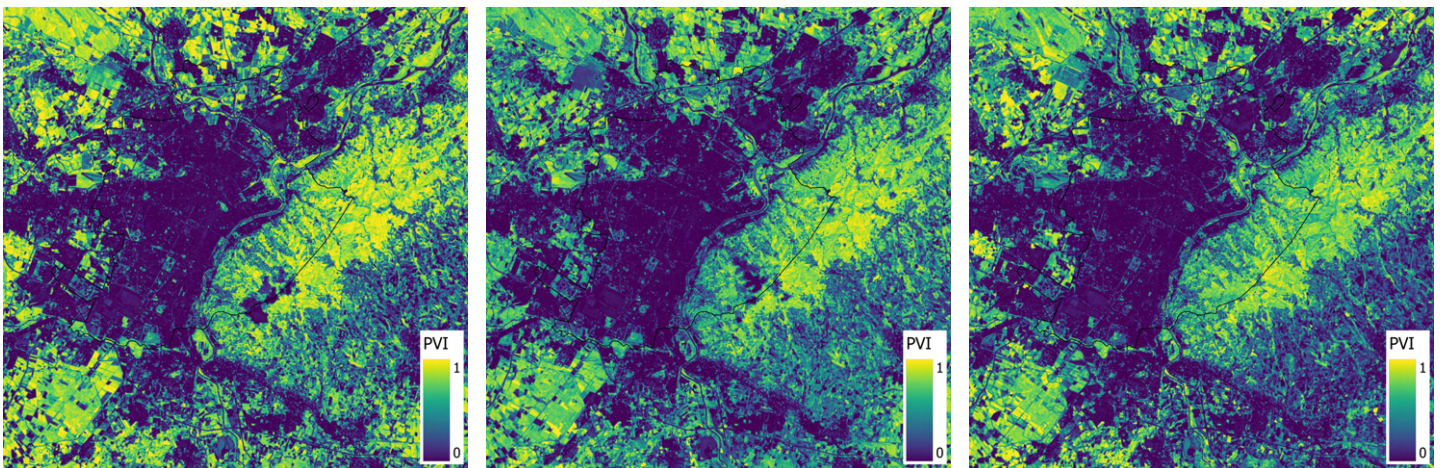
Figure 33 - PVI summer 2013, 2018, 2023

Given that this index is closely related to the NDVI, it is logical to expect that the PVI differs significantly between winter months and summer or mid-season months. Taking 2023 as an example, below are the summary histograms for each class (in the order of winter, mid-season, summer):
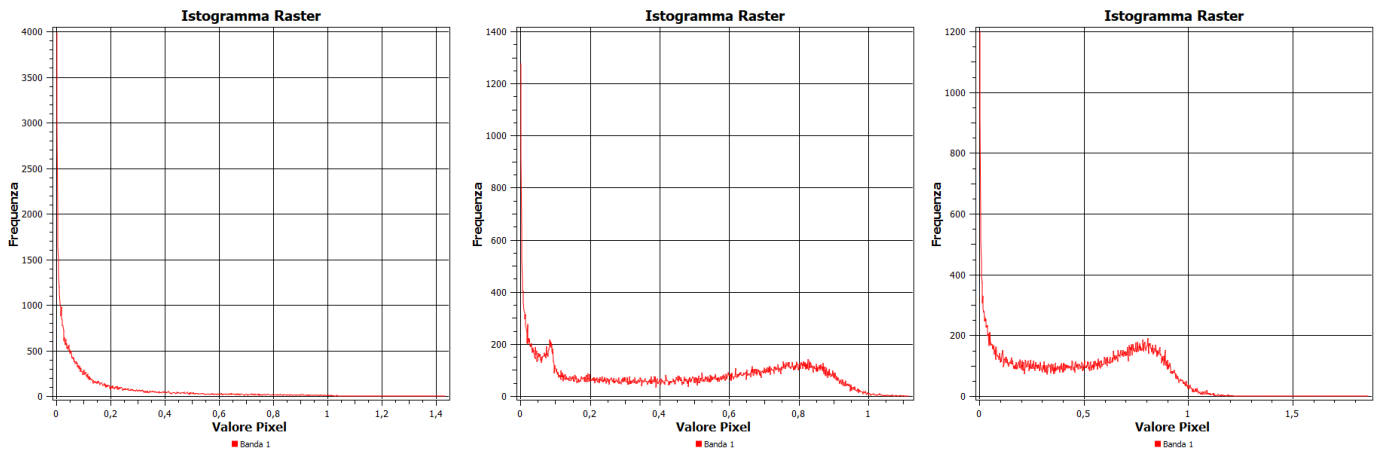
Graph 11 - Histograms winter, mid-season. summer 2023, PVI

The histograms also indicate that during winter, areas characterized by vegetation are relatively low compared to mid-season and summer.

Emissivity

Land surface emissivity refers to how effectively a surface emits thermal radiation, and it is measured in comparison to an ideal blackbody, which is a perfect emitter of heat.

Emissivity is calculated as follows:

$$0.004 * PVI + 0.986$$

The index ranges from 0 (perfect reflector) to 1 (perfect emitter) and depends on the nature of the surface and its temperature.
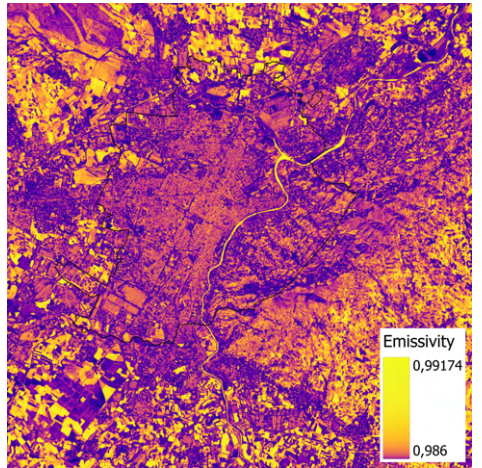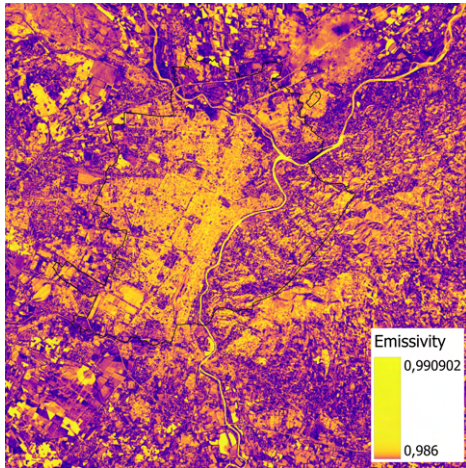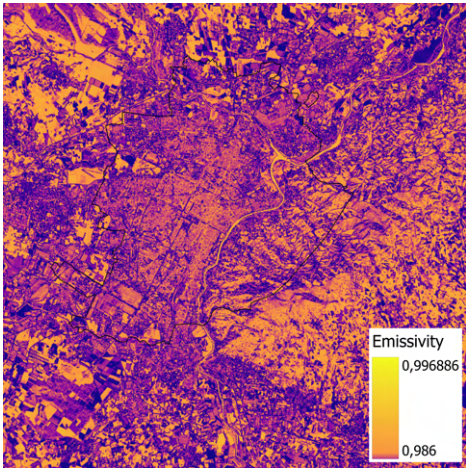
Figure 34 - Emissivity winter 2013, 2018, 2023
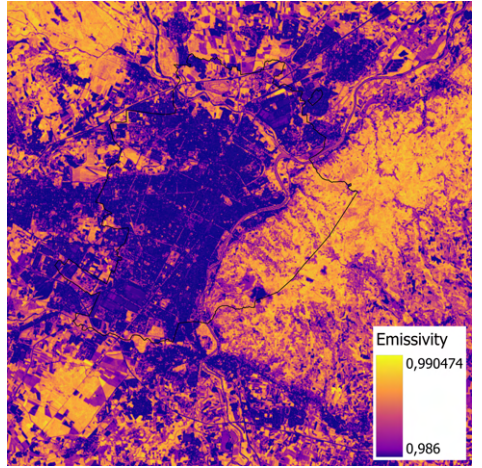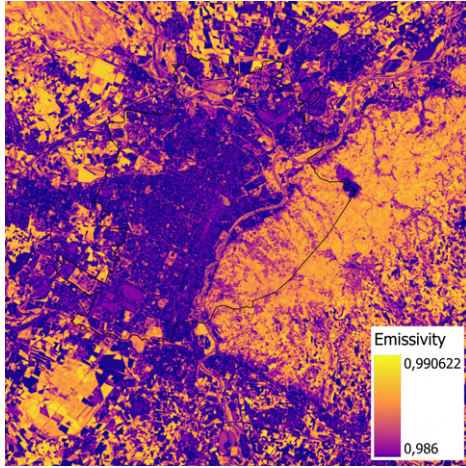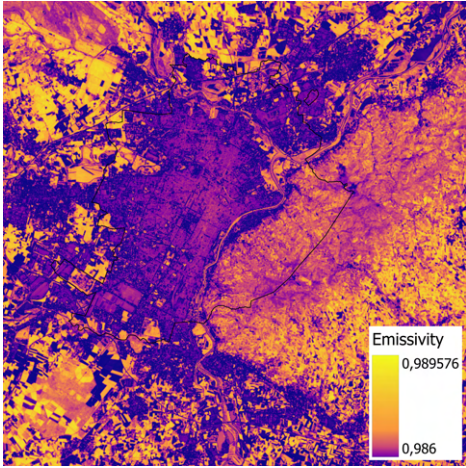
Figure 35 - Emissivity mid-season 2013, 2018, 2023
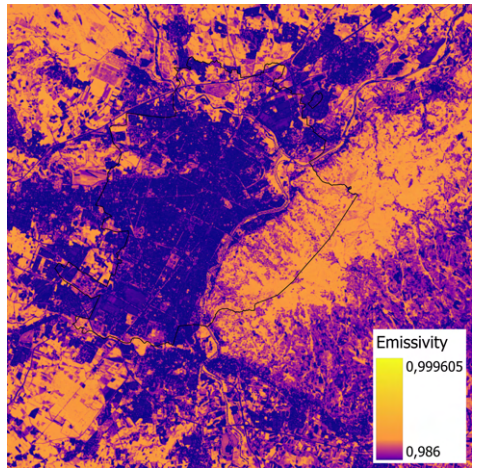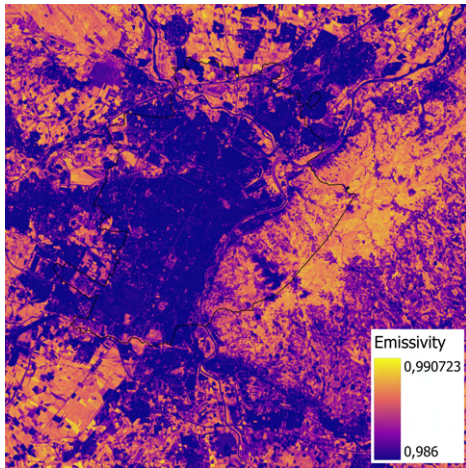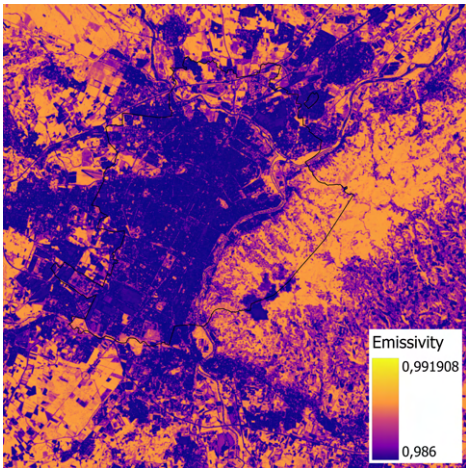
Figure 36 - Emissivity summer 2013, 2018, 2023

Emissivity is closely related to PVI (and thus indirectly to NDVI). In winter, emissivity shows less variation compared to the summer and mid-season months. Considering the year 2023, the following histograms summarize the data by class (in order: winter, mid-season, summer):
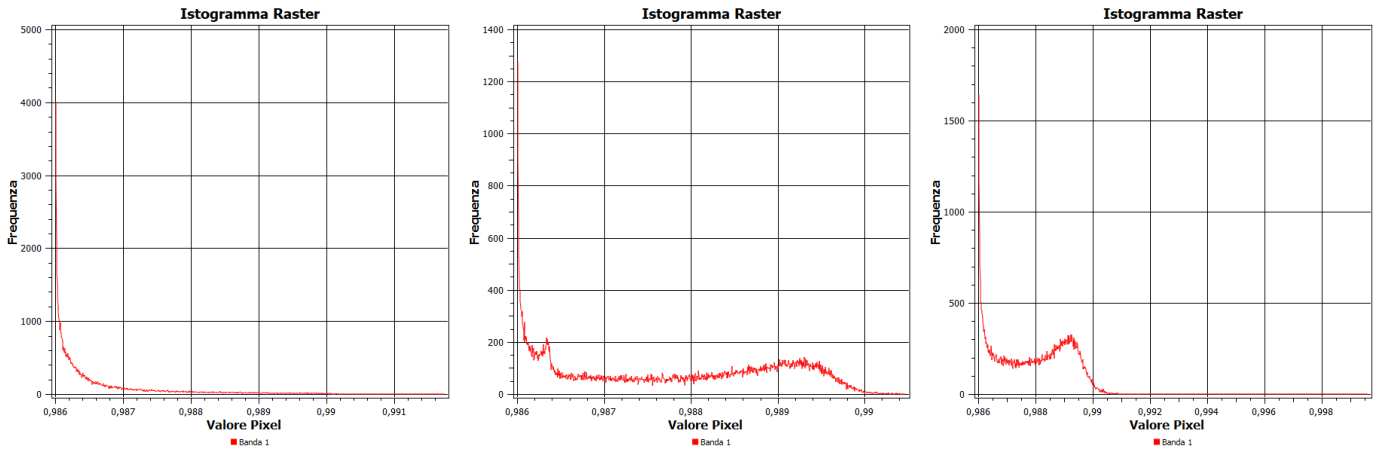
Graph 12 - Histograms winter, mid-season. summer 2023, Emissivity

During the mid-season, the values of emissivity are relatively widespread, while in the summer there is a peak between 0,988 and 0,99.

Land surface temperature

Thanks to the previous analyses, it is possible to estimate the land surface temperature (LST). This important parameter measures the emission of thermal radiation and the ground temperature that results from solar radiation. The LST describes the processes between the atmosphere and the ground that influence, for example, plant growth.

To estimate the LST, the Landsat 8 band was used. Below are the steps for the calculation:

Conversion from Digital Number to Radiance:

$$L_y = M_L * Q_{CAL} + A_L$$

Where:

M_L: band-specific multiplicative rescaling factor [from image metadata]

Q_{CAL}: corresponds to Band 10

A_L: band-specific additive rescaling factor [from image metadata]

Calculation of brightness temperature [°C]:

$$\left(\frac{(K_2)}{\ln\left(\frac{(K_1)}{L_y} + 1 \right)} \right) - 273.15$$

Where:

K1: band-specific thermal conversion constant [from image metadata]

K2: band-specific thermal conversion constant [from image metadata]

L: Radiance

Calculation of proportion vegetation index:

$$\left(\frac{(\text{NDVI} - \text{NDVI}_{\text{min}})}{(\text{NDVI}_{\text{max}} + \text{NDVI}_{\text{min}})} \right)^2$$

Where:
NDVI: Normalized difference vegetation index
NDVI$_{min}$: minimum value - Normalized difference vegetation index
NDVI$_{max}$: maximum value - Normalized difference vegetation index

Calculation of emissivity:

$$0.004 * \text{PV} + 0.986$$

Where:
PV: proportion of vegetation
0,986: correction value

Calculation of LST [°C]:

$$\frac{\text{BT}}{1 + \left(\lambda * \dfrac{\text{BT}}{\text{C}_2} \right) * \ln(\text{E})}$$

Where:
BT: brightness temperature
λ: wavelenght of emitted radiance
*C$_2$: 14388 (h * c / s)*
E: emissivity

The analysis of land surface temperature (LST) was conducted for the same years and periods (winter, mid-season, summer) selected based on defined criteria. From a climate perspective, the LST is fundamental because changes in land use and albedo transformations influence land surface temperature. Additionally, cloud cover and climate shifts also contribute to variations in this parameter.

The table below relates the selected day to the corresponding temperature:

Seasonality	2013		2018		2023	
	Day	Air temerature [°C]	Day	Air temerature [°C]	Day	Air temerature [°C]
Winter	28/11	-0,8	11/2	1,6	10/2	-1,9
Mid – season	18/4	21,3	25/4	21,7	24/5	19,7
Summer	1/8	32,3	6/8	34,9	21/8	35,9

Table 16 - Temperature related to day selected

The following summarizes the LST data obtained from the previous images:

Seasonality	2013			2018			2023		
	Day	T min °C	T max °C	Day	T min °C	T max °C	Day	T min °C	T max °C
Winter	28/11	-3,4	13	11/2	-1,8	14,8	10/2	7,5	-7,3
Mid – season	18/4	9,9	37,4	25/4	9,3	42,4	24/5	7,8	35,4
Summer	1/8	15	45,1	6/8	13,1	42	21/8	11,3	35,8

Table 17 - LST related to day selected

The images clearly indicate that the hottest areas correspond to urbanized zones, with a particular focus on commercial and/or industrial areas, which are the hottest overall. In contrast, the hilly areas of Turin tend to be the coolest and least affected by high land surface temperatures (LST), likely because of the greater amount of vegetation in these regions. However, it's important to note that the analysis was based on Landsat 8 images with a 100-meter resolution, which could influence the accuracy of the findings. As such, the results should be seen as generally indicative rather than exact.
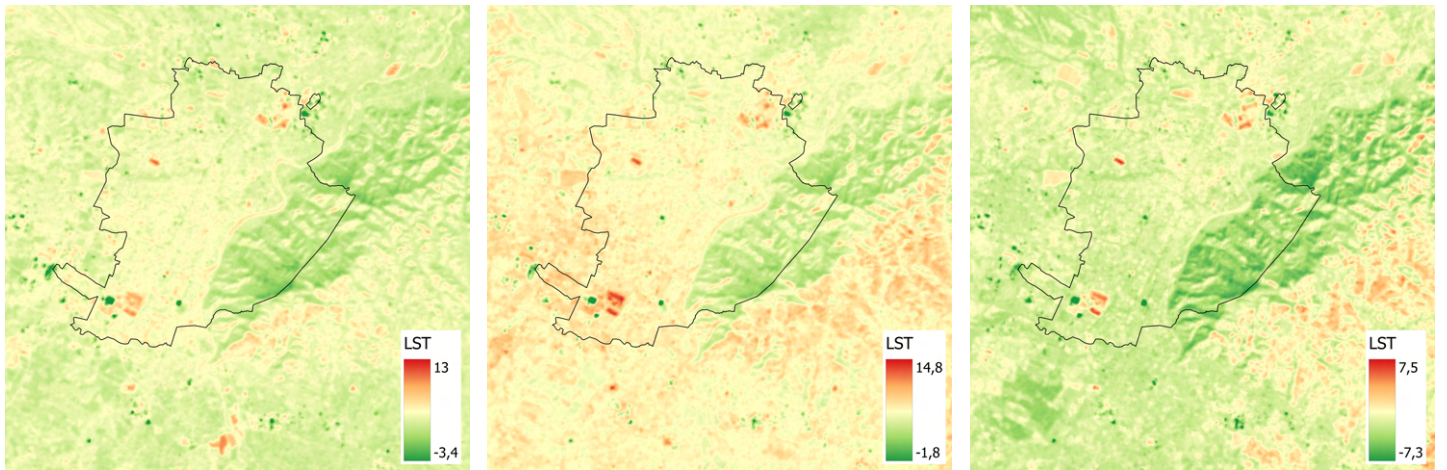
Figure 37 - LST [°C] winter 2013, 2018, 2023
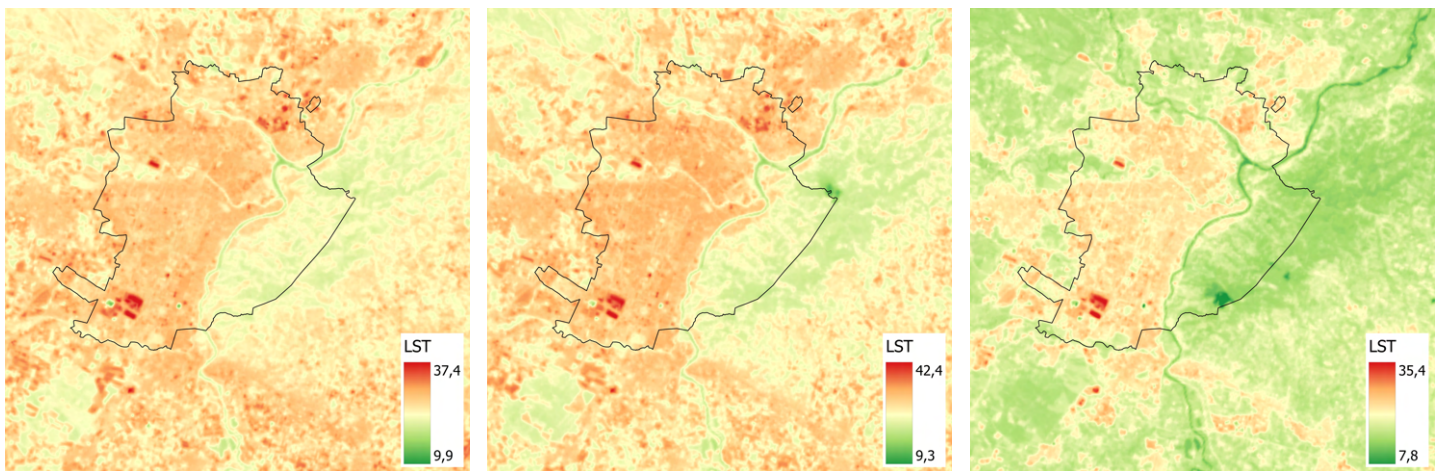
Figure 38 - LST [°C] mid-season 2013, 2018, 2023
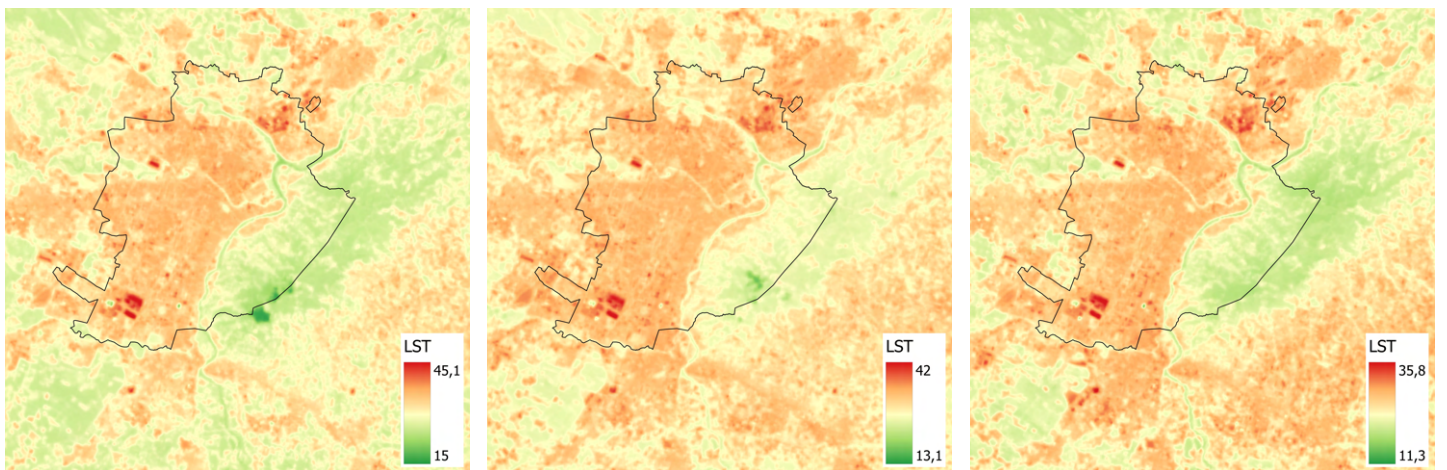
Figure 39 - LST [°C] summer 2013, 2018, 2023

63

Considering the year 2023, the following are the summary histograms for each class (in order: winter, mid-season, summer):
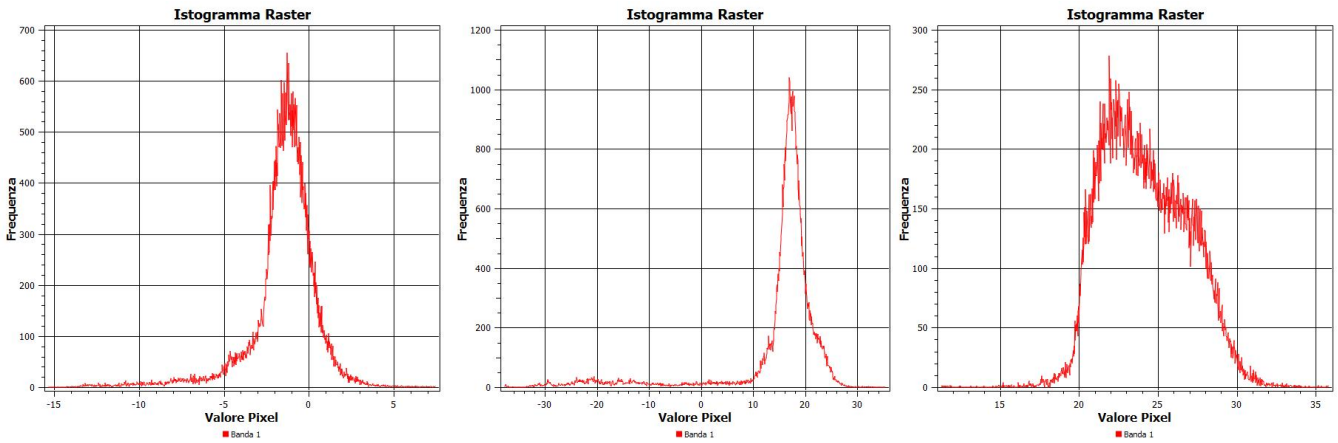
Graph 13 - Histograms winter, mid-season. summer 2023, LST

It is evident how and to what extent the Land Surface Temperature (LST) varies according to seasonal changes.

At this point, it would be useful to demonstrate how and to what LST and albedo varies according to its type. The points for the classification has been selected as follows:

Figure 40 - Localization of selected point (soil type)

Below is a summary table presenting the LST based on different soil types (the classification considers the year 2023, corresponding to the post-intervention phase of the projects discussed in the previous chapters):

	Soil Type	Temperature in winter [°C]	Temperature in mid-season [°C]	Temperature in summer [°C]
1	Water	0,4	10,4	19,1
2	Forest - Hilly Area	-5,3	15,2	20,2
3	Built-up Area (City Center)	0,1	24,2	29,5
4	Built-up Area (Suburban Area)	-0,7	22,8	27,3
5	Paving (Dark Surface)	0,3	24,9	31,2
6	Paving (Light Surface)	-0,8	23,3	27,4
7	Industrial Zone	3,6	33,4	35,6
8	Urban Green Space	-1,2	19,2	23,4

Table 18 - Surface temperatures depending on soil type and seasons (radiometric calculation)

The same table has been presented for the albedo results:

	Soil Type	Albedo in winter	Albedo in mid-season	Albedo in summer
1	Water	0,41	0,48	0,57
2	Forest - Hilly Area	0,10	0,13	0,18
3	Built-up Area (City Center)	0,12	0,11	0,12
4	Built-up Area (Suburban Area)	0,12	0,12	0,11
5	Paving (Dark Surface)	0,04	0,04	0,06
6	Paving (Light Surface)	0,11	0,10	0,13
7	Industrial Zone	0,10	0,12	0,13
8	Urban Green Space	0,09	0,12	0,16

Table 19 - Albedo depending on soil type and seasons (radiometric calculation)

Soil types exhibit different temperature behaviors due to a combination of physical, chemical, and biological factors. The key reasons for these temperature variations include:

• Composition and Structure: The mineral content, water, and organic matter in the soil affect its ability to retain or dissipate heat.

• Albedo: Albedo refers to the ability of a surface to reflect solar radiation. Lighter-colored soils, which reflect more solar radiation, tend to stay cooler, whereas darker soils absorb more radiation and heat up more.

• Moisture: Moist soils take longer to warm up because they need more energy to evaporate the water they contain. On the other hand, dry soils heat up faster since there is less moisture to evaporate.

• Vegetation: Vegetation helps to moderate temperature changes by providing shade and cooling the soil through transpiration. This cooling effect occurs at a microscopic level and influences the overall temperature of the soil.

• Thermal Conductivity: Soils with high thermal conductivity, such as clayey soils, transfer heat more efficiently. On the other hand, soils with low thermal conductivity, such as sandy or organic soils, warm up more slowly.

• Depth and Stratification: Soil temperature varies with depth, with deeper soils generally maintaining more stable temperatures, while surface soils are more susceptible to thermal fluctuations.

In conclusion, soil temperature is influenced by the interaction of these factors, causing different types of soil to respond differently to solar radiation, moisture, and other environmental conditions.

In this context, it is evident that soils exhibit different temperatures both seasonally and based on their type. When considering vegetation, it generally results in cooler temperatures, while water behaves in a more tempered manner (cool in summer and warm in winter). In terms of surfaces, light-colored pavements are cooler than dark-colored ones, confirming that the type of paving contributes to higher temperatures. In urban areas, where this type of soil is predominant or prevalent, it significantly impacts the urban temperature and, consequently, the intensity of the urban heat island effect.

UHI intensity

It is important to emphasize that the UHI intensity was calculated based on the LST results, as the thesis focuses on mitigation measures related to pavement surfaces. Therefore, the calculation differs from the standard UHI analysis, which typically pertains to air temperature.

The Urban Heat Island (UHI) intensity can be measured using a standardized method that tracks the rise in temperatures in urban areas.

$$\frac{LST - LST_{mean}}{LST_{std}}$$

Where:
LST: land surface temperature
LST$_{mean}$: mean land surface temperature
LST$_{std}$: standard deviation land surface temperature

The formula standardizes the value of LST by taking into account its deviation from the average LST. A positive value of UHI would mean that, at that particular location, the LST is greater than the average and hence an urban area of intensified heat. On the other hand, negative UHI value indicates that LST is lower than the average in the regional scale, implying a cooling effect compared to the surroundings.

This calculation provides a context-independent measure of temperature modification and give a wider understanding of the dynamics involved in UHI, assisting in the informed development of strategies for urban planning and environmental management.

In the following pages, the results of this calculation will be presented. As in previous analyses, the evaluation was conducted for the same years and the same periods (winter, mid-season, summer), selected based on defined criteria.

UHI intensity winter 2013

Mean air temperature:
-0,8°C
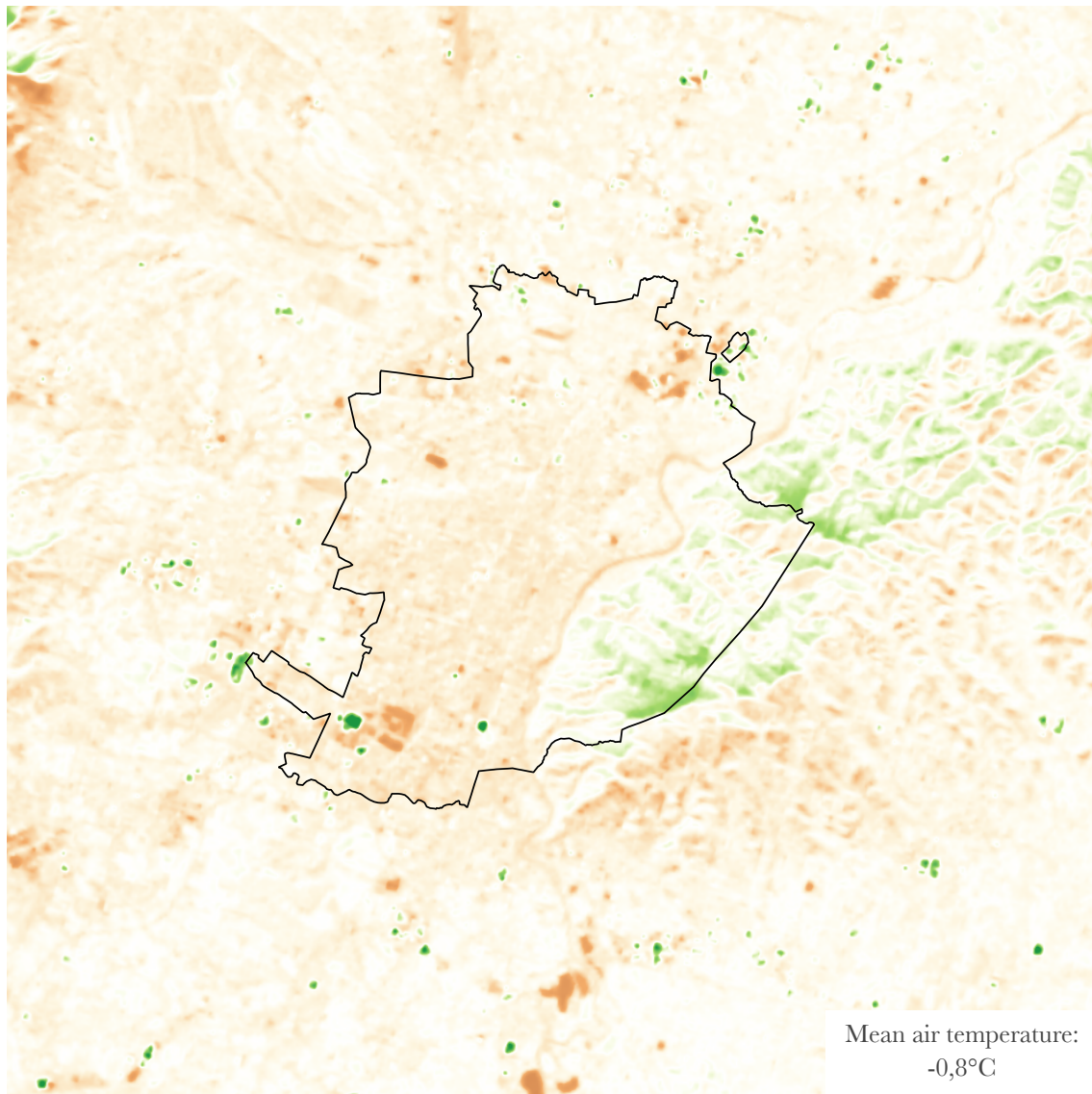
Figure 41 - UHI effect, winter 2013

- ☐ -1 [medium-low cooling effect]
- ☐ -0,5 [low cooling effect]
- ☐ 0 [area of balance]
- ☐ 1 [medium-low heating effect]
- ☐ 2 [medium heating effect]

RESULTS:

In the winter of 2013, Turin exhibited a notable urban heat island effect. The majority of the urban area was characterized by a medium-low heating effect, which may have been influenced by factors such as building density, heating practices, and materials that absorb heat.

UHI intensity winter 2018

Mean air temperature:
1,6°C
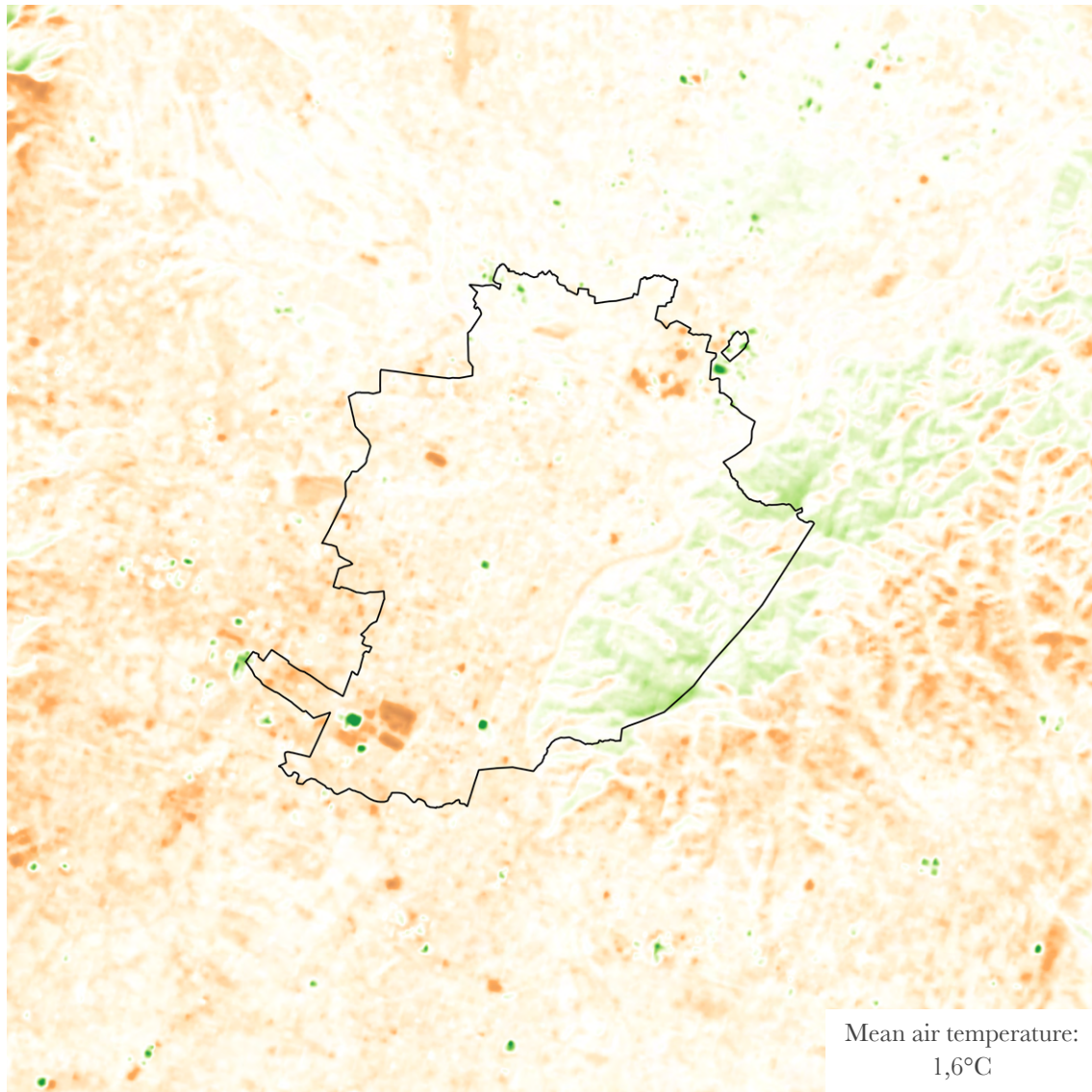
Figure 42 - UHI effect, winter 2018

RESULTS:

- 🟩 -1 [medium-low cooling effect]
- 🟩 -0,5 [low cooling effect]
- ⬜ 0 [area of balance]
- 🟧 1 [medium-low heating effect]
- 🟧 2 [medium heating effect]

Compared to the winter of 2018, there are significant differences in terms of heating effect peaks. The urban heat island (UHI) is characterized by less balance than in the previous year, also indicating a greater cooling effect in the hilly areas.

UHI intensity winter 2023

Mean air temperature:
-1,9°C
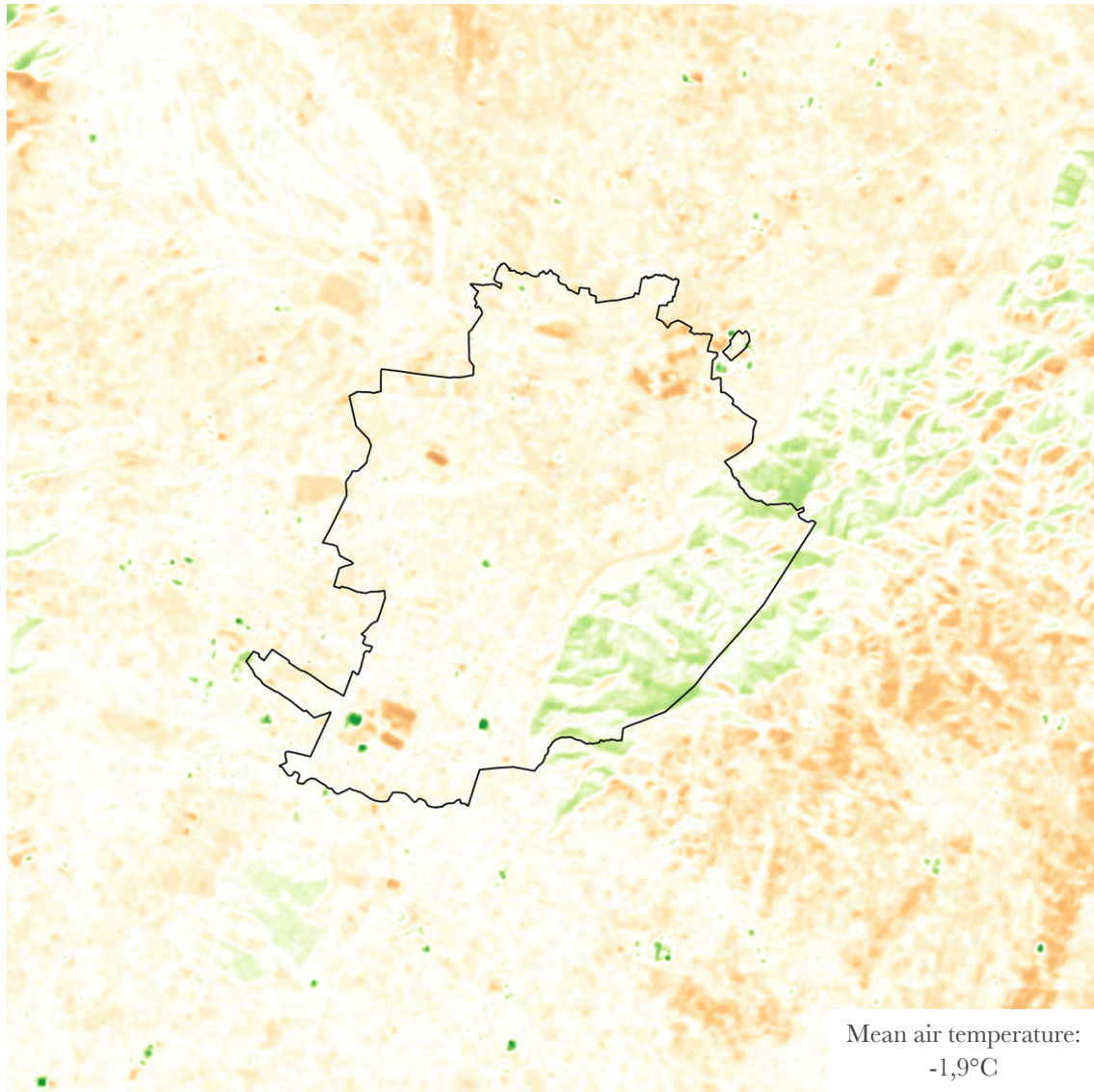
Figure 43 - UHI effect, winter 2023

- [ ] -1 [medium-low cooling effect]
- [ ] -0,5 [low cooling effect]
- [ ] 0 [area of balance]
- [ ] 1 [medium-low heating effect]
- [ ] 2 [medium heating effect]

RESULTS:

In comparison to winter 2018, the UHI pattern in 2023 resembles that of 2013 more closely: there are more balanced areas, and the UHI phenomenon appears more homogeneous across the analyzed territory. However, the industrial zones continue to exhibit a pronounced heating effect.

UHI intensity mid-season 2013

Mean air temperature: 21,3°C
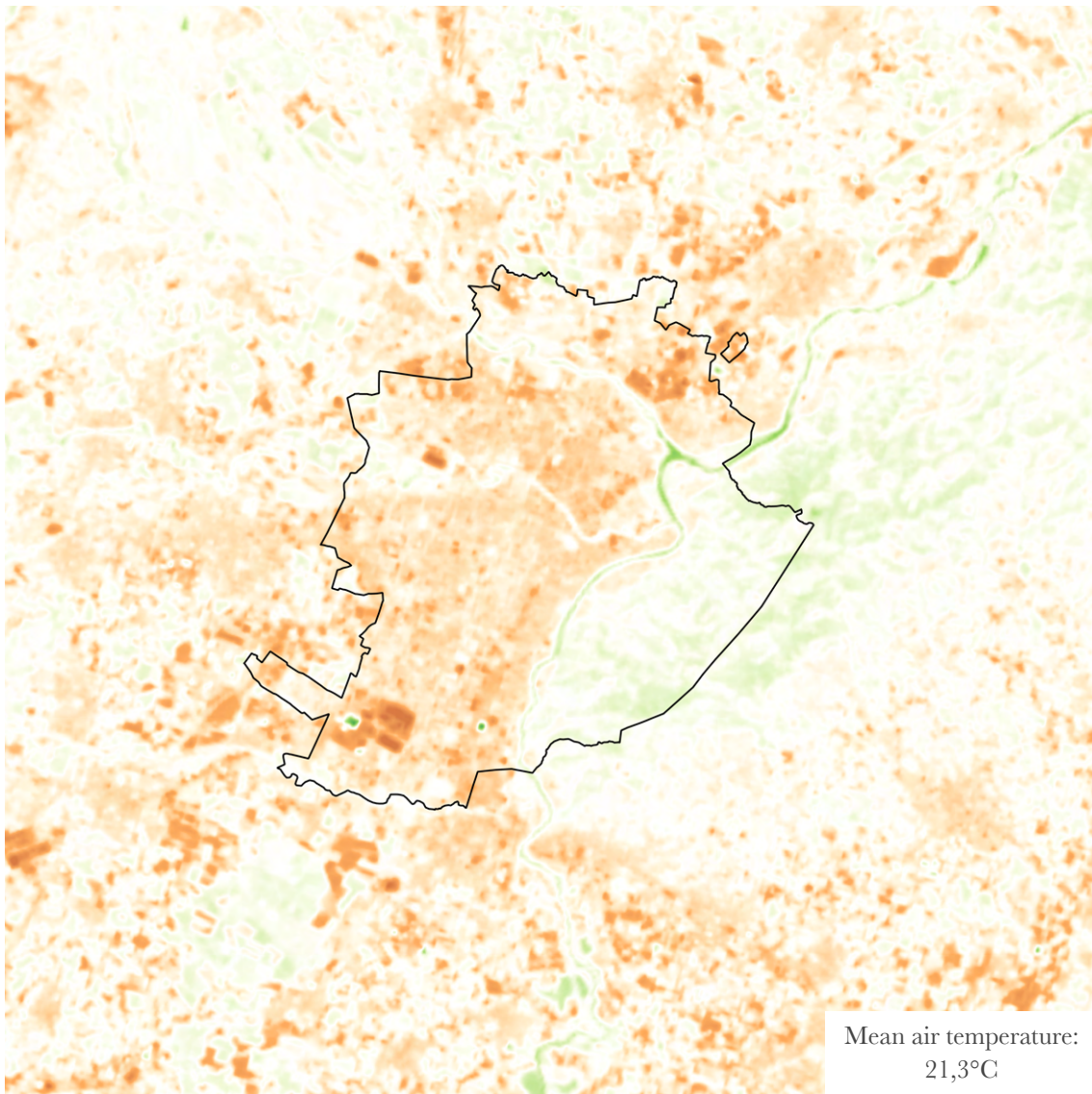
Figure 44 - UHI effect, mid-season 2013

■ -3 [high cooling effect]

■ -2[medium cooling effect]

■ -1 [low cooling effect]

□ 0 [area of balance]

□ 1 [medium-low heating effect]

■ 2 [medium heating effect]

■ 3 [high heating effect]

RESULTS:

During the mid-season of 2013, the UHI phenomenon is clearly concentrated in the urban area, while some hilly regions are cooler in comparison to the urban core. As observed in the winter cases, industrial hubs are characterized by the highest intensity heating effect.

UHI intensity mid-season 2018

Mean air temperature:
21,7°C
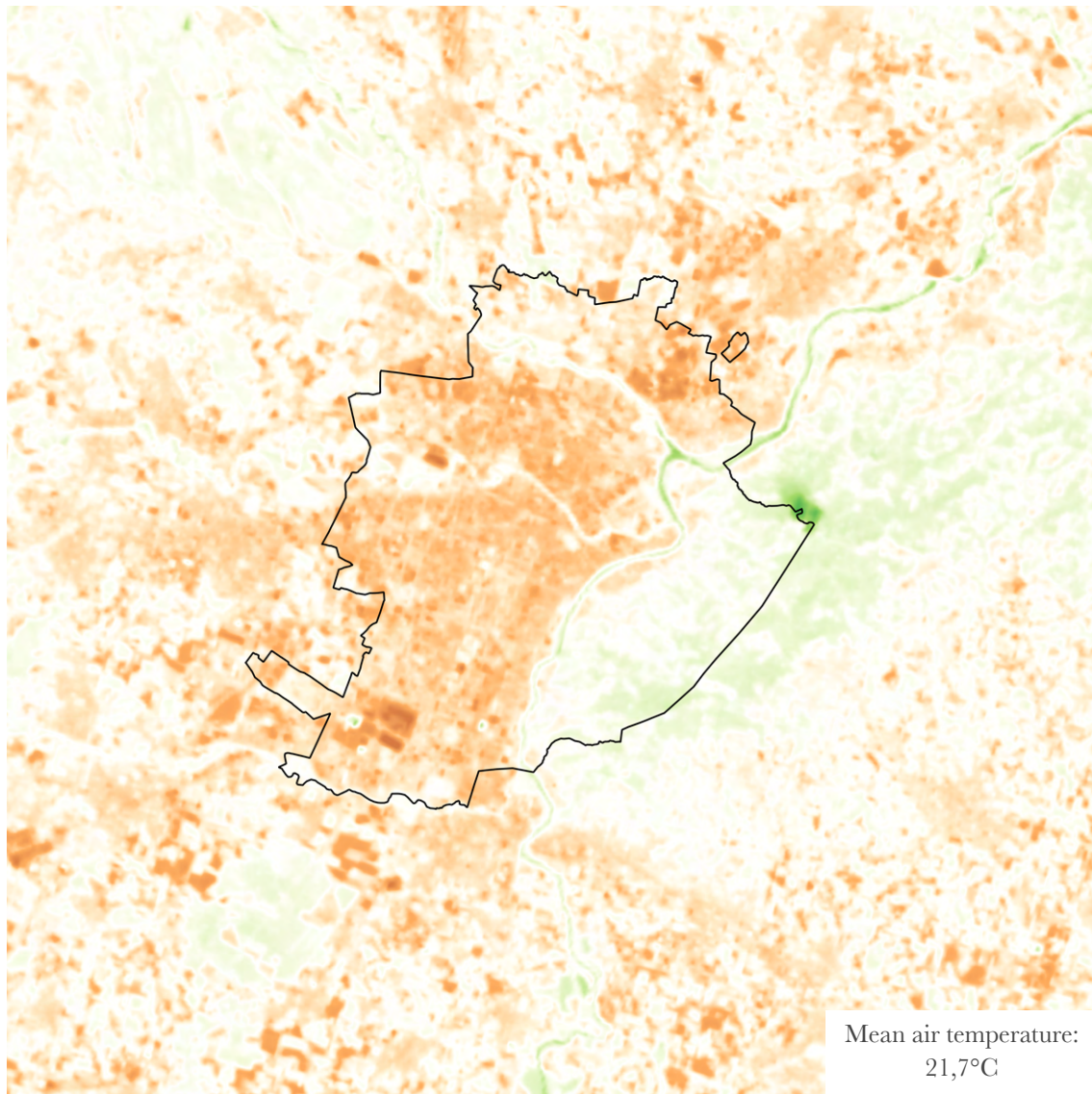
Figure 45 - UHI effect, mid-season 2018

■ -3 [high cooling effect]
■ -2[medium cooling effect]
■ -1 [low cooling effect]
□ 0 [area of balance]
□ 1 [medium-low heating effect]
■ 2 [medium heating effect]
■ 3 [high heating effect]

RESULTS:

Compared to the mid-season of 2013, the mid-season of 2018 was characterized by a more pronounced UHI phenomenon: the hilly areas experienced less cooling than in 2013, leading to a greater balance within the region. Conversely, the urban area continued to experience a relatively high heating effect, particularly in industrial zones.

Mean air temperature:
19,7°C
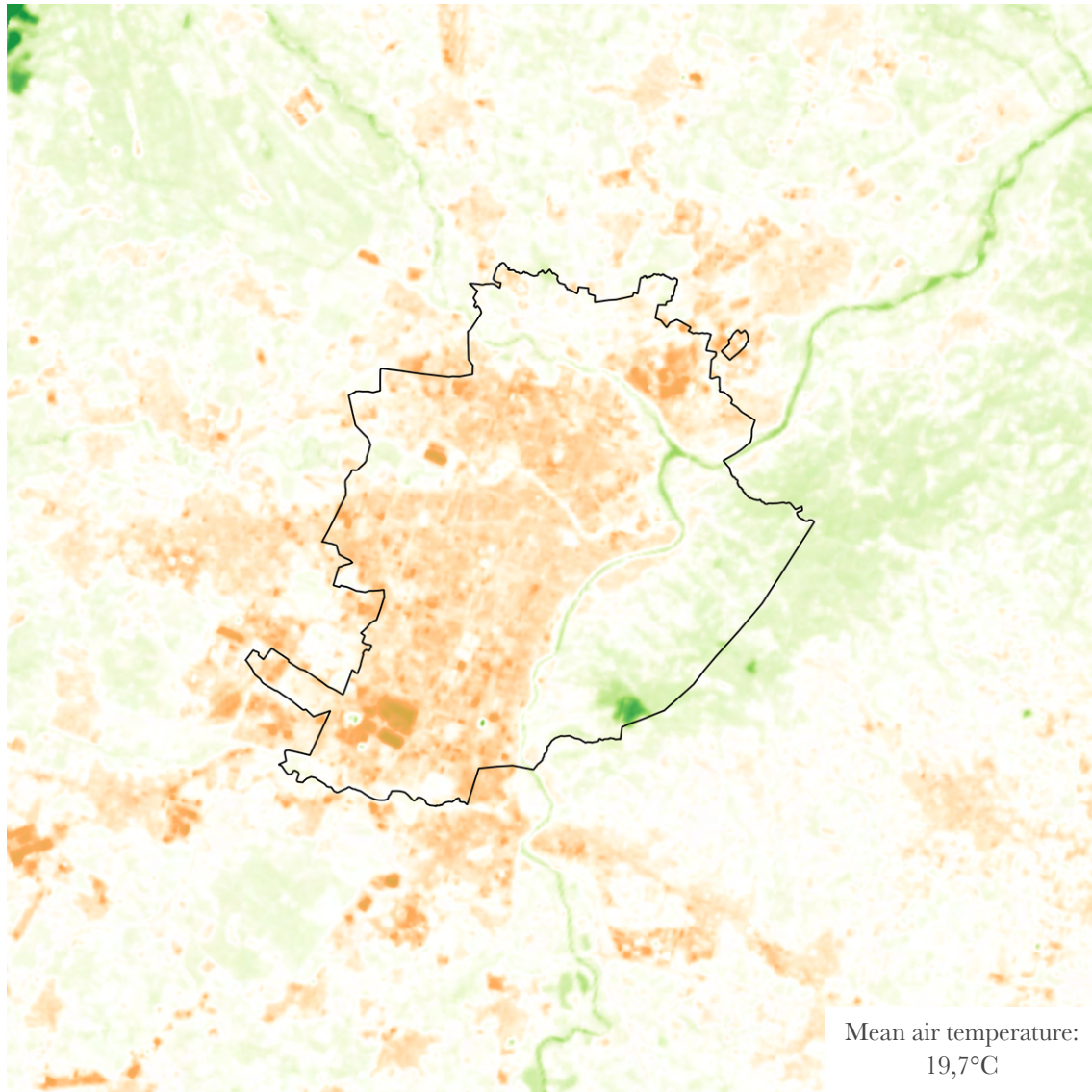
Figure 46 - UHI effect, mid-season 2023

-3 [high cooling effect]
-2[medium cooling effect]
-1 [low cooling effect]
0 [area of balance]
1 [medium-low heating effect]
2 [medium heating effect]
3 [high heating effect]

RESULTS:

The mid-season of 2023 exhibited a more mitigated UHI effect, as the areas affected by heating were fewer, resulting in a map that appears "whiter" with values around 0 (indicating balanced areas). Additionally, the hilly regions experienced a greater cooling effect compared to the previous years of analysis.

UHI intensity summer 2013

Mean air temperature:
32,3°C
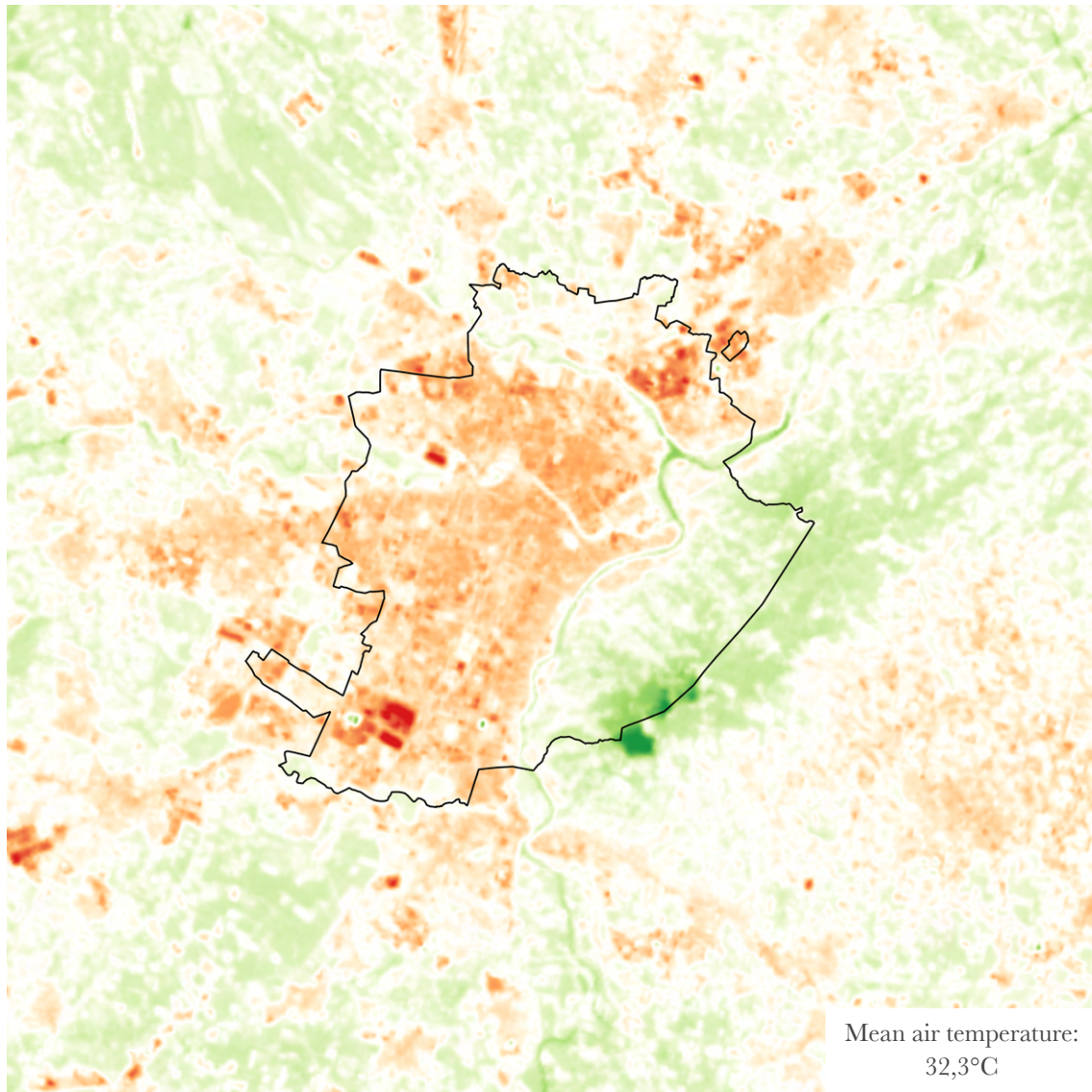
Figure 47 - UHI effect, summer 2013

■ -3 [high cooling effect]

■ -2,5 [medium-high cooling effect]

■ -2[medium-low cooling effect]

■ -1,5 [low cooling effect]

□ 0 [area of balance]

■ 1,5 [low heating effect]

■ 2 [medium-low heating effect]

■ 2,5 [medium heating effect]

■ 3 [medium-high heating effect]

■ 3,5 [high heating effect]
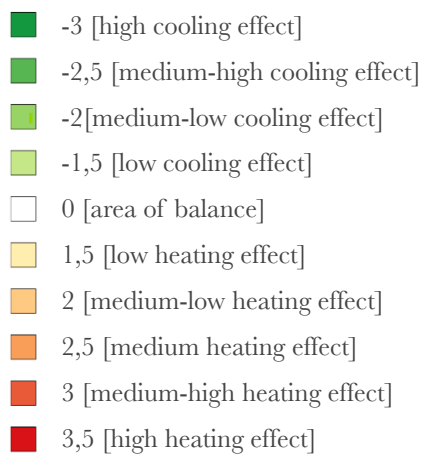
RESULTS:

In the summer of 2013, the disparity between urban areas and green spaces is evident, as the built-up areas of the city are characterized by significant heating phenomena, while the hilly regions experienced a cooling effect. The areas surrounding the city also exhibit a cooling effect in comparison to the constructed urban landscape.

UHI intensity summer 2018

Mean air temperature:
34,9°C
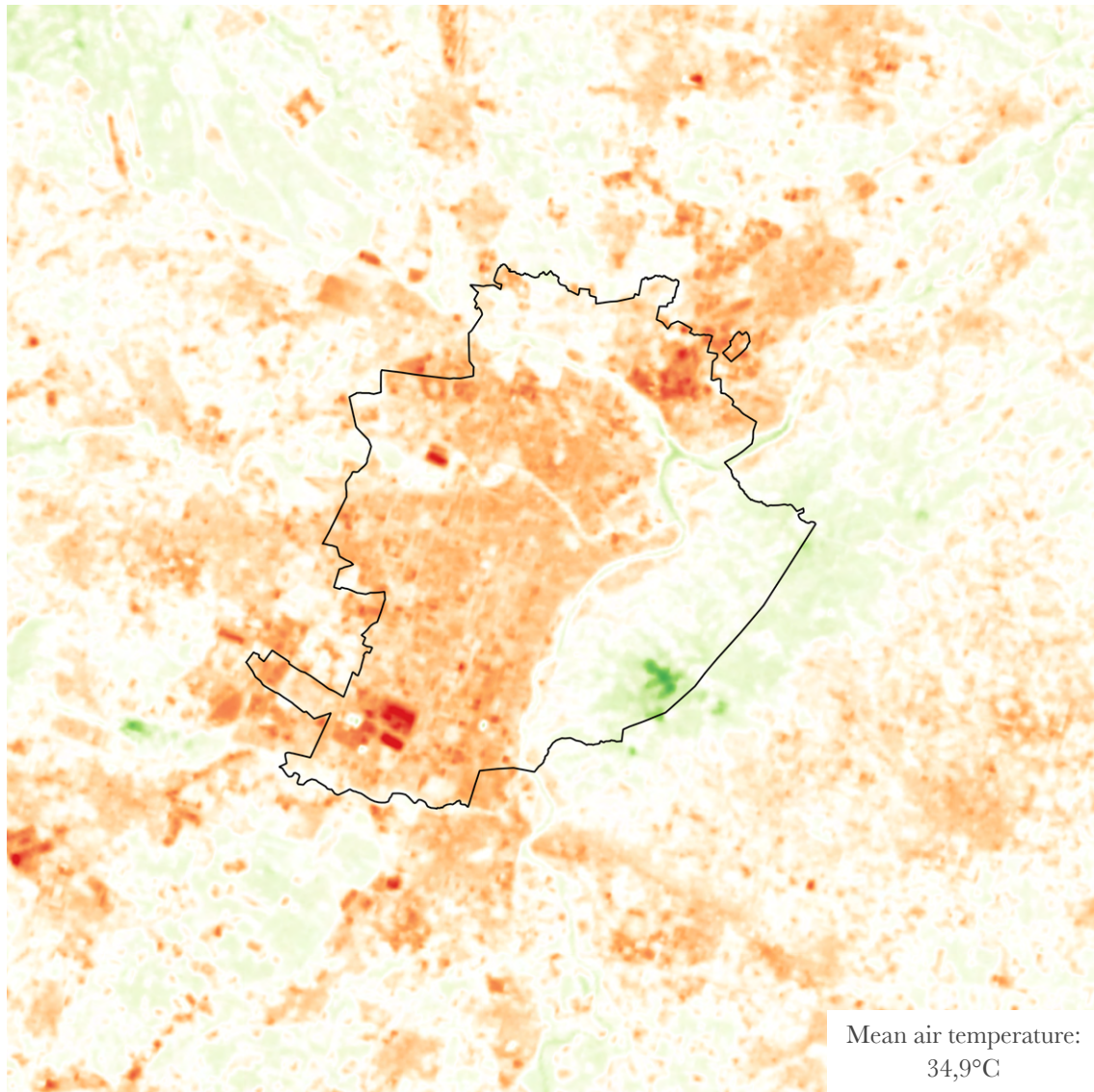
Figure 48 - UHI effect, summer 2018

- ■ -3 [high cooling effect]
- ■ -2,5 [medium-high cooling effect]
- ■ -2[medium-low cooling effect]
- ■ -1,5 [low cooling effect]
- □ 0 [area of balance]
- □ 1,5 [low heating effect]
- ■ 2 [medium-low heating effect]
- ■ 2,5 [medium heating effect]
- ■ 3 [medium-high heating effect]
- ■ 3,5 [high heating effect]
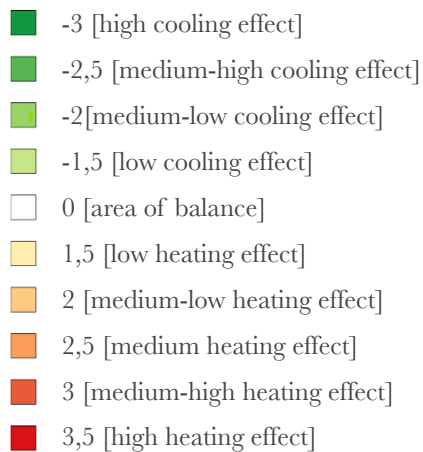
RESULTS:

Compared to the summer of 2013, in 2018 the UHI effect was less diversified, showing a more homogeneous heating trend, with only a few restricted and localized cooling areas. The balance zones were primarily located in the pre-hilly region and in the surrounding areas of the city.

UHI intensity summer 2023

Mean air temperature:
35,9°C
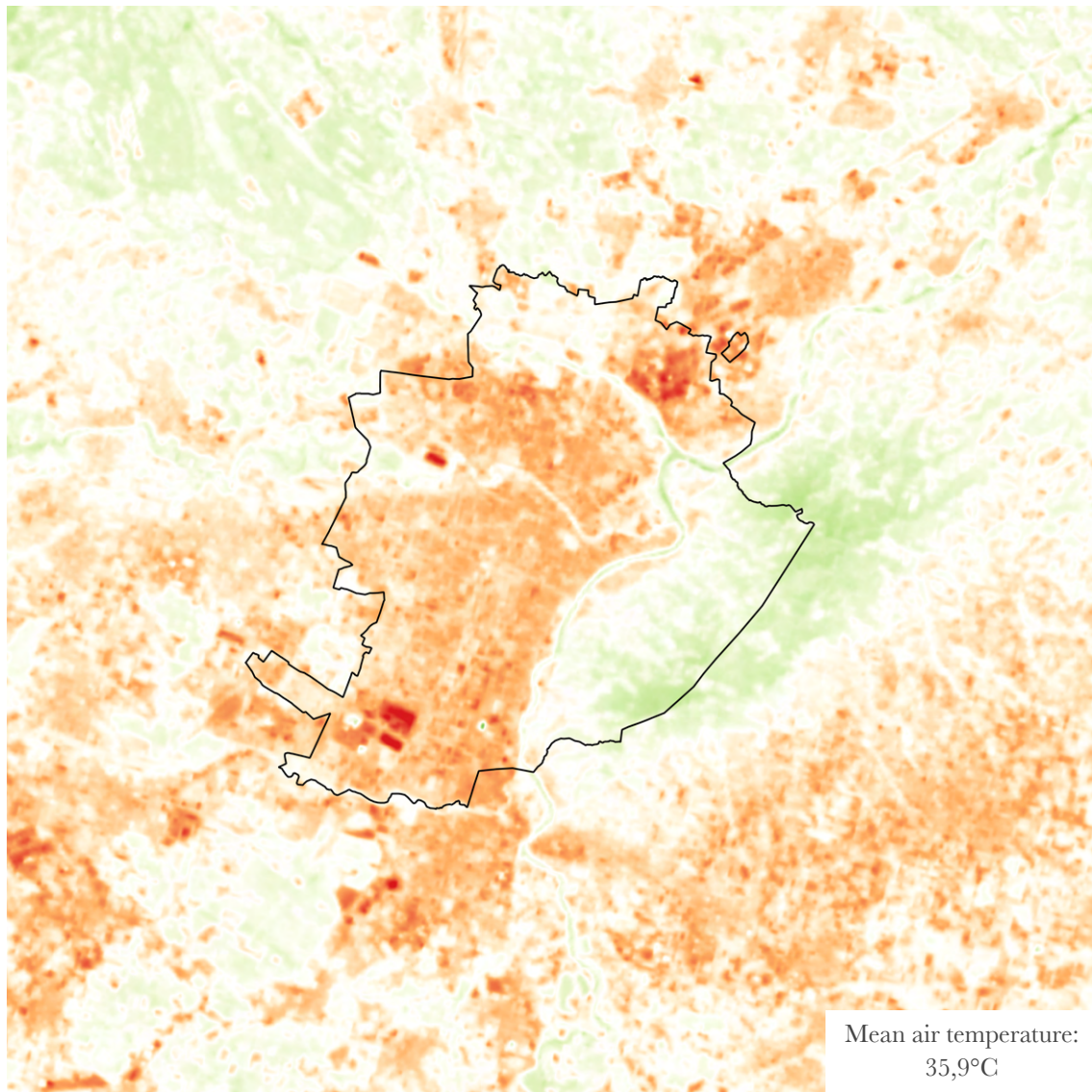
Figure 49 - UHI effect, summer 2023

■ -3 [high cooling effect]

■ -2,5 [medium-high cooling effect]

■ -2[medium-low cooling effect]

■ -1,5 [low cooling effect]

□ 0 [area of balance]

■ 1,5 [low heating effect]

■ 2 [medium-low heating effect]

■ 2,5 [medium heating effect]

■ 3 [medium-high heating effect]

■ 3,5 [high heating effect]
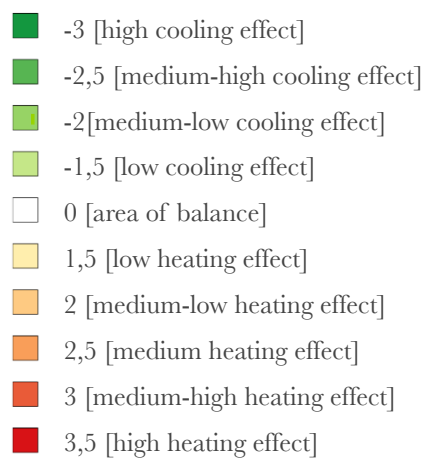
RESULTS:

In 2023, the urban heat island effect in Turin exhibited an increase in both diversification and intensity: the "hot" areas became even hotter, while the "cool" areas remained significantly cooler. Compared to previous years, the surrounding zones of the city also experienced an increase in heating effect.

5 ON-SITE DATA ACQUISITION

Pyranometer, albedometer and temperature probes

On-site measurements were conducted using various probes. Below are the tables detailing the technical specifications for each probe:

Probe	Description	Photo
Pyranometer DELTA OHM, LP PYRA 12	The pyranometer measures global solar irradiance within the spectral range of 0.3 mm to 3 mm. Equipped with a shading ring for direct components, it allows for the measurement of the diffuse component of solar radiation as well.	
Albedometer DELTA OHM, LP PYRA 06	The albedometer measures the net total radiation and the albedo of surfaces (albedo is defined as the ratio of the radiation reflected by a given surface to the amount of radiation incident on that surface).	
Temperature probe TESTO, 175 T3	The temperature datalogger is equipped with two connections for external probes with thermocouples (Type T or Type K). This device is ideal for measuring temperature on two channels, with a measurement range from -50 °C to +1000 °C.	

Table 20 - Probes identification

[12] WMO (2023), Guide to Instruments and Methods of Observation, Volume I – Measurement of Meteorological Variables

According to the WMO [12], measurements with the albedometer should be taken at a height between 1 and 1.5 meters to avoid discrepancies and shading. Nearby obstacles can cause shading or errors in reflectance measurements, as light or dark surfaces significantly influence the results. Therefore, shading should be avoided. The installation manual for the LP PYRA 06 albedometer also recommends placing the probe at a height of 1 to 2 meters above the ground. Considering the guidelines from both manuals, the measurements with the albedometer were conducted at a height of 1.5 meters.

For the pyranometer, measurements were taken by positioning the instrument on the ground while ensuring it was kept at a relatively high distance from obstacles such as poles, benches, trees, or any other objects that could influence the results.

For the temperature measurements, a datalogger was used with two external probes: one to measure air temperature and the other to measure soil temperature. To ensure accurate results, different types of surfaces were chosen to see how temperature changes depending on the type of pavement.

It is essential that during measurements the sky is clear and free from clouds and obstructions. For this reason, the selection of the measurement site is a crucial factor for the effectiveness and success of the experiment.

Sites definition

To assess how and to what extent different pavements influence the urban heat island effect, it is essential to carefully select the measurement sites, seeking diverse pavements in terms of both color (and consequently albedo) and composition.

The two sites where measurements were conducted are:
• Parking lot of the Politecnico of Turin (Corso Peschiera/Corso Castelfidardo):
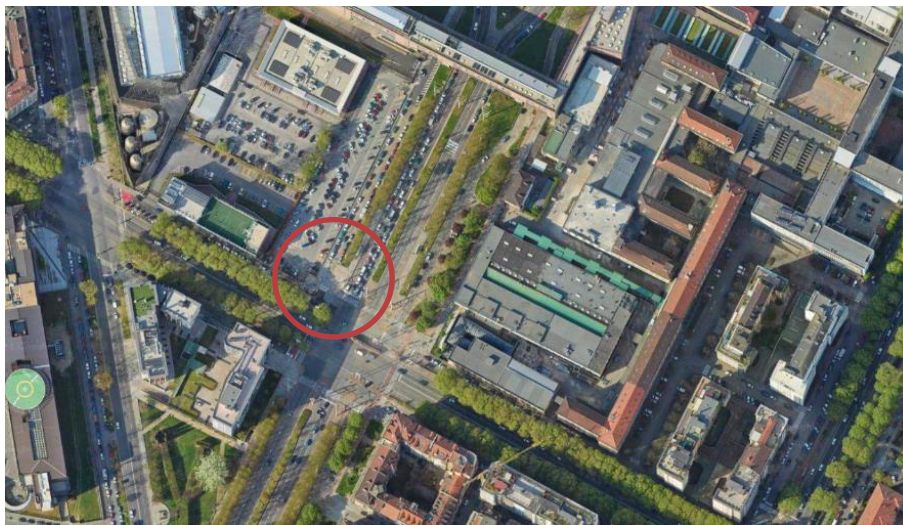
• Corso Marconi (post-intervention - mentioned in Chapter 3.2):
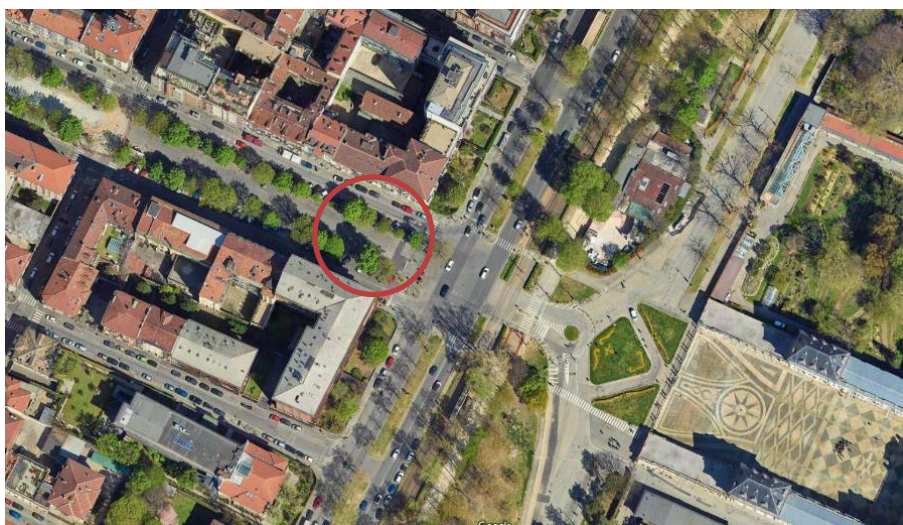
Data acquisition

Data were collected on September 14, 2024, at the sites previously indicated. Below are the data from the meteorological station at the Polytechnic University of Turin, aimed at ensuring consistency in the results obtained from the measurements:
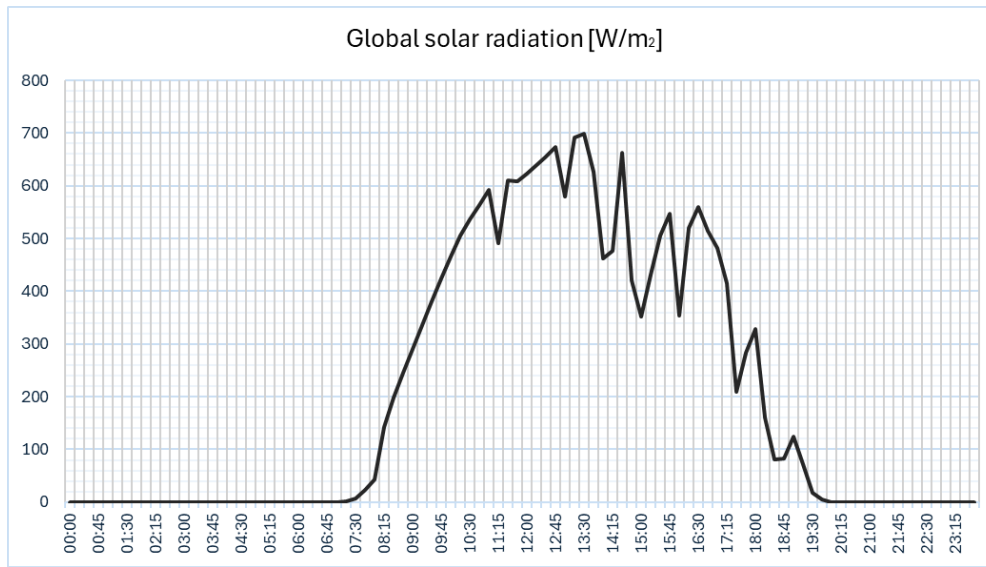
Graph 14 - Global solar radiation in Turin on 14/09/2024
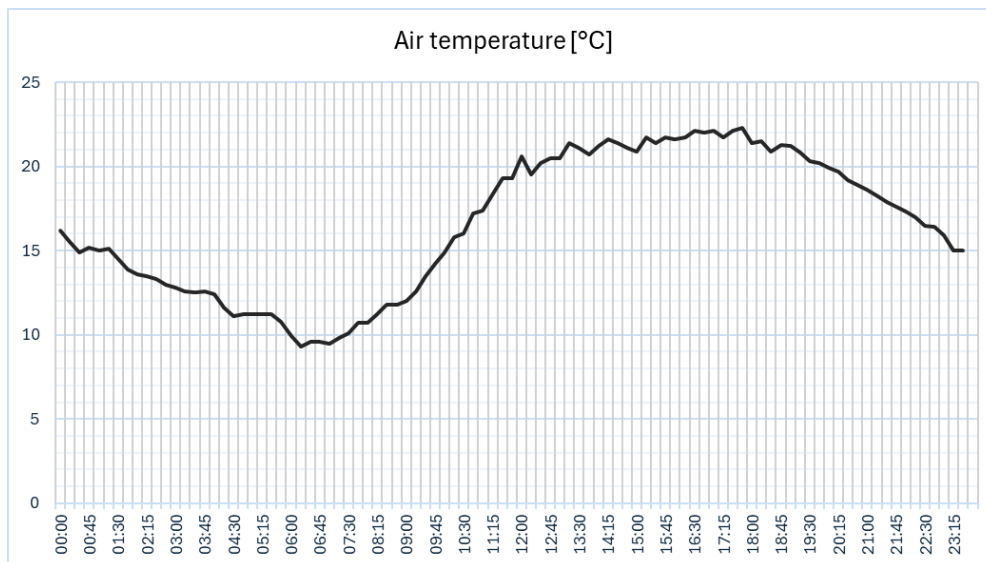
Graph 15 - Air temperature in Turin on 14/09/2024

Measurements were conducted between 11 AM and 1 PM (from 11:00 to 11:30 AM at the Polytechnic parking lot and from 12:30 to 1:00 PM at Corso Marconi).

As indicated by WMO guidelines and the instruction manual for the LP PYRA 06 probe:

• The albedometer was positioned at a height of approximately 1 meter.

• The pyranometer was maintained at a relatively high distance from obstacles (such as poles, benches, trees, or any other objects that could influence the results).

• The temperature data logger measures both air temperature and soil temperature. For consistency in the results, different soil types were selected to verify how temperature varies based on the type of pavement.

Figure 50 - Localizzazione della strumentazione, parcheggio Politecnico

Figure 51 - Localizzazione della strumentazione, Corso Marconi

Regarding the measurements, the probes were used as follows:

- Temperature Probe: air temperature [°C] and soil temperature [°C];

- Pyranometer: direct solar radiation [W/m2] - refers to the sum of short wave radiation that reaches the earth's surface, incident horizontally - and diffuse solar radiation [°W/m2] - with the help of a pyrometer, only the diffused light from the sky is measured, keeping the sun covered with the help of a shadow projector;

- Albedometer: albedo, which refers to the reflected solar radiation and indicates the ability of a surface to reflect solar rays.

The results of the measurements are presented below:

POLITECNICO DI TORINO PARKING

11:10 PM	T air 20.7°C / T soil 28.2°C	Albedo: 0.13	Direct radiation: 708.2 W/m²
11:20 PM	T air 22.0°C / T soil 34.2°C	Albedo: 0.11	Direct radiation: 681.6 W/m²
11:30 PM	T air: 22.2°C / T soil: 33.2°C	Albedo: 0.11	Direct radiation: 692.0 W/m²
11:35 PM	T air: 26.1°C / T soil: 30.7°C	Diffuse radiation: 60.2 W/m²	Direct radiation: 701.9 W/m²

Table 21 - On site measures, Politecnico Parking

12:30 PM		 Albedo: 0.24	 Diffuse radiation: 71 W/m²
12:35 PM	 T air 26.5°C / T soil 39.3°C	 Albedo: 0.25	 Direct radiation: 785.9 W/m²
12:55 PM	 T air: 25.9°C / T soil: 34.5°C	 Diffuse radiation: 170.37 W/m²	 Direct radiation: 614.8W/m²
1:00 PM	 T air: 25.4°C / T soil: 32.8°C	 T air: 26.4°C / T soil: 39.8°C	 Direct radiation: 605.9 W/m²

Table 22 - On site measures, Corso Marconi

Results

As previously mentioned, the on-site analysis involved measuring both temperature and solar radiation to establish a direct correlation between the two results.

Below is a summary table that includes all the temperature measurements [°C] of the floorings taken on-site. For measurements recorded multiple times, the highest temperature value is considered:

Pedestrian Stripe (on asphalt)	39.8°C - Corso Marconi, 1pm
Light Yellow Flooring	30.7°C - Politecnico parking, 11:35am
Medium-Light Beige Flooring	31.8°C - Corso Marconi, 12:30pm
Red Flooring	34,5°C - Corso Marconi, 34.5°C, 12:55pm
Cement Flooring	39.3°C - Corso Marconi, 12:30 pm
Pedestrian Stripe (on asphalt)	32.8°C - Corso Marconi, 01:00 pm

Table 23 - Temperature results [°C]

Temperature is essential for understanding climatic conditions (air temperature) and how these conditions affect various surfaces (surface temperature). Meanwhile, solar radiation is important for highlighting how not only temperature impacts the urban heat island effect but also how the amount of radiation reaching the ground alters microclimatic dynamics.

Regarding the initial measurements conducted at the Politecnico di Torino parking lot, the chosen pavement type was asphalt (relatively dark and uniformly applied).

In terms of temperature, the pavement demonstrated a significantly higher temperature compared to the air: at 11:10, the temperature difference was approximately 8°C; by 11:20, the difference increased to 12°C, and at 11:30, it decreased to 11°C. To illustrate how color, and consequently albedo, influences temperature results, at 11:35, the temperature probe was moved to the white parking stripes, where the temperature difference between air and pavement was only about 4°C.

Concerning solar radiation (both diffuse and direct) measured with the pyranometer, direct solar radiation ranged between 680 and 708 W/m², while the diffuse solar radiation measured at 11:35 showed a value of 60 W/m².

As for reflected solar radiation—albedo—the albedometer recorded values consistent with those in Tables 1 and 2 of Chapter 2 of this thesis, oscillating between 0,11 and 0,13 (with reference values of 0,1 for aged asphalt and 0,125).

The pavement on Corso Marconi is varied because of changes implemented by the City of Turin. As a result, different types of surfaces can be found along the street.

In terms of temperature, various pavement types were tested: the medium-light pavement showed a temperature difference between air and ground of about 7°C, the red pavement exhibited a difference of approximately 13°C, the medium-dark pavement indicated a difference of about 9°C, while the relatively light cement pavement also showed a 7°C difference. For reference, the temperature difference on asphalt was 13°C.

The reason for the higher temperature differences compared to previous measurements is that solar radiation values were elevated; for instance, at 12:35, solar radiation reached 785.9 W/m², explaining why the red pavement was notably warm relative to air temperature. Additionally, measurements were taken about an hour apart; considering both factors (higher solar radiation on Corso Marconi and the timing difference), the results are compatible and comparable.

The albedo of the medium-light pavement on Corso Marconi ranged from 0.24 to 0.25, which is consistent with Tables 1 and 2, where the brick has an albedo of 0.27 and the tile has an albedo of 0.21.

Both measurements were conducted on September 14 in late morning (between 11:30 pm and 01:00 pm), allowing for comparison. It can be concluded that "dark" pavements (such as the asphalt in the parking lot and the asphalt and red pavement on Corso Marconi) have higher temperatures than lighter pavements. Given that the measurements were taken in mid-September with air temperatures between 20 and 26°C, along with relatively intense solar radiation and a mostly clear sky, it can be asserted that the urban heat island effect is significantly influenced by pavement type.

Comparing the results obtained from the measurements with those from the UHI estimation analysis (and all related urban variables), a strong correlation can be observed. It is important to emphasize that the on-site measurements are significantly influenced by factors such as time of day, weather conditions, and cloud cover—and, consequently, by the season (in this case, mid-September, which is not typically a very hot period).

As for the estimation analyses using QGIS, the Landsat images provide an indicative overview of the situation, as the resolution is 30 meters (and for the thermal band 10, it is 100 meters, adjusted to 30 meters).

However, when correctly correlated, these two tools provide an indicative picture of the critical situation in the city of Turin in terms of temperature rise. It should be noted, however, that between 2018 and 2023, a slight decline in terms of LST and, consequently, UHI intensity was observed. One factor to consider is that the city of Turin has been investing in interventions aimed at improving outdoor environmental comfort (as extensively outlined in Chapter 2). Although the numerous projects are localized and targeted, they have significant effects on the local microclimate: thus, increasing the number of such targeted projects could yield substantial improvements in terms of environmental comfort and UHI intensity mitigation.

Of course, having selected only one representative day (the warmest, average, and coldest days of the year for the three years under study) does not provide a comprehensive picture. The analysis of trends in temperature and solar radiation supports the thesis and helps to understand the city's climatic dynamics.

Pavements, covering approximately 35% of the city's land surface, have a significant impact on soil temperature. Therefore, it can be stated that interventions on pavements - whether large or small - will have positive effects on the urban microclimate. This can be observed in the analysis of the 2018 and 2023 summer LSTs: the maximum surface temperatures decreased from 42°C to 35.8°C (considering that the Landsat 8 remote sensor recorded the data around 10 a.m.).

The following is a summary table in terms of albedo calculated from Landsat 8 images (radiometric variables), from literature, and from on-site calculation:

Soil Type	Albedo (from Landsat8, winter)	Albedo (from Landsat8, mid-season)	Albedo (from Landsat8, summer)	Albedo (from literature)	Albedo (from on-site calculation)
Water	0,41	0,48	0,57	0,5	n/a
Forest - Hilly Area	0,10	0,13	0,18	0,15	n/a
Built-up Area (City Center)	0,21	0,11	0,12	0,27	n/a
Built-up Area (Suburban Area)	0,12	0,12	0,11	0,27	n/a
Paving (Dark Surface)	0,04	0,04	0,06	0,05 - 0,125	0,11
Paving (Light Surface)	0,18	0,17	0,19	0,205	0,25
Industrial Zone	0,10	0,12	0,13	0,13	n/a
Urban Green Space	0,09	0,12	0,16	0,15	n/a

Table 24 - Albedo depending on soil type and seasons (radiometric calculation)

It can be stated that the values calculated from the Landsat 8 images and those measured on-site are consistent with the findings in the literature.

6 CONCLUSIONS

Combating UHI through Urban Planning

As urbanization accelerates, cities are experiencing rising temperatures due to the urban heat island effect, creating significant challenges for public health, energy consumption, and overall urban livability.

Dark materials like asphalt absorb a lot of heat, which can lead to higher temperatures in urban areas. On the other hand, lighter, more reflective pavements help to reduce this heat buildup. Newer materials, such as permeable pavements and reflective coatings, are designed to boost the Solar Reflectance Index (SRI) and reduce their overall environmental impact.

In essence, both the SRI and the types of pavements used are key factors in sustainable urban design, helping to create cooler, more comfortable, and energy-efficient environments.

"Cool materials" are construction and surfacing materials designed to reduce heat absorption and mitigate the urban heat island effect. These materials reflect more solar radiation than they absorb, helping to lower surface temperatures. Cool materials, which typically have a high albedo, are used in applications such as roofing, paving, and walls in urban areas. By reflecting a greater percentage of incoming solar radiation, they reduce surface overheating and the accumulation of heat in densely built environments.

Permeable pavements offer a valuable "soft engineering" solution for sustainable urban drainage (SuDS), providing integrated approaches to manage stormwater and address environmental issues in cities. These pavements help manage runoff, recharge groundwater, and improve road safety when properly designed. However, they also present challenges, such as the need for careful maintenance in certain conditions.

Pavements play a vital role in the Urban Heat Island (UHI) phenomenon, directly impacting surface temperatures in urban areas. Innovative materials, such as reflective and permeable pavements, along with integrated urban design strategies, can help mitigate the negative effects of UHI, creating cooler, healthier, and more energy-efficient environments. In this context, pavements should be considered a key element in the planning of sustainable cities.

Addressing the Urban Heat Island (UHI) intensity requires careful and thoughtful urban planning. As climate change worsens, the impact on local temperatures becomes even more pronounced, highlighting the growing link between global climate trends and the heat we experience in cities. This makes it all the more important to integrate climate action into urban development, ensuring our cities are not just sustainable, but also resilient and livable for future generations.

- Suitable Land Use: The impact of the built environment in cities is significant and can lead to pronounced effects on urban form. Urban planning should prioritize mixed land use to prevent the over-concentration of built-up areas.

- Energy-Efficient Buildings: Efficient buildings reduce energy consumption and heat dispersion, staying cooler in summer and warmer in winter, and therefore not contributing to local heat generation.

- Green Spaces, Vegetation, and Urban Forestry: It is well-established that urban greenery helps mitigate the effects of the heat island. In UHI analyses (such as NDVI calculations), greener areas in cities like Turin are cooler. Trees reduce heat absorption, provide shade, and, when placed in parks, enhance evaporative cooling. Proper management of urban forests is essential for keeping trees healthy, as they play a key role in cooling and improving the local microclimate.

- Green/Cool Roofs and Pavements: These types of surfaces reflect more solar radiation, contributing to cooling effects by absorbing less heat compared to conventional materials.

- Reflective Surfaces: Reflective surfaces help reduce heat absorption. However, care should be taken not to use excessively bright surfaces in terms of albedo, as they can cause glare and create maintenance challenges.

The Urban Heat Island (UHI) effect creates a vicious cycle where rising temperatures lead to increased use of cooling systems, which in turn drive higher energy consumption and emissions, further exacerbating heat and increasing the demand for cooling. Urban areas must find ways to adapt to and mitigate the effects of UHI. The more committed cities are to mitigation, the easier it will be to address global warming. Collaboration between urban planners, communities, and policymakers is essential for a smoother, more effective transition, ensuring greater environmental justice in cities.

By embracing innovative urban planning and understanding the connection between the Urban Heat Island (UHI) effect and climate change, cities can become a driving force in building a more sustainable and resilient future. Humidity, whether from soil, plants, or the atmosphere, has a natural cooling effect that helps reduce the intensity of the UHI, making urban areas more comfortable and livable. Plants, in particular, are crucial: through transpiration and shading, they significantly lower the temperatures of surrounding surfaces.

Urban regeneration projects can integrate reflective surfaces, such as cool roofs and reflective pavements, which deflect more solar radiation and absorb less heat, thus helping to reduce the UHI effect. The intensity of this phenomenon varies depending on the characteristics and layout of different urban areas. For example, densely built city centers with tall buildings and limited green spaces tend to experience a stronger UHI effect, as they accumulate more heat and offer fewer opportunities for natural cooling. In contrast, more open areas with green spaces generally exhibit lower UHI intensities.

Turin has implemented two strategic plans to enhance its resilience to climate change: the Piano Strategico dell'Infrastruttura Verde Torinese (2020) and the Piano di Resilienza Climatica (2020). The latter focuses on analyzing and identifying risks associated with the UHI effect, proposing nature-based solutions and initiatives to mitigate the impacts of warming.

BIBLIOGRAPHY

Agar-Ozbek, A. S., Weerheijm, J., Schlangen, E., & van Breugel, K. (2013). Investigating porous concrete with improved strength: Testing at different scales. Construction and Building Materials, 41, 480-490. https://doi.org/10.1016/j.conbuildmat.2013.01.028

AlShareedah, O., & Nassiri, S. (2020). Pervious concrete mixture optimization, physical, and mechanical properties and pavement design: A review. Journal of Cleaner Production, 288, 125095. https://doi.org/10.1016/j.jclepro.2020.125095

Anandababu, D., & Purushothaman, B. M. (2018). Estimation of land surface temperature using LANDSAT 8 data. International Journal of Advance Research, Ideas and Innovations in Technology, 4(2). Retrieved from http://www.ijariit.com

Baldinelli, G., & Bonafoni, S. (2015). Analysis of albedo influence on surface urban heat island by spaceborne detection and airborne thermography. In Proceedings of the International Conference on Image Analysis and Processing. https://doi.org/10.1007/978-3-319-23222-5_12

Bradley, A. V., Thornes, J., Chapman, L., & Unwin, D. J. (2002). Modeling spatial and temporal road thermal climatology in rural and urban areas using a GIS. Climate Research, 22(1), 41-55. https://doi.org/10.3354/cr022041

Busato, F., Lazzarin, R. M., & Noro, M. (2014). Three years of study of the Urban Heat Island in Padua: Experimental results. Sustainable Cities and Society, 10, 251-258. https://doi.org/10.1016/j.scs.2013.12.001

Chen, J., Chu, R., Wang, H., Zhang, L., Chen, X., & Du, Y. (2019). Alleviating urban heat island effect using high-conductivity permeable concrete pavement. Journal of Cleaner Production, 237, 117722. https://doi.org/10.1016/j.jclepro.2019.117722

Chen, J., Zhou, Z., Wu, J., Hou, S., & Liu, M. (2019). Field and laboratory measurement of albedo and heat transfer for pavement materials. Construction and Building Materials, 202, 46-57. https://doi.org/10.1016/j.conbuildmat.2018.12.024

Chen, Z., Zhang, H., Yang, X., Leng, Z., & Tang, Y. (2024). Cooling efficiency of thermochromic asphalt pavement material and its contribution to field performance enhancement of asphalt mixture. Construction and Building Materials, 411, 134562. https://doi.org/10.1016/j.conbuildmat.2024.134562

Cunha, J., Nóbrega, R. L. B., Rufino, I., Erasmi, S., Galvão, C., & Valente, F. (2020). Surface albedo as a proxy for land-cover clearing in seasonally dry forests: Evidence from the Brazilian Caatinga. Remote Sensing of Environment, 238, 111250. https://doi.org/10.1016/j.rse.2019.111250

Diem, P. K., Nguyen, C. T., Diem, N. K., Diep, N. T. H., Thao, P. T. B., Hong, T. G., & Phan, T. N. (2024). Remote sensing for urban heat island research: Progress, current issues, and perspectives. Remote Sensing Applications: Society and Environment, 33, 101081. https://doi.org/10.1016/j.rsase.2023.101081

Digavinti, J., Reddy, S. N., & Manikiam, B. (2017). Land surface temperature retrieval from LANDSAT data using emissivity estimation. International Journal of Applied Engineering Research, 12(20), 9679-9687. Retrieved from https://www.ripublication.com/ijaer17/ijaerv12n20_57.pdf

Ellena, M., Melis, G., Zengarini, N., Di Gangi, E., Ricciardi, G., Mercogliano, P., & Costa, G. (2023). Micro-scale UHI risk assessment on the heat-health nexus within cities by looking at socio-economic factors and built environment characteristics: The Turin case study (Italy). Urban Climate, 49, 101514. https://doi.org/10.1016/j.uclim.2023.101514

Gronlund, C. J. (2014). Racial and socioeconomic disparities in heat-related health effects and their mechanisms: A review. Current Epidemiology Reports, 1(3). https://doi.org/10.1007/s40471-014-0014-4

Higashiyama, H., Sano, M., Nakanishi, F., Takahashi, O., & Tsukuma, S. (2016). Field measurements of road surface temperature of several asphalt pavements with temperature rise reducing function. Case Studies in Construction Materials, 4, 73-80. https://doi.org/10.1016/j.cscm.2016.06.004

Howard, L. (1833). The Climate of London. London, UK: Harvey and Darton.

Huang, Z., Tang, L., Qiao, P., He, J., & Su, H. (2024). Socioecological justice in urban street greenery based on green view index: A case study within the Fuzhou Third Ring Road. Urban Forestry & Urban Greening, 95, 128313. https://doi.org/10.1016/j.ufug.2024.128313

Kousis, I., & Pisello, A. L. (2023). Evaluating the performance of cool pavements for urban heat island mitigation under realistic conditions: A systematic review and meta-analysis. Urban Climate, 49, 101470. https://doi.org/10.1016/j.uclim.2023.101470

Liao, W., Hong, T., & Heo, Y. (2021). The effect of spatial heterogeneity in urban morphology on surface urban heat islands. Energy and Buildings, 244, 111027. https://doi.org/10.1016/j.enbuild.2021.111027

Liu, Y., Chu, C., Zhang, R., Chen, S., Xu, C., Zhao, D., Meng, C., Ju, M., & Cao, Z. (2024). Impacts of high-albedo urban surfaces on outdoor thermal environment across morphological contexts: A case of Tianjin, China. Sustainable Cities and Society, 100, 105038. https://doi.org/10.1016/j.scs.2023.105038

Lopez-Cabeza, V. P., Alzate-Gaviria, S., Diz-Mellado, E., Rivera-Gomez, C., & Galan-Marin, C. (2022). Albedo influence on the microclimate and thermal comfort of courtyards under Mediterranean hot summer climate conditions. Sustainable Cities and Society, 81, 103872. https://doi.org/10.1016/j.scs.2022.103872

Matthews, T. (2012). Heat islands: Understanding and mitigating heat in urban areas. Australian Planner, 49(4), 363-364. https://doi.org/10.1080/07293682.2011.591742

Mutani, G., & Beltramino, S. (2022). Geospatial assessment and modeling of outdoor thermal comfort at urban scale. International Journal of Heat and Technology, 40(4), 871-878. https://doi.org/10.18280/ijht.400402

Mutani, G., Matsuo, K., & Todeschi, V. (2019). Urban heat island mitigation: A GIS-based model for Hiroshima. Instrumentation Mesure Métrologie, 18(4), 323-335. https://doi.org/10.18280/i2m.180401

Mutani, G., Todeschi, V., & Beltramino, S. (2021). How to improve the liveability in cities: The effect of urban morphology and greening on outdoor thermal comfort. Tecnica Italiana. https://dx.doi.org/10.18280/ti-ijes.652-433

Mutani, G., Todeschi, V., & Beltramino, S. (2022). Improving outdoor thermal comfort in built environment: Assessing the impact of urban form and vegetation. International Journal of Heat and Technology, 40(1), 23-31. https://doi.org/10.18280/ijht.400104

Mutani, G., Todeschi, V., & Matsuo, K. (2022). Urban heat island mitigation: A GIS-based model for Hiroshima. Instrumentation Mesure Métrologie, 18(4), 323-335. https://doi.org/10.18280/i2m.180401

Oke, T. R. (1982). The energetic basis of urban heat island. Quarterly Journal of the Royal Meteorological Society, 108(455), 1-24. https://doi.org/10.1002/qj.49710845502

Oke, T. R. (2010). The distinction between canopy and boundary-layer urban heat islands. International Journal of Climatology, 30(2), 268-277. https://doi.org/10.1002/joc.1502

Qin, Y., Tan, K., & Liang, J. (2016). Theory and procedure for measuring the albedo of a roadway embankment. Cold Regions Science and Technology, 126, 30-35. https://doi.org/10.1016/j.coldregions.2016.03.002

Qin, Y., Tan, K., Meng, D., & Li, F. (2016). Theory and procedure for measuring the solar reflectance of urban prototypes. Energy and Buildings, 126, 44-50. https://doi.org/10.1016/j.enbuild.2016.04.025

Rahman, M. N., Rony, M. R. H., Jannat, F. A., Pal, S. C., Islam, M. S., Alam, E., & Towfiqul Islam, A. R. M. (2022). Impact of urbanization on urban heat island intensity in major districts of Bangladesh using remote sensing and geo-spatial tools. Climate, 10(1), 3. https://doi.org/10.3390/cli10010003

Rahman, T., Irawan, M. Z., Tajudin, A. N., Amrozi, M. R. F., & Widyatmoko, I. (2023). Knowledge mapping of cool pavement technologies for urban heat island mitigation: A systematic bibliometric analysis. Energy and Buildings, 291, 113133. https://doi.org/10.1016/j.enbuild.2023.113133

Sen, S., Li, H., & Khazanovich, L. (2022). Effect of climate change and urban heat islands on the deterioration of concrete roads. Results in Engineering, 16, 100736. https://doi.org/10.1016/j.rineng.2022.100736

Shamsaei, M., Carter, A., & Vaillancourt, M. (2022). A review on the heat transfer in asphalt pavements and urban heat island mitigation methods. Construction and Building Materials, 359, 129350. https://doi.org/10.1016/j.conbuildmat.2022.129350

United Nations. (2015). 2030 Agenda for Sustainable Development. https://sdgs.un.org/2030agenda

Vujovic-Smolarski, S., Haddad, B., Karaky, L. H., & Sebaibi, N. (2021). Urban heat island: Causes, consequences, and mitigation measures with emphasis on reflective and permeable pavements. CivilEng, 2(2), 459-484. https://doi.org/10.3390/civileng2020026

Wardeh, Y., Kinab, E., Escadeillas, G., Rahme, P., & Ginestet, S. (2022). Review of the optimization techniques for cool pavements solutions to mitigate urban heat islands. Building and Environment, 223, 109482. https://doi.org/10.1016/j.buildenv.2022.109482

Wang, S., Cai, W., Tao, Y., Sun, Q. C., Wong, P. P. Y., Huang, X., & Liu, Y. (2023). Unpacking the inter- and intra-urban differences of the association between health and exposure to heat and air quality in Australia using global and local machine learning models. Science of The Total Environment, 871, 162005. https://doi.org/10.1016/j.scitotenv.2023.162005

World Meteorological Organization. (2023). Guide to instruments and methods of observation: Volume I – Measurement of meteorological variables (WMO-No. 8). Geneva: WMO. Retrieved from https://library.wmo.int/records/item/68695-guide-to-instruments-and-methods-of-observation?language_id=13&back=&offset=

Zhang, R., Jiang, G., & Liang, J. (2015). The albedo of pervious cement concrete linearly decreases with porosity. Advances in Materials Science and Engineering, 2015, Article 746592. https://doi.org/10.1155/2015/746592

SITOGRAPHY

ALBEDO DEFINITION

https://www.britannica.com/science/albedo

Copernicus Land Monitoring Service, EAGLE

https://land.copernicus.eu/en/eagle

Interventi di Torino, Torino Cambia

https://www.torinocambia.it/interventi

Landsat Images download

https://earthexplorer.usgs.gov/

NDVI, NDWI and NDMI definition & calculation

https://eos.com/make-an-analysis

Piano di Resilienza Climatica, Torino

http://www.comune.torino.it/torinosostenibile/documenti/
200727_Piano_Resilienza_Climatica_allegati.pdf

Piano Strategico dell'Infrastruttura Verde, Torino

http://www.comune.torino.it/verdepubblico/il-verde-a-torino/piano-infrastruttura-
verde/

UNI 8477/1

https://uni-8477-1

FIGURES

TABLES

GRAPHS

Graph 1 - Climograph (temperature and precipitation)
Graph 2 - Temperature trends 2013 - 2023 (from January to June)
Graph 3 - Temperature trends 2013 - 2023 (from July to December)
Graph 4 - Irradiance trends 2013 - 2023 (from January to June)
Graph 5 - Irrandiace trends 2013 - 2023 (from July to December)
Graph 6 - Percentage of use of soil in Turin
Graph 7 - Histograms winter, mid-season. summer 2023, NDVI
Graph 8 - Histograms winter, mid-season. summer 2023, NDVWI
Graph 9 - Histograms winter, mid-season. summer 2023, NDMI
Graph 10 - Histograms winter, mid-season. summer 2023, Albedo
Graph 11 - Histograms winter, mid-season. summer 2023, PVI
Graph 12 - Histograms winter, mid-season. summer 2023, Emissivity
Graph 13 - Histograms winter, mid-season. summer 2023, LST
Graph 14 - Global solar radiation in Turin on 14/09/2024
Graph 15 - Air temperature in Turin on 14/09/2024

LITERATURE TABLE

N°	TITLE	YEAR	PLACE	SCALE	OBJECT	FACTORS	TOOLS/ANALYSIS	RESULTS
1	*A review on the heat transfer in asphalt pavements and urban heat island mitigation methods*	2022			A considerable amount of solar energy is absorbed by asphalt concrete affecting the environment and mechanical properties of asphalt pavements	Thermal diffusivity, thermal emissivity, density, heat capacity, thermal conductivity, solar reflectance index, albedo	Indoor and outdoor tests	Regarding UHI mitigation methods, three ways are common, including using the cooling effects of water inside the pavement, increasing the reflectivity of pavements, and altering the thermal conductivity of pavement which are fully investigated in this study
2	*Albedo influence on the microclimate and thermal comfort of courtyards under Mediterranean hot summer climate conditions*	2022	Seville	Subdistrict	Evaluate the impact of different surface albedo on the thermal performance and comfort of a courtyard	Dry bulb temperature, relative humidity, wind speed, albedo	On-site test, ENVI-met	The influence of albedo on the temperature of the surfaces is high, as is the mean radiant temperature of the courtyard, affected by reflected solar radiation and surface temperature radiation
3	*Alleviating urban heat island effect using high-conductivity permeable concrete pavement*	2019			Develop high-conductivity permeable concrete and investigate its potential in alleviating UHI effect under both dry and wet conditions	Heat transfer theories, surface temperature	Indoor and outdoor tests	Permeable concrete pavement caused slightly greater heat output on sunny days but much smaller heat output on rainy days to the near-surface environment, as compared to conventional concrete pavement
4	*Analysis of Albedo Influence on Surface Urban Heat Island by Spaceborne Detection and Airborne Thermography*	2015	Florence	Urban	Detection of the surface urban heat island and the identification of the surface thermal and optical properties (albedo, in particular, is consequently connected with the surface temperatures)	Albedo, LST	Remote sensing, Landsat satellite images	Peculiar surface properties, such as the surface temperature and albedo, occupy a key position in the material classification and recognition in a urban texture
5	*Cooling efficiency of thermochromic asphalt pavement material and its contribution to field performance enhancement of asphalt mixture*	2024			Fill the research gaps about thermochromic asphalt pavement material in its cooling efficiency verification and field performance evaluation aspects	Albedo, cooling efficiency, outdoor solar radiation	Indoor and outdoor tests	The cooling efficiency of thermochromic asphalt material to pavement in hot summertime was verified through the experimental test combined with numerical simulation
6	*Effect of climate change and urban heat islands on the deterioration of concrete roads*	2022	Phoenix, Boston		Explore the mechanism by which changes to the hourly weather lead to a change in the performance of concrete pavements	Air temperature, pavements characteristic	Mechanistic-Empirical Pavement Design Guide (PavementME)	Concrete pavements, just like asphalt pavements, are sensitive to variability in air temperatures due to climate change and UHI
7	*Estimation of Land Surface Temperature using LANDSAT 8 Data*	2019	India, Hosur	Subdistrict	Estimate land surface temperature by NDVI, TOA data	NDVI, TOA, LST	Landsat 8 imagery, GIS	Image processing method to estimate LST and can be used to understand the urban development impacts on environment
8	*Evaluating the performance of cool pavements for urban heat island mitigation under realistic conditions: A systematic review and meta-analysis*	2023			Help towards the establishment of efficient standards and protocols that may be adopted in order to evaluate cooling performance under a uniform and consistent framework dedicated to effectively mitigate urban overheating	Cool pavement, Pavement monitoring	Bibliometric analysis	The three main Coll Pavement techniques that were reviewed in the study are reflective pavements, evaporative pavements and thermal energy storage pavements
9	*Field and laboratory measurement of albedo and heat transfer for pavement materials*	2019			Develop a new system for laboratory testing of albedo and temperatures at different depths in pavement slabs to overcome the defects of field measurement	Albedo, coating materials	Laboratory testing	Solar radiation intensity, incident angle and surrounding environment have remarkable effect on the field measured value of albedo, which makes it difficult to measure pavement albedo accurately. The developed laboratory albedometer can accurately measure the albedo and the internal temperature of pavement materials
10	*Field measurements of road surface temperature of several asphalt pavements with temperature rise reducing function*	2016		Urban	Utilization of ceramic waste powder as a part of components in water retaining pavements is investigated and evaluated to measure the surface temperature of pavements through field measurements conducted in the summer season	Surface temperature, water retention	Laboratory testing, on-site testing	All of the cement-based grouting materials application to the urban area can have great potential in reducing the surface temperature and contribute to the mitigation of the urban heat island phenomenon

N°	TITLE	YEAR	PLACE	SCALE	OBJECT	FACTORS	TOOLS/ANALYSIS	RESULTS
11	*Geospatial Assessment and Modeling of Outdoor Thermal Comfort at Urban Scale*	2022	Turin	Urban	Outdoor thermal condition at urban scale	Urban morphology, vegetation, outdoor thermal comfort, sky View factor, mean radiant temperature, urban surfaces	QGIS (UMEP-SOLWEIG), DSM	SOLWEIG is a more suitable tool for ssessment and analyses at the urba scale, whine ENVI-met is more useful for feasibility studies with high spatial and temporal resolution or for the pre-design phase of little neighboroods
12	*Guide Instruments and Methods of Observation, Volume I - Measurement of Meteorological Variables*	2023			Instructions and definition of measurements with probes	Measurements, probes		The albedometer measurements should be taken at a height of between 1 and 1.5 metres, so as to avoid discrepancies and shadowing. Obstacles in the vicinity of the probe can cause shadowing or errors in terms of reflectance
13	*Heat Islands: Understanding and Mitigating Heat in Urban Areas*	2008			Describes how heat islands are formed, what problems they cause, which technologies mitigate heat island effects and what policies and actions can be taken to cool communities	UHI, Cool roofing and paving		Presents the results of numerous quantitative studies that document and model the problem. The emphasis is on mitigation efforts, tried and true as well as experimental
14	*How to Improve the Liveability in Cities: The Effect of Urban Morphology and Greening on Outdoor Thermal Comfort*	2021	Turin	Subdistrict	Thermal comfort conditions at pedestrian level	Outdoor thermal comfort, urban morphology, green roofs, vegetated areas, neighborhood scale	ENVI-met	The use of urban geometries together with the use of greenery can helpto design better built environments. The use of new indexes and tools as ENVI-met is fundamental to have good results
15	*Impact of Urbanization on Urban Heat Island Intensity in Major Districts of Bangladesh Using Remote Sensing and Geo-Spatial Tools*	2022	Banglad esh	Urban	The research aims to analyze how rapid urbanization has affected the intensity of Urban Heat Islands (UHIs) during the winter dry period in major districts of Bangladesh from 2000 to 2019	LULC maps, Hotspots and LST, Urbanization, UHI, NDVI	Landsat (5,7,8), GIS	The research in seven urbanized districts of Bangladesh over 20 years revealed that urban growth resulted in less vegetation, higher land temperatures, and increasing Urban Heat Island (UHI) intensities, with Mymensingh having the highest UHI intensity (10°C) and Dhaka the lowest (1.46°C), highlighting significant thermal changes and underscoring the importance of sustainable urban planning to address UHI effects and potential regional climate impacts
16	*Impacts of high-albedo urban surfaces on outdoor thermal environment across morphological contexts: A case of Tianjin, China*	2024	Tianjin	Urban	Evaluate the effects of high-albedo urban surfaces using three thermal environment-related indicators	Weather data, urban morphology	Urban Weather Generator, GIS	Increasing road albedo is more effective in mitigating UHI in fringe areas, whereas increasing wall and roof albedo is more effective in mitigating UHI in central areas
17	*Improving Outdoor Thermal Comfort in Built Environment Assessing the Impact of Urban Form and Vegetation*	2022	Turin	Subdistrict	Impact of urban variables and quantification of greening's influence on outdoor thermal comfort conditions	Greening, neighborhood scale, utdoor thermal comfort, thermal comfort indexes, urban morphology	ENVI-met	Outdoor thermal comfort is significantly affected by urban morphology, but the use of green areas and trees can mitigate the local climate conditions
18	*Investigating porous concrete with improved strength: Testing at different scales*	2013			Designing porous concretes that fracture into small fragments and have improved strength	Aggregate properties, porosity, compressive strenght	Computed tomography, electron microscopy, X-ray diffraction analysis	Experiments at different scales were performed to determine the effectiveness of the various factors while the outcome of the tests guided the modification process of the material
19	*Knowledge mapping of cool pavement technologies for urban heat island Mitigation: A Systematic bibliometric analysis*	2023			Gather scientific publications from subject-specific indexed databases, analyse and categorise the publications manually, analyse the publications using bibliometric software, and interpret the technologies	Cooling pavement technologies	Bibliometric analysis	The production of documents related to cool pavements has increased exponentially since 1993. Most research on cool pavement technology has focused on increasing the solar reflectance of the pavement surface
20	*Land Surface Temperature Retrieval from LANDSAT data using Emissivity Estimation*	2017	India, Chittoor	Subdistrict	Land Surface Emissivity (LSE) values needed in order to apply the method have been estimated from a procedure that uses the visible and near infrared bands	LSE, LST, NDVI	Landsat 8 images	Image processing method to estimate LST and can be used to understand the urban development impacts on environment

N°	TITLE	YEAR	PLACE	SCALE	OBJECT	FACTORS	TOOLS/ANALYSIS	RESULTS
21	*Micro-scale UHI risk assessment on the heat-health nexus within cities by looking at socio-economic factors and built environment characteristics: The Turin case study (Italy)*	2023	Turin	Urban	Empirical example of a flexible and replicable methodology to estimate the micro-scale UHI risks within an urban context	Inequalities, risk assessment, vulnerabilities	GIS	Improved the knowledge base for the implementation of micro-scale UHI risk assessment by looking at the heat-health nexus within cities
22	*Modeling spatial and temporal road thermal climatology in rural and urban areas using a GIS*	2002	West Midlands	Urban	Estimate the spatial variation of surface variables across the West Midlands. Spatial analysisof the topography was achieved using a GIS database	Latitude, SVF, albedo, emissivity, surface temperature	GIS	Shows how values for albedo, sky-view factor, and roughness can be derived for any urban or rural grid. The most influential of the variables was the weighting of surface emission with a sky-view factor
23	*Pervious concrete mixture optimization, physical, and mechanical properties and pavement design: A review*	2021			Help to efficiently navigate the existing literature and respond promptly to new challenges and issues that arise by the rapid adoption of permeable pavement technology	Pervious concrete, Permeable pavement, Sustainable construction material	Bibliometric analysis	Efforts in computational modeling of mechanical, structural, and hydrological behavior of pervious concrete materials and pervious concrete pavements are also presented
24	*Protocollo ITACA a Scala Urbana - SINTETICO*	2020	Italy	Urban				
25	*Racial and Socioeconomic Disparities in Heat-Related Health Effects and Their Mechanisms: a Review*	2014	Michigan		Examine the ways in which race and socioeconomic status contribute to disparities in heat-related healh outcomes. The objective is to identify strategies for reducing disparities	Access to air conditioning, outdoor occupation, social isolation, pre-existing medical conditions, urban design, environmental factors	Bibliometric analysis	The study found out that race and low-income background affect negative experiences regarding health impacts due to heat waves. This was due to factors such as lack of access to air conditioning, outdoor occupations, social isolation and pre-existing medical conditions
26	*Remote sensing for urban heat island research: Progress, current issues, and perspectives*	2024			Importance of understanding UHI impacts, exploring effective mitigation and adaptation strategies, and addressing methodological challenges	Control factors, mitigation interventions, surface urban heat island,	Satellite images (Landsat, Modis), LST	Landsat and MODIS are the two most popular satellite data used for SUHI. Landsat is the most used, it however has limitations. Data fusion is a potential solution to exploit both high temporal resolution from MODIS and high spatial resolution from Landsat
27	*Review of the optimization techniques for cool pavements solutions to mitigate Urban Heat Islands*	2022			Technique of cool pavements or evaporative pavements	Cool pavements, Evaporation, Durability		In order to decrease the air temperature through cool pavements, it is necessary, first of all, to decrease the surface temperature of these pavements by increasing their albedo, their thermal conductivity and their evaporation flux
28	*Socioecological justice in urban street greenery based on green view index-A case study within the Fuzhou Third Ring Road*	2024	Fujian	Subdistrict	Measures the distribution of street greenery using a GVI indicator and to assess the fairness of the spatial distribution of street green space	Urban greenery, green view index, socioecological justice	Street view images, GIS, LiDAR	Subdistricts with a lower green view index have a less equitable street greenery distribution, people with low socioeconomic status may suffer from green injustice, and seniors have a lower accessibility to street green space than people with the average social status
29	*Surface albedo as a proxy for land-cover clearing in seasonally dry forests: Evidence from the Brazilian Caatinga*	2020	Caatinga forest	Local	Identification of changes in terrestrial forest biomass on an annual basis is a prerequisite for improving estimates of terrestrial water, energy, and carbon sources and exchanges	Surface albedo (SA), Enhanced Vegetation Index (EVI), Normalized Difference Vegetation Index (NDVI)	Remote sensing, Landsat satellite images	The spatial resolution and temporal coverage series of Landsat images allows a systematic assessment
30	*The Albedo of Pervious Cement Concrete Linearly Decreases with Porosity*	2015			Measures the albedo of pervious concrete with a range of porosities. Four Portland cement concrete mixes are cast with designed amounts of sand to control the porosities. A spectrophotometer is used to measure the reflectances	Albedo, reflectance	Laboratory testing	It is cautious to develop pervious concrete to mitigate the urban heat island

N°	TITLE	YEAR	PLACE	SCALE	OBJECT	FACTORS	TOOLS/ANALYSIS	RESULTS
31	*The climate of London*	1833		Urban	Provide a meteorological and environmental analysis of the climate of London	Temperature, humidity, Wind direction/speed, atmospheric phenomena	Thermometers, hygrometer, wind vane	Temperature in London veries from 8°C (january) to 18°C (july). Humidity in London is higher in early morning. Wind speed tends to be higher in winter. Heaviest rainall in october and november
32	*The distinction between canopy and boundary-layer urban heat island*	2010	Vancouver	Urban	Define the causes of UHI and how it is influenced	Land use, building density, vegetation	Review article	Difference between canopy and boundary layers can lead to differen mitigation strategies
33	*The effect of spatial heterogeneity in urban morphology on surface urban heat islands*	2021	London, Seoul	Urban	Quantify spatial heterogeneity of urban morphology based on GIS data and improve the understanding of the effects of spatial variation on SUHIs	LST, Urban spatial heterogeneity, urban microclimate	GIS	The analysis results suggest a necessity for further exploration on underlying physical mechanisms between urban spatial heterogeneity and SUHIs
34	*The energetic basis of the urban heat island*	1980	Vancouver	Urban	Define physical processes that are responsible for the UHI effect	Building materials, weather conditions, surface cover	Metereological measurements, remote sensing	Urban areas have higher temperatures due to absorption and storage of heat. Highlight the importance of energy balance in urban environments
35	*Theory and procedure for measuring the albedo of a roadway embankment*	2016			Develops a theoretical model to measure the albedo of an embankment prototype	Albedo, solar reflectance, reflectivity, view factor	Albedometer	A theoretical model and its associated experimental procedure are developed to measure the albedo of the curved surface like a roadway embankment
36	*Theory and procedure for measuring the solar reflectance of urban prototypes*	2016			Proposes a new, simplistic method to measure the albedo of the urban prototype. The proposed method introduces a black urban prototype that is the same configuration as the measured urban prototype	Multiple reflections, albedo, reflectivity, urban surface	Albedometer	The proposed method can be applied to characterize whether coating urban surfaces with high-reflective paints can effectively reduce the urban solar absorption on a larger scale
37	*Three years of study of the Urban Heat Island in Padua: Experimental results*	2014	Padova	Urban	Controllable and uncontrollable factors could further be categorized as the temporary effect variables, permanent effect variables, and cyclic effect variables	Solar reflectance, air temperature, relative humidity, cloud coverage, wind speed	Weather station	The higher air temperature of sub-urban zones with respect to rural ones is noteworthy, but without the typical "bell-shaped" form. In nearly all the graphs there is a local minimum after 8000 m, corresponding to a shaded road
38	*Unpacking the inter- and intra-urban differences of the association betweenhealth and exposure to heat and air quality in Australia using global and local machine learning models*	2023	Australia	National	Quantify and identify the potential confunders that are importat to the heat-air-health relationship, unveil the cumulative heat and air pollution on self-reported physical and mental health	Census, health, land use, Google Earth, LST	GIS	Social and built environmental factors are more influential to physical and mental health outcomes than heat and air pollution, especially in rural areas
39	*Urban Heat Island Mitigation: A GIS-based Model for Hiroshima*	2019	Hiroshima	Urban	GIS tool can be used to analyze the microclimate of outdoor spaces, considering the relationship between air temperature and characteristics of an urban environment	Urban morphology, vegetation, density population, surfaces types	GIS, Satellite images (Landsat)	UHI effect decreases proportionally with the presence of vegetation and with higher values of the albedo of urban surfaces, as well as the altitude and the distance from the sea. The UHI effect instead increases proportionally for higher values of the canyon height-to-width ratio, the building density and the LST
40	*Urban Heat Island: Causes, Consequences, and Mitigation Measures with Emphasis on Reflective and Permeable Pavements*	2020	More places has been taken in consideration	Urban	The objective of this research is to investigate the economic and social development in urban and rural areas of developing countries in the context of increasing impervious surfaces, primarily paved surfaces, and its consequences on urban heat island formation	Green areas, building materials, morphology, weather condition		The study highlights the importance of landscape design in urban planning and the potential of cool pavements for improving the urban microclimate. The study suggests the need for further research through experimental models or numerical simulations to assess the efficiency of combined strategies involving reflective and permeable pavements as potential UHI mitigation measures
41	*2030 Agenda for Sustainable Development,*	2015	World	National, Urban, Subdistrict	17 Sustainable Development Goals as urgent call for action by all countries	Poverty, health, education,equality, energy, economic growth,climate action, water and land		Ending poverty must go with strategies that improve health and education while tackling climate change and working for preservation

RINGRAZIAMENTI

Desidero ringraziare la Professoressa Mutani, la mia relatrice, per avermi guidata fin dal primo giorno, per avermi trasmesso le conoscenze di cui avevo bisogno e la passione che spronerà il mio futuro.

Desidero ringraziare il Professor Bassani e il Professor Tefa per avermi fornito ulteriori spunti di sviluppo per questa tesi.

Desidero ringraziare i miei genitori e tutta la mia famiglia per l'affetto e il sostegno che mi hanno sempre dimostrato.

Desidero, infine, ringraziare tutti i miei amici che mi hanno fatta sorridere e divertire anche nei momenti più duri.